

# **NUMERICAL STUDY OF A THREE-BED ADSORPTION CHILLER WITH DIFFERENT CYCLES**

Submitted by  
GULSHAN KHATUN  
Student No. 100609007P  
Session: October-2006

MASTER OF PHILOSOPHY  
IN  
MATHEMATICS



Department of Mathematics  
BANGLADESH UNIVERSITY OF ENGINEERING AND  
TECHNOLOGY, DHAKA-1000  
December-2013

The thesis entitled

**NUMERICAL STUDY OF A THREE-BED ADSORPTION CHILLER WITH  
DIFFERENT CYCLES**

Submitted by

GULSHAN KHATUN

Student No. 100609007P, Session: October-2006, a part time student of M.Phil.

(Mathematics) has been accepted as satisfactory in partial fulfillment for the degree of

**Master of Philosophy in Mathematics**

On December, 08-2013

**BOARD OF EXAMINERS**

- |    |  |                              |
|----|--|------------------------------|
| 1. | <hr/> <b>Dr. Md. Zafar Iqbal Khan</b><br>Professor<br>Department of Mathematics, BUET, Dhaka-1000              | Chairman<br><br>(Supervisor) |
| 2. | <hr/> <b>Head</b><br>Department of Mathematics, BUET, Dhaka-1000   | Member<br><br>(Ex-Officio)   |
| 3. | <hr/> <b>Dr. Md. Mustafa Kamal Chowdhury</b><br>Professor<br>Department of Mathematics, BUET, Dhaka-1000       | Member                       |
| 4. | <hr/> <b>Dr. Md. Abdul Hakim Khan</b><br>Professor<br>Department of Mathematics, BUET, Dhaka-1000              | Member                       |
| 5. | <hr/> <b>Dr. Md. Abdus Samad</b><br>Professor<br>Department of Mathematics<br>University of Dhaka, Dhaka-1000. | Member<br><br>(External)     |

# Abstract

This thesis deals with the numerical results of a three-bed adsorption chiller with different cycles, using mass recovery scheme to improve the cooling effect. In the present numerical solution, the heat source temperature variations are taken from 50<sup>0</sup>C to 65<sup>0</sup>C (for cycle1) and from 50<sup>0</sup>C to 90<sup>0</sup>C (for cycle 2) and along with coolant inlet temperature at 30<sup>0</sup>C and the chilled water inlet temperature at 14<sup>0</sup>C. Silica gel-water is chosen as adsorbent-refrigerant pair. In the new strategy, mass recovery process occurs in all bed. In operational strategy1, the configuration of beds in the three bed chiller with mass recovery are taken as uniform in size, but in operational strategy2, the configuration of Hex3 is taken as half of Hex1 or Hex2. A cycle simulation computer program is constructed to analyze the influence of operating conditions (hot and cooling water temperature) on COP (coefficient of performance), CC (cooling capacity) and chilled water outlet temperature. The performances in terms of cooling capacity (CC) and coefficient of performances (COP) are compared with those of conventional three-bed mass recovery scheme. Results show that the optimum COP values are obtained for hot water inlet temperature at 65<sup>0</sup>C along with the coolant and chilled water inlet temperature are at 30<sup>0</sup>C and 14<sup>0</sup>C, respectively. It is also seen that the cooling capacity (CC) and coefficient of performances (COP) can be improved up to 50%, 13% (for cycle1) and 8%, 9.5% (for cycle 2) respectively than that of the conventional mass recovery cycle if heat source temperature is considered to be 65<sup>0</sup>C.

## **Author's Declaration**

I am here by declaring that the work in this dissertation entitled “NUMERICAL STUDY OF A THREE-BED ADSORPTION CHILLER WITH DIFFERENT CYCLES” is being carried out in accordance with the regulations of Bangladesh University of Engineering and Technology (BUET), Dhaka, Bangladesh. The work is also original except where indicated by and attached with special reference in the context and no part of it has been submitted for any attempt to get other degree or diplomas.

All views expressed in the dissertation are those of the author and in no way or by no means represent those of Bangladesh University of Engineering and Technology, Dhaka. This dissertation has not been submitted to any other University for examination either in home or abroad.

(Gulshan Khatun)

Date: December, 08-2013

## Acknowledgement

At the outset I am pronouncing my thankfulness to the almighty who give me the ability to carry out such a research work.

My gratitude will always be there to Dr. Md. Zafar Iqbal Khan, Professor, Department of Mathematics, BUET, my supervisor who continuously guided me from all the directions. It is my great gratification having the opportunity to work under his supervision. I would like to have the opportunity to express my heart-rending admiration to my supervisor who has encouraged and rightly initiated me to step into the wide arena of mathematics and its application in the engineering fields.

I am not less grateful and thankful to the efforts, perseverance, sincerity, enormous will-force, clarity, accuracy, completeness, monumental patience, generous co-operation and fellow-feeling he made for me to venture this research and bring this painstaking task to a successful end.

I am as well intensely beholden to all my teachers of the Department of Mathematics, BUET for their intelligent and open-minded support in providing me all necessary help from the department during my course of M. Phil. Degree. They all have helped me immensely over the last school period either in the courses or mentally with advices.

I would like to utter here the name of my colleagues of Eastern University for their co-operation.

I am really grateful to my husband and my son for his burly bona fide aid.

I must acknowledge my debt to my parents for whom I have been able to see the beautiful sights and sounds of the world.

# Contents

Abstract.....	iii
Author's Declaration.....	iv
Acknowledgements.....	v

## Contents

Nomenclature.....	viii
List of Tables.....	ix
List of Figures.....	x

## Chapter 1

Introduction	1
1.1 Introduction.....	1
1.2 Literature Review.....	1
1.3 Present Problems.....	5
1.4 Objectives of the present study.....	5
1.5 Outline of the Thesis.....	6

## Chapter 2

Numerical Study of a Three-Bed Adsorption Chiller With Mass Recovery (Equal Bed)..	7
2.1 Introduction.....	7
2.2 Working Principle of the Mass Recovery Chiller.....	7
2.3 Formulation of the problem.....	21
2.3.1 Energy balance for the adsorber/desorber.....	21
2.3.2 Energy balance for the evaporator.....	22
2.3.3 Energy balance for the condenser.....	22
2.3.4 Mass balance.....	23
2.3.5 Absorption rate.....	23
2.3.6 Measurement of system performance.....	24
2.4 Solution procedure.....	26
2.5 Results and discussion.....	30

2.6 Comparison of the results.....	34
2.7 Conclusion.....	36
<b>Chapter 3</b>	<b>37</b>
Performance Evaluation on Mass Recovery Three-Bed Adsorption Chiller (Unequal Bed)..	37
3.1 Introduction.....	37
3.2 Working Principle of the Mass Recovery Chiller.....	37
3.3. Results and discussion.....	51
3.4 Comparison of the results.....	55
3.5 Conclusion.....	57
<b>Chapter 4</b>	<b>58</b>
Comparison of the Result between Two Cycles.....	58
4.1 Introduction.....	58
4.2 Comparison of the result between two cycles.....	58
4.3 Conclusion.....	60
<b>Overall Conclusion</b>	<b>61</b>
<b>Extension of this work</b>	<b>62</b>
<b>References</b>	<b>63</b>

## Nomenclature

A	area (m <sup>2</sup> )
C <sub>p</sub>	Specific heat (J kg <sup>-1</sup> K <sup>-1</sup> )
D <sub>so</sub>	Pre-exponential constant (m <sup>2</sup> s <sup>-1</sup> )
E <sub>a</sub>	activation energy (J kg <sup>-1</sup> )
L	latent heat of vaporization (J kg <sup>-1</sup> )
$\dot{m}$	mass flow rate (kg s <sup>-1</sup> )
P <sub>s</sub>	saturated vapor pressure (Pa)
q	concentration (kg refrigerant / kg adsorbent)
q <sup>*</sup>	Concentration equilibrium (kg refrigerant / kg adsorbent)
Q <sub>st</sub>	isosteric heat of adsorption (J kg <sup>-1</sup> )
R	gas constant (J kg <sup>-1</sup> K <sup>-1</sup> )
R <sub>p</sub>	average radius of a particle (m)
T	temperature (K)
t	time (s)
U	heat transfer coefficient (W m <sup>-2</sup> K <sup>-1</sup> )
W	weight (kg)

## Subscripts

ads	adsorber, adsorption	hw	hot water
cond	condenser	in	inlet
chill	Chilled water	out	outlet
cw	Cooling water	s	silica gel
des	desorber, desorption	se	sorption element
eva	evaporator	w	water
hex	heat exchanger	w <sub>v</sub>	water vapor



## List of Tables

Table 2.1	Operational strategy1 of three bed chiller with mass recovery.	8
Table 2.2	Baseline parameters.	25
Table 2.3	Standard operating conditions.	26
Table 2.4	Heat source temperature variation on CC, COP and chilled water outlet temperature for proposed cycle1.	34
Table 2.5	Heat source temperature variation on CC, COP and chilled water outlet temperature for Khan et al. [2].	35
Table 3.1	Operational strategy 2 of three bed chiller with mass recovery.	38
Table 3.2	Standard operating conditions.	51
Table 3.3	Heat source temperature variation on CC, COP and chilled water outlet temperature for proposed cycle2.	55
Table 3.4	Heat source temperature variation on CC, COP and chilled water outlet temperature for Khan et al. [2].	56
Table 4.1	Heat source temperature variation on CC, COP and chilled water outlet temperature for cycle1 and cycle 2.	58

## List of Figures

Figure 2.1	Schematic of three bed chiller with mass recovery Mode (A-T).	9-18
Figure 2.2(a)	The effect of heat source temperature on CC.	31
Figure 2.2(b)	The effect of heat source temperature on COP.	31
Figure 2.3(a)	The effect of cooling water inlet temperature on CC.	32
Figure 2.3(b)	The effect of cooling water inlet temperature on COP.	32
Figure 2.4(a)	The effect of heat source temperature on waste heat recovery efficiency [-].	33
Figure 2.4(b)	The effect of heat source temperature on chilled water outlet temperature.	33
Figure 2.5(a)	Cycle time effect on CC and COP.	34
Figure 2.5(b)	Effect of mass recovery time on CC and COP.	34
Figure 3.1	Schematic of three bed chiller with mass recovery Mode (A-T).	39-48
Figure 3.2(a)	The effect of heat source temperature on CC.	52
Figure 3.2(b)	The effect of heat source temperature on COP.	52
Figure 3.3(a)	The effect of cooling water inlet temperature on CC.	53
Figure 3.3(b)	The effect of cooling water inlet temperature on COP.	53
Figure 3.4(a)	The effect of heat source temperature on waste heat recovery efficiency [-].	54
Figure 3.4(b)	The effect of heat source temperature on chilled water outlet temperature.	54
Figure 3.5(a)	Cycle time effect on CC and COP.	55
Figure 3.5(b)	Effect of mass recovery time on CC and COP.	55

Figure 4.1(a)	Performance comparison of CC between the proposed cycle1 and cycle 2.	59
Figure 4.1(b)	Performance comparison of COP between the proposed cycle1 and cycle 2.	59
Figure 4.1(c)	Performance comparison of outlet chilled water between the proposed cycle1 and cycle 2.	60

## Introduction

### 1.1 Introduction

Over the past few decades there have been considerable efforts to use adsorption (solid/vapor) for cooling and heat pump applications, but intensified efforts were initiated only since the imposition of international restrictions on the production and utilization of CFCs and HCFCs. The severity of the ozone layer destruction problem due to CFCs and HCFCs has been calling for rapid developments in environment friendly air conditioning technologies. With regard to energy use, global warming prevention has been requiring a thorough revision of energy utilization practices towards greater efficiency. From this perspective, interest in adsorption systems has been increased as they do not use ozone depleting substances as refrigerants nor do they need electricity or fossil fuels as driving sources.

### 1.2 Literature Review

Most of the advanced cycles in adsorption refrigeration/heat pump are proposed to achieve high Coefficient of Performance (COP) and/or Cooling Capacity (CC) values. Few cycles, however, are proposed to utilize relatively low temperature heat source. Saha et al. [1] proposed two-stage chiller where the driving heat source temperature was validated experimentally. A two-stage silica gel-water adsorption refrigeration cycle can exploit the heat source of temperature around 60<sup>0</sup>C with the cooling source at 30<sup>0</sup>C. Khan et al. [2] studied the performance investigation on mass recovery three-bed adsorption cycle. Later, Khan et al. [3] proposed and investigated numerically the advanced three-bed adsorption chiller employing mass recovery scheme. Saha et al. [4] studied waste heat driven dual-mode, multi-stage, multi-bed regenerative adsorption system. A novel adsorption chiller, namely, “Three-bed adsorption chiller” is also investigated by Saha et

al. [5] and shown that waste heat recovery efficiency of the three-bed system is about 35% higher than that of the two-bed system.

In the promotion of environmentally friendly energy utilization systems, one major goal is to develop CFC-free refrigeration/ heat pump systems that utilize waste heat or renewable energy sources. Heat driven sorption (adsorption/ desorption) cycle is one of the promising candidates to utilize waste heat at near environment temperature so that waste heat below 100<sup>0</sup>C can be recovered. In the moment absorption (liquid-vapor) is the most promising technology in area of heat driven heat pump/refrigeration technologies, however, adsorption (solid-vapor) cycles have some distinct advances over the other systems in view points of their ability to be driven by relatively low temperature heat source, which is highly desirable and investigated by Kashiwagi et al. [6]. In the last three decades, extensive investigations on the performances of adsorption refrigeration/heat pump systems have been conducted considering various adsorbent/refrigerant pairs, such as zeolite/water, activated carbon/ammonia, activated carbon/methanol and silica gel/water. It is well known that the performance of adsorption cooling/heating system is lower than that of other heat driven heating/cooling systems. Specially, absorption system provided that the available heat source temperature is at 75<sup>0</sup>C or higher. From this context, many authors proposed and/or investigated the adsorption cooling and heating system to improve the performance. In order to improve the performance of such cooling systems, Douss and Meunier [7] proposed a cascading cycle with a higher COP of 1.06. Stitou et al. [8] analyzed different cascading cycles which coupled solid-gas reactions with the liquid-gas absorption process. Wang et al. [9] incorporated heat and mass recovery processes into the continuous cycle to improve its thermal performance. Recently, Leong and Liu [10] modeled a combined heat and mass recovery adsorption cycle employing a compact zeolite adsorbed bed and obtained COP values which are slightly better than those of Wang and Wang [9]. To improve the coefficient of performance, Shelton et al. [11] proposed a thermal wave regenerative adsorption heat pump system. In a similar effort, Critoph [12] proposed a forced convection adsorption cycle. Meunier [13] investigated the system performance of cascaded adsorption cycles in which an active/methanol cycle is topped by zeolite/water

cycle. Pons and Poyelle [14] investigated the effect of mass recovery process in conventional two bed adsorption cycle to improve the cooling power. Later, Wang [15] showed that mass recovery process is very effective for the high evaporating pressure lift as well as for the low regenerating temperature. Akahira et al. [16] investigated two-bed mass recovery cycle with novel strategy, which shows that mass recovery cycle with heating/cooling improves the cooling power. Alam et al. [17] analyzed four-bed mass recovery cycle with silica gel/water pair employing a new strategy to improve the cooling effect. Recently, Saha et al. [18] analyzed a dual-mode, multi-bed adsorption chiller to improve the heat recovery efficiency and Khan et al. [19] studied two-stage adsorption chiller using re-heat parametrically to utilize low-temperature waste heat as heat source.

Adsorption cooling system is a noiseless, non-corrosive and environment-friendly energy conversion system. So, many researchers around the world have made significant efforts to study such a cooling system in order to commercialize it. Following are some representative examples.

The silica gel/water adsorption chiller driven by the waste heat source has been successfully commercialized in Japan, as reported by Saha et al. [20]. Waste heat at the temperature between 50<sup>0</sup>C and 90<sup>0</sup>C abounds in industry. It is seldom utilized, but usually discharged into the environment at present. A multi-bed regenerative adsorption chiller design has been proposed by Chua et al. [21]. The simulation results have showed that, using the same waste heat source, a four-bed chiller generated 70% refrigerating capacity improvement compared with a typical two-bed chiller, and a six-bed chiller generated 40% refrigerating capacity improvement compared with a four-bed chiller. Alam et al. [22] proposed and analyzed re-heat two-stage adsorption chiller which can be operated with driving heat source temperature range between 50<sup>0</sup>C and 90<sup>0</sup>C along with a heat sink at 30<sup>0</sup>C, COP of the re-heat two-stage chiller is higher than that of two-stage chiller and also found, the re-heat two-stage chiller produces effective cooling even though heat source temperature fluctuated between 50<sup>0</sup>C and 90<sup>0</sup>C.

Adsorption chillers are usually driven by heat, so these chillers are attractive for reducing electric power demand peaks resulting from air-conditioning and refrigeration equipment loads. The variety of heat sources available for driving the adsorption refrigeration cycle

makes this a technology that contributes to CO<sub>2</sub> reduction by utilizing non-fossil fuel, such as solar energy or waste heat from industrial process, as its driving source by Ng et al. [23]. It has been reported that the fixed beds of porous materials in the adsorption refrigeration cycles tend to be low performance, long cycle time and make the system over-sized due to poor heat and mass transfer rates in the adsorption bed by Qu et al. [24].

Most of the research in this field focuses on developing advanced cycles in order to improve chiller performance to be competitive with other systems. Silica gel-water is widely used as an adsorbent-adsorbate pair in adsorption refrigeration system. Compared to other adsorbents, silica gel can be regenerated at a relatively low temperature that is below 100<sup>0</sup>C. It also has a large uptake capacity for adsorption of water up to 35%-40% of its dry mass, which has a high latent heat of evaporation. Because of the low regeneration temperature, a silica gel-water adsorption chiller can utilize industrial waste heat or renewable energy resources in Chu et al. [25] and Ng et al. [26].

The intensive research on developing silica gel-water adsorption chiller has been done by many researchers. For example, the multi-bed multi-stage cycle is able to produce a cooling effect at low heat source temperature such as below 100<sup>0</sup>C. To utilize the low heat source temperature, a three-stage silica gel-water adsorption cycle was proposed and examined by Saha et al. [27].

The performance of the adsorption refrigeration cycle can be enhanced by applying a mass recovery cycle into the adsorption cycle. The mass recovery cycle is produced by interconnecting the two beds for depressurizing and pressurizing after desorption and adsorption process, respectively. Akahira et al. [28, 29] determined that the mass recovery cycle provides heating to the desorber and cooling to the adsorber. They reported that the cycle produces better performance than that of conventional mass recovery without heating and cooling. The mass recovery cycle can also be applied to multi-bed and multi-stage cycles. Alam et al. [30] introduced the mass recovery cycle into a two-stage adsorption cycle, namely, a re-heat two-stage adsorption cycle. A similar effort was also made by Khan et al. [31], applying the scheme to a three-stage adsorption

cycle. They reported that the cycle produces a higher COP value than those of conventional two-stage and three-stage cycles. The advanced mass recovery cycle was also applied to a three-bed cycle. Khan et al. [32] proposed and numerically evaluated a three-bed mass recovery cycle. They reported that the cycle performance is better than that of the three-bed single stage proposed by Saha et al. [2]. Uyun et al. [33] proposed and investigated numerically the advanced three-bed adsorption cycle employing heat and mass recovery cycle. They obtained that the performance of the cycle are superior to those of three-bed of single stage and mass recovery cycle. Recently, Khan et al. [34] studied experimentally on a three-bed adsorption chiller and reported that it provides better COP values for 65<sup>0</sup>C-75<sup>0</sup>C heat source temperature.

### **1.3 Present Problems**

In the present work, mass recovery process occurs in all bed. In the new strategy additional heating and cooling accelerate the desorption/adsorption process; thus the system provides the better cooling output. A cycle simulation computer program is constructed to analyze the influence of operating conditions (hot and cooling water temperature) on COP (coefficient of performance), CC (cooling capacity),  $\eta$  (chiller efficiency) and chilled water outlet temperature.

### **1.4 Objectives of the present study**

The primary objective of the study is to determine the numerical result of a three-bed adsorption chiller with different cycles. To get the optimum cooling capacity (CC) and the coefficient of performance (COP) of the chiller, we want to investigate the following

- To determine the highest COP values, it is important to operate the chiller with renewable energy or waste heat of temperature below 100°C as the driving heat source.
- To investigate the influence of the heat source temperature on a three-bed adsorption chiller which calculate the cooling capacity and its improvement ratios.



- Numerical results are analyzed in terms of cooling capacity and coefficient of performance by varying heat transfer fluid (hot and cooling water) inlet temperatures and adsorption/desorption cycle time.

## **1.5 Outline of the Thesis**

This dissertation contains four chapters. In chapter 1, a brief introduction is presented with aim and objective. This chapter also consists a literature review of the past studies.

In chapter 2, we have numerically studied the performance of a three-bed adsorption chiller (equal bed) with mass recovery scheme. Mass recovery process occurs in all bed. The performances in terms of cooling capacity (CC) and coefficient of performances (COP) are compared with those of conventional three-bed mass recovery scheme [4]. The cycle simulation calculation indicates that the optimum COP value is 0.6214 for hot water inlet temperature at 65<sup>0</sup>C along with the coolant and chilled water inlet temperature are at 30<sup>0</sup>C and 14<sup>0</sup>C, respectively.

In chapter 3, the numerical results of a three-bed adsorption chiller (unequal bed) using silica gel-water as the adsorbent-refrigerant pair are presented. The configuration of Hex1 and Hex2 are identical, but the configuration of Hex3 is taken as half of Hex1 or Hex2. A cycle simulation computer program is constructed to analyze the influence of operating conditions (hot and cooling water temperature) on COP (coefficient of performance), CC (cooling capacity),  $\eta$  (chiller efficiency) and chilled water outlet temperature.

The comparison of the numerical results between the proposed cycle 1 and the proposed cycle 2 are discussed in chapter 4. Both of the cycles were tested at the same conditions based on the input parameters. The proposed cycle 1 gives better CC and COP value than the proposed cycle 2. Finally, the dissertation is rounded off with the overall conclusion and recommendations for further study of the present problem are outlined.

### **Numerical Study of a Three-Bed Adsorption Chiller With Mass Recovery (Equal Bed)**

#### **2.1 Introduction**

In this chapter the performance of a three-bed adsorption chiller with mass recovery has been numerically studied. The mass recovery scheme is used to improve the cooling effect and a CFC-free-based sorption chiller driven by the low-grade waste heat or any renewable energy source can be developed for the next generation of refrigeration. Silica gel/water is taken as adsorbent/adsorbate pair for the present chiller. The three-bed adsorption chiller comprises with three adsorber/desorber heat exchanger, one evaporator and one condenser. In the present numerical solution, the heat source temperature variation is taken from 50<sup>0</sup>C to 65<sup>0</sup>C along with coolant inlet temperature at 30<sup>0</sup>C and the chilled water inlet temperature at 14<sup>0</sup>C. In the new strategy, mass recovery process occurs in all bed. A cycle simulation computer program is constructed to analyze the influence of operating conditions (hot and cooling water temperature) on COP (coefficient of performance), CC (cooling capacity),  $\eta$ (chiller efficiency) and chilled water outlet temperature.

#### **2.2 Working Principle of the Mass Recovery Chiller**

The schematic diagram and time allocation of the proposed three-bed mass recovery chiller are shown in Fig.2.1 and Table 2.1, respectively. The three-bed mass recovery chiller comprises with three sorption elements (adsorber / desorber heat exchangers), a condenser, an evaporator, and metallic tubes for hot, cooling and chilled water flows as shown in Fig. 2.1. The design criteria of the three-bed mass recovery chiller are almost similar to that of the three-bed chiller without mass recovery which is proposed and developed by Saha et al. (2003) and (2006). The configuration of beds in the three bed chiller with mass recovery were taken as uniform in size. Operational strategy1 of the proposed chiller is shown in Table 2.1. In proposed design, mass recovery process occurs in all bed. To complete a full cycle for the proposed system, the chiller needs 20 modes,

namely A, B, C, D, E, F, G, H, I, J, K, L, M, N, O, P, Q, R, S and T as can be seen from Table 2.1.

Table 2.1: Operational strategy1 of three bed chiller with mass recovery

Mode	A	B	C	D	E	F	G	H	I	J	K	L	M	N	O	P	Q	R	S	T	
Hex1	Desorption		Mass recovery with heating	Pre-heating	Adsorption		Mass recovery with cooling	Pre-cooling	Desorption		Mass recovery with heating	Pre-heating	Adsorption		Mass recovery with cooling	Pre-cooling	Desorption		Mass recovery with heating	Pre-heating	
Hex2	Adsorption		Mass recovery with cooling	Pre-cooling	Desorption		Mass recovery with heating	Pre-heating	Adsorption		Mass recovery with cooling	Pre-cooling	Desorption		Mass recovery with heating	Pre-heating	Adsorption		Mass recovery with cooling	Pre-cooling	
Hex3	Desorption	Mass recovery with heating	Pre-heating	Adsorption	Mass recovery with cooling	Pre-cooling	Desorption	Mass recovery with heating	Pre-heating	Adsorption	Mass recovery with cooling	Pre-cooling	Desorption	Mass recovery with heating	Pre-heating	Adsorption	Mass recovery with cooling	Pre-cooling	Desorption	Mass recovery with heating	Pre-heating

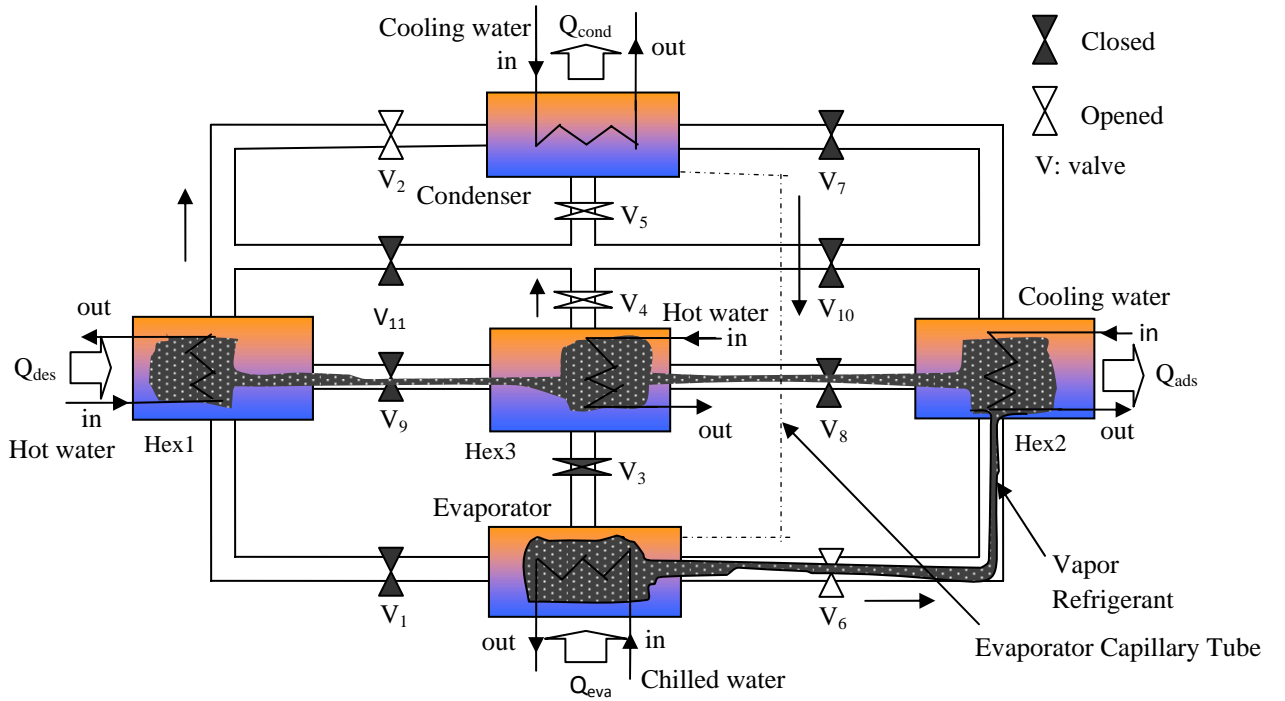


Fig2.1: Schematic of three bed chiller with mass recovery

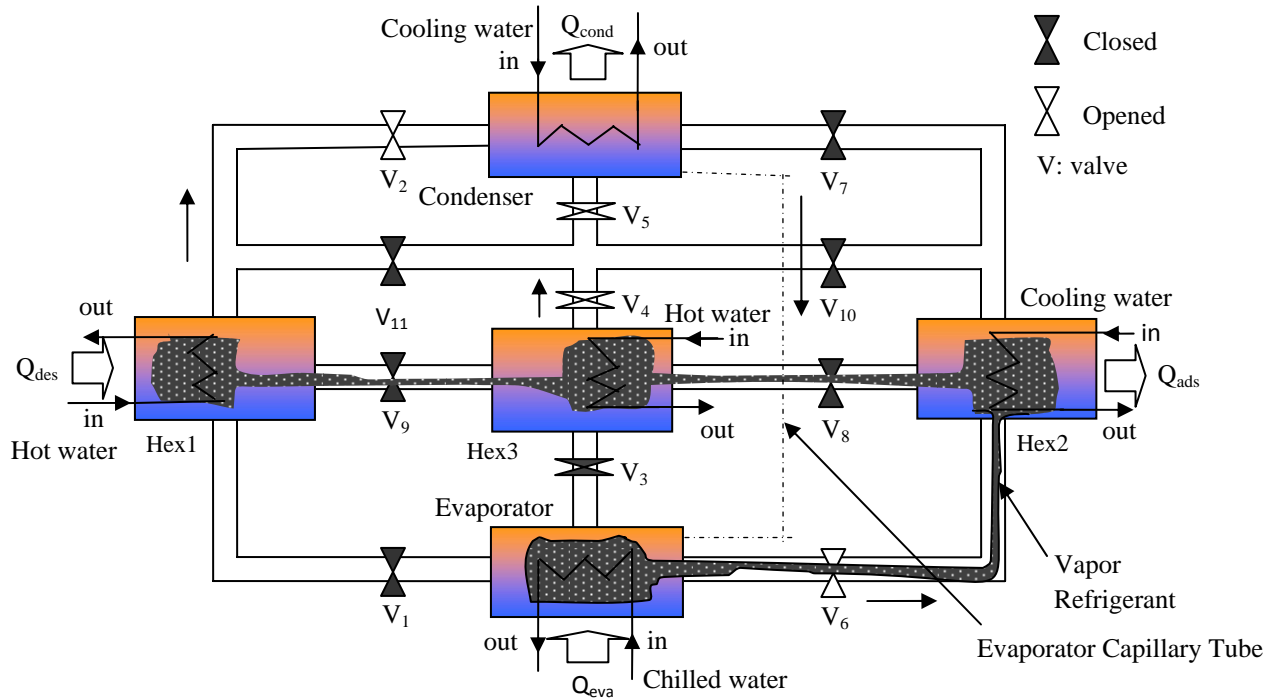


Fig2.1: Schematic of three bed chiller with mass recovery (Mode-A)

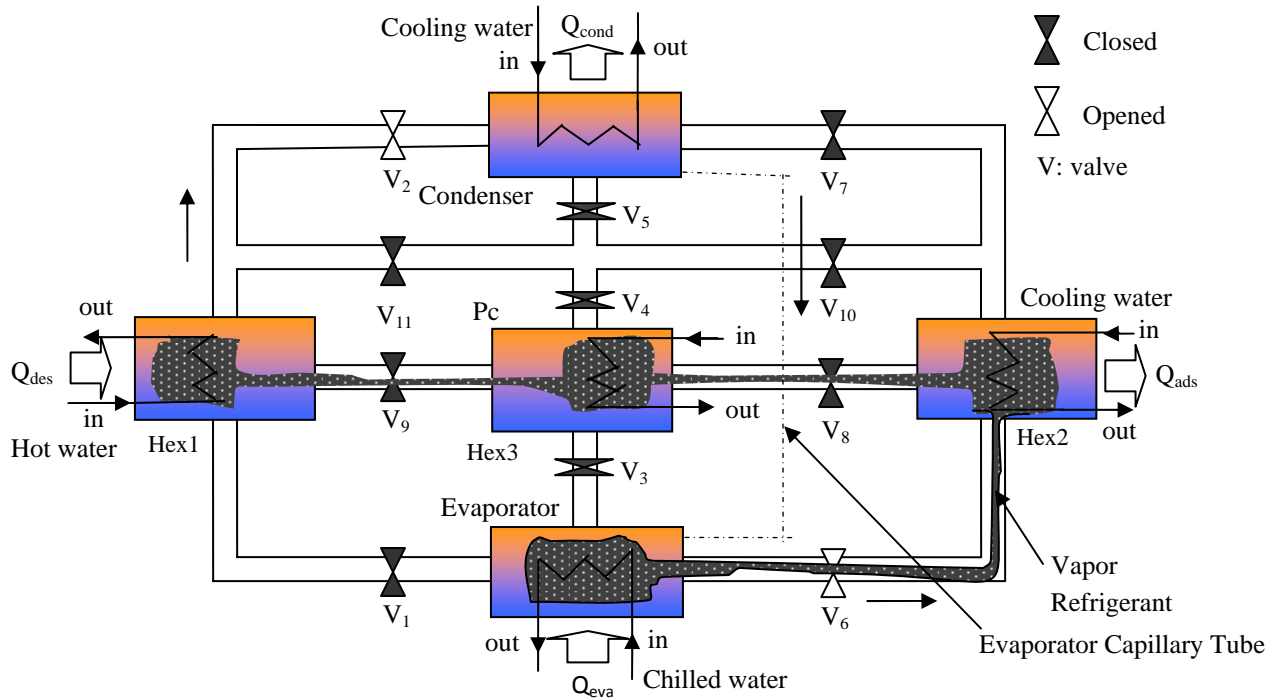


Fig2.1: Schematic of three bed chiller with mass recovery (Mode-B)

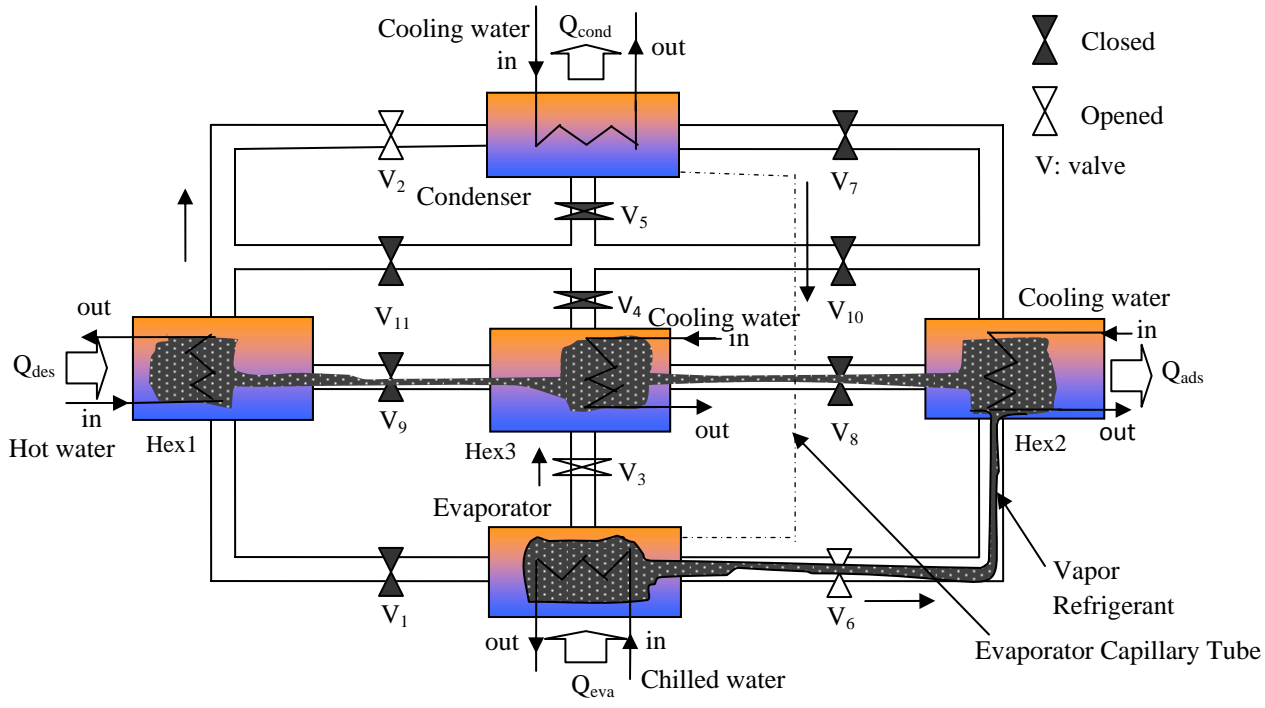


Fig2.1: Schematic of three bed chiller with mass recovery (Mode-C)

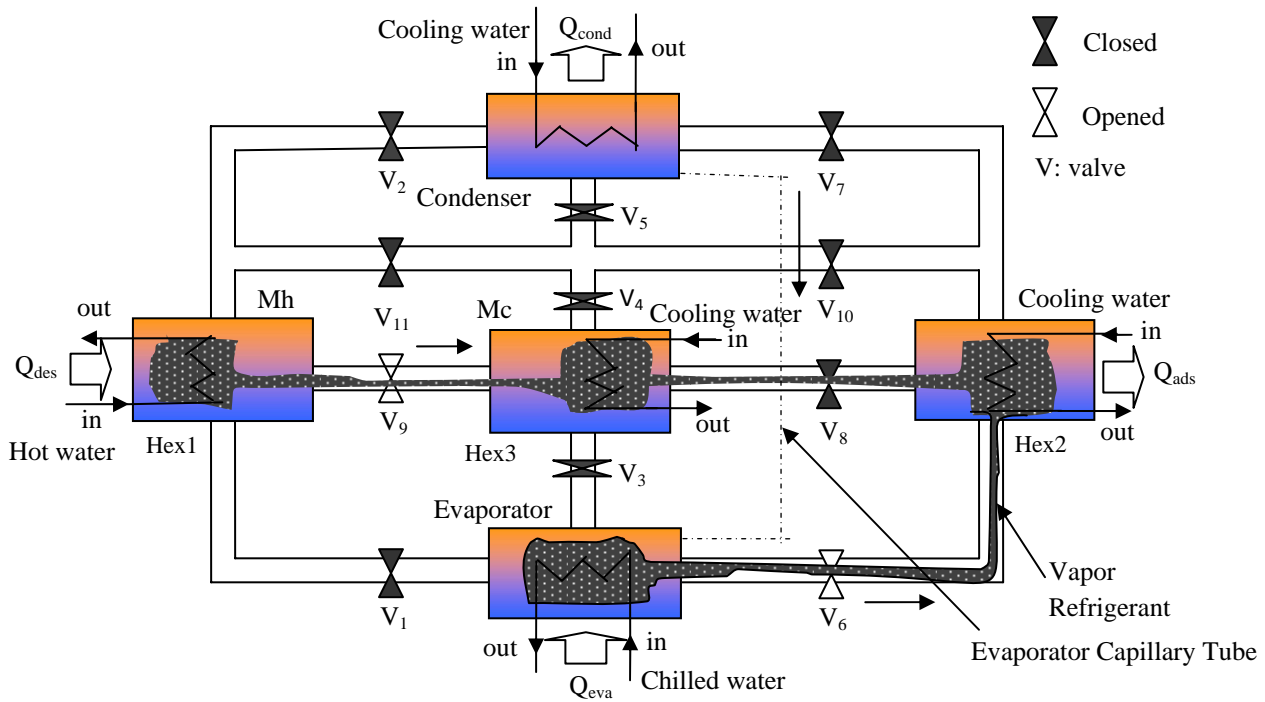


Fig2.1: Schematic of three bed chiller with mass recovery (Mode-D)

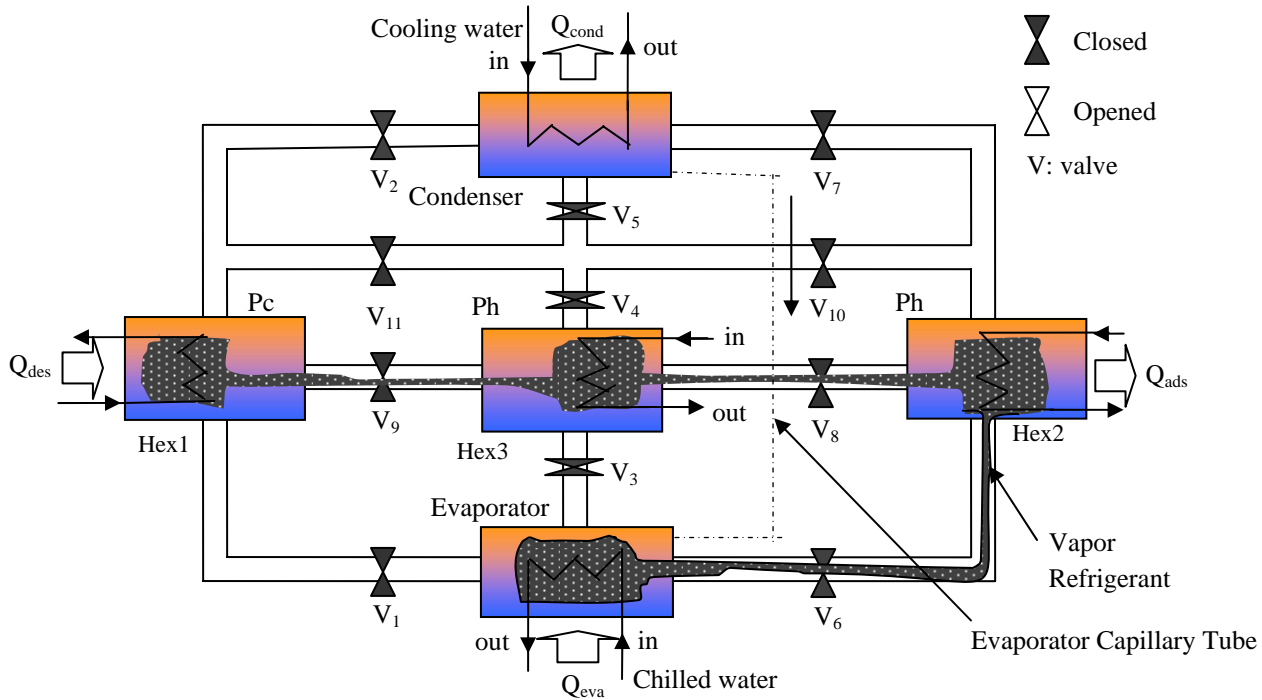


Fig2.1: Schematic of three bed chiller with mass recovery (Mode-E)

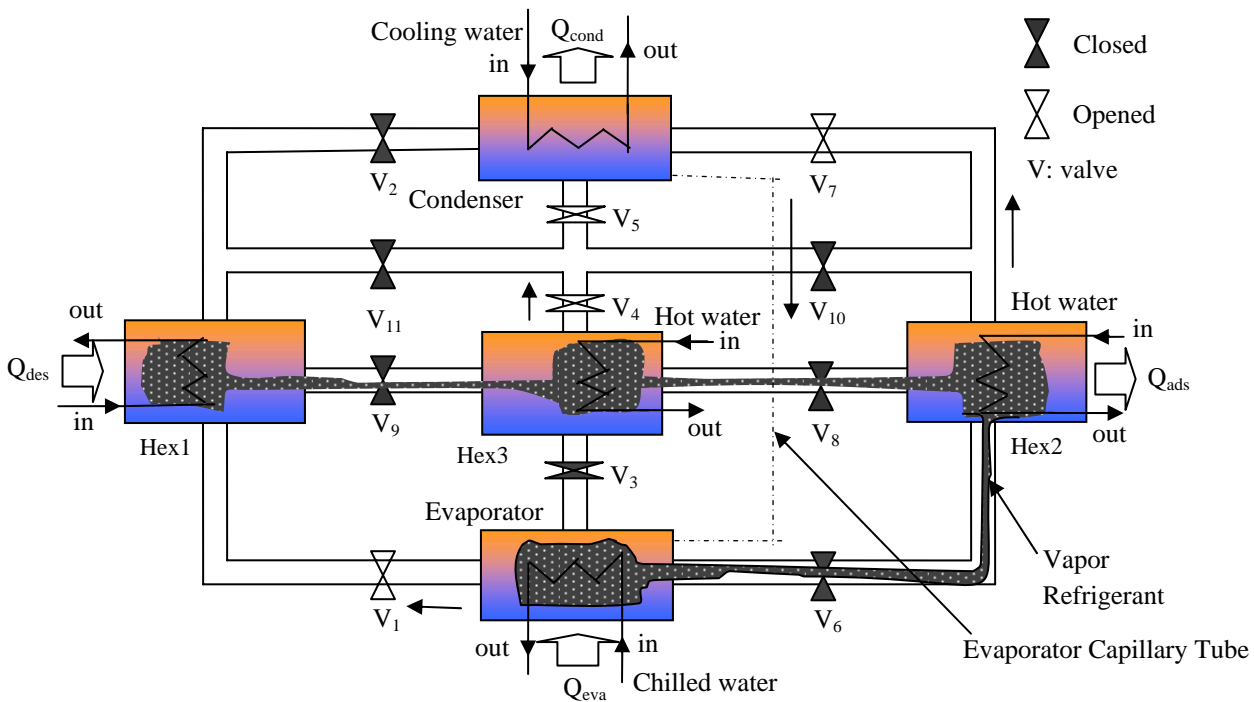


Fig2.1: Schematic of three bed chiller with mass recovery (Mode-F)

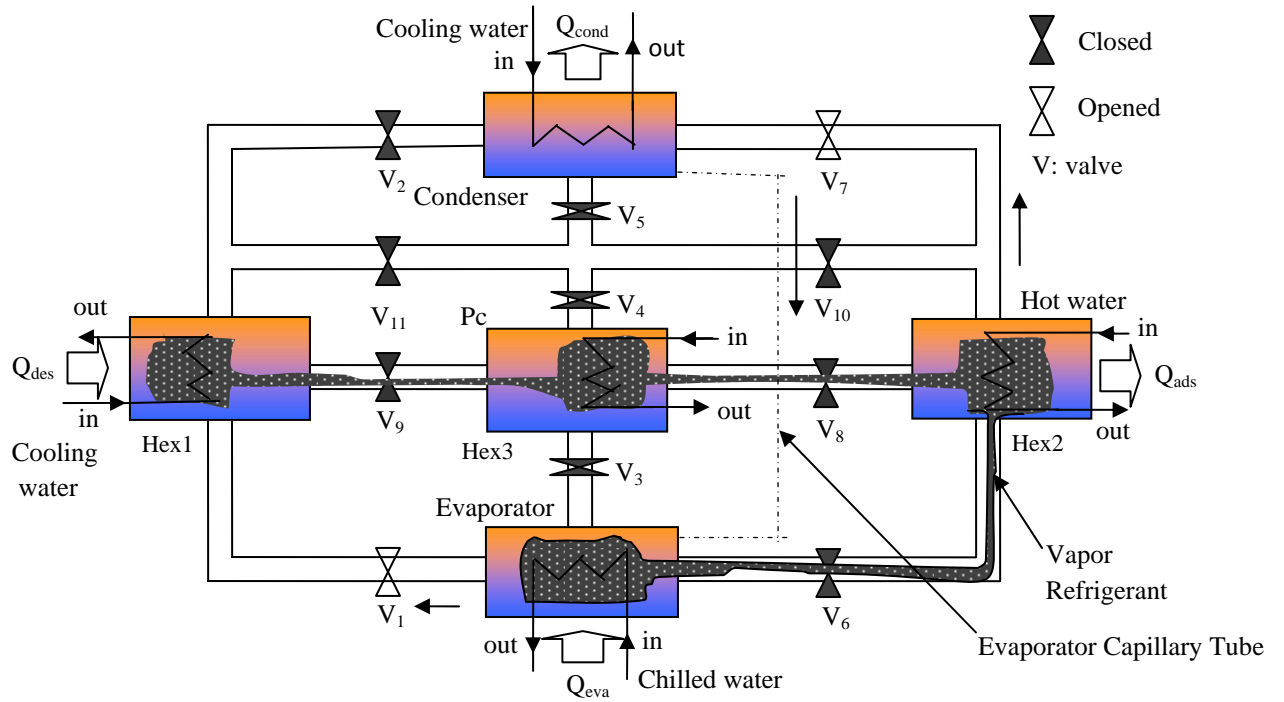


Fig2.1: Schematic of three bed chiller with mass recovery (Mode-G)

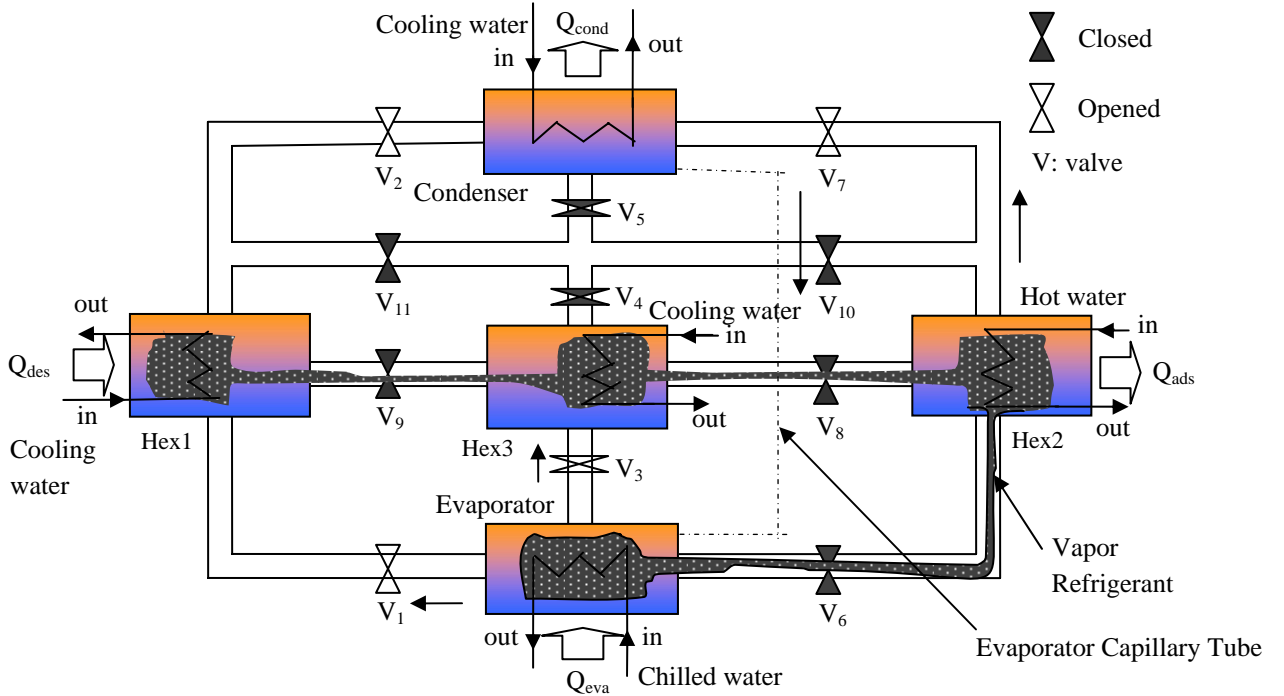


Fig2.1: Schematic of three bed chiller with mass recovery (Mode-H)

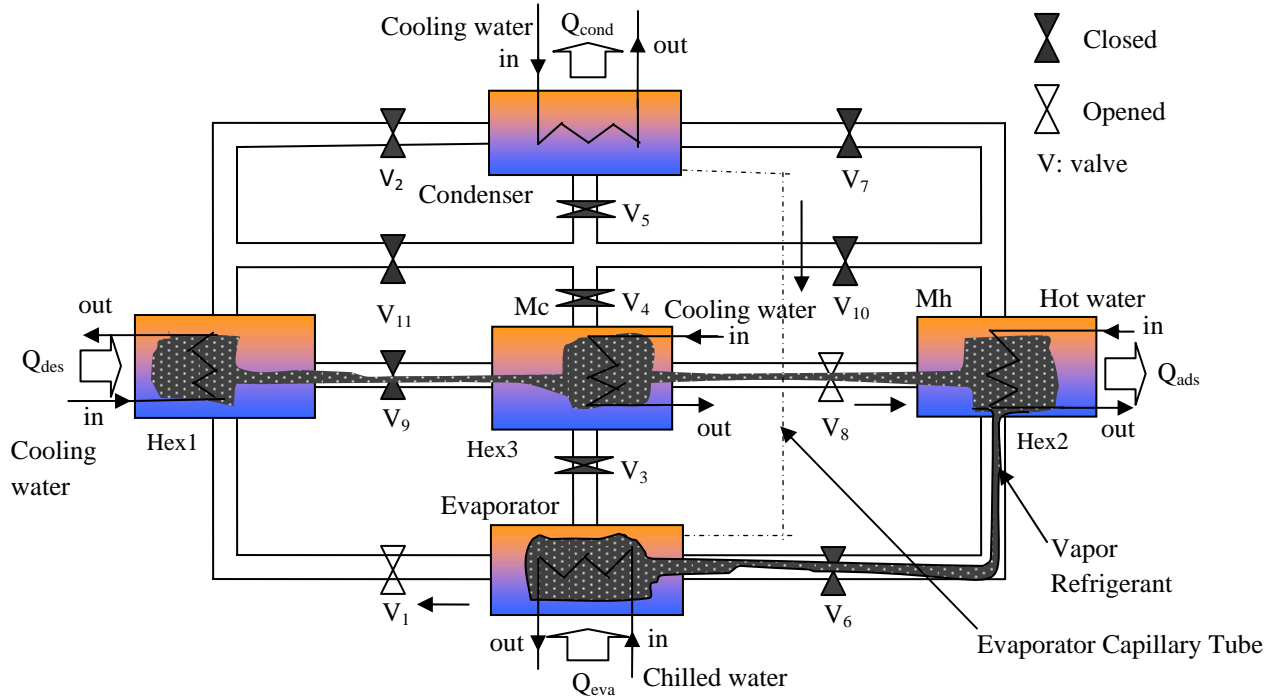


Fig2.1: Schematic of three bed chiller with mass recovery (Mode-I)

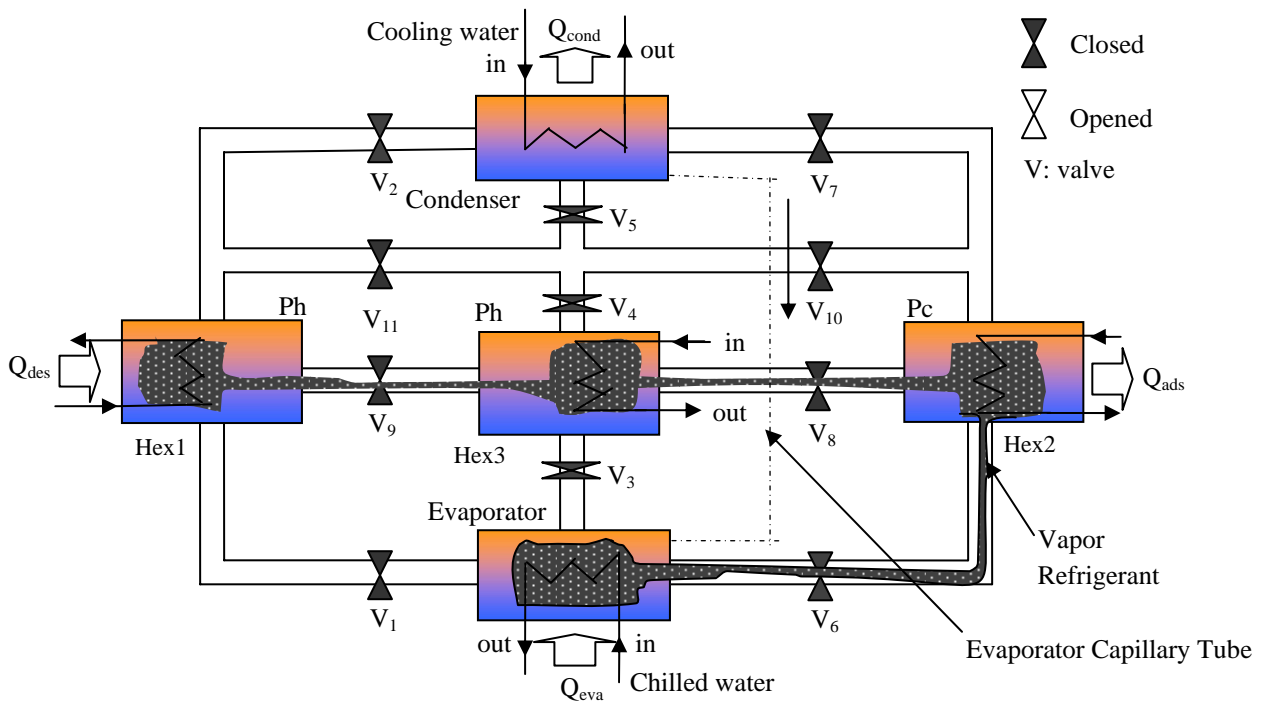


Fig2.1: Schematic of three bed chiller with mass recovery (Mode-J)



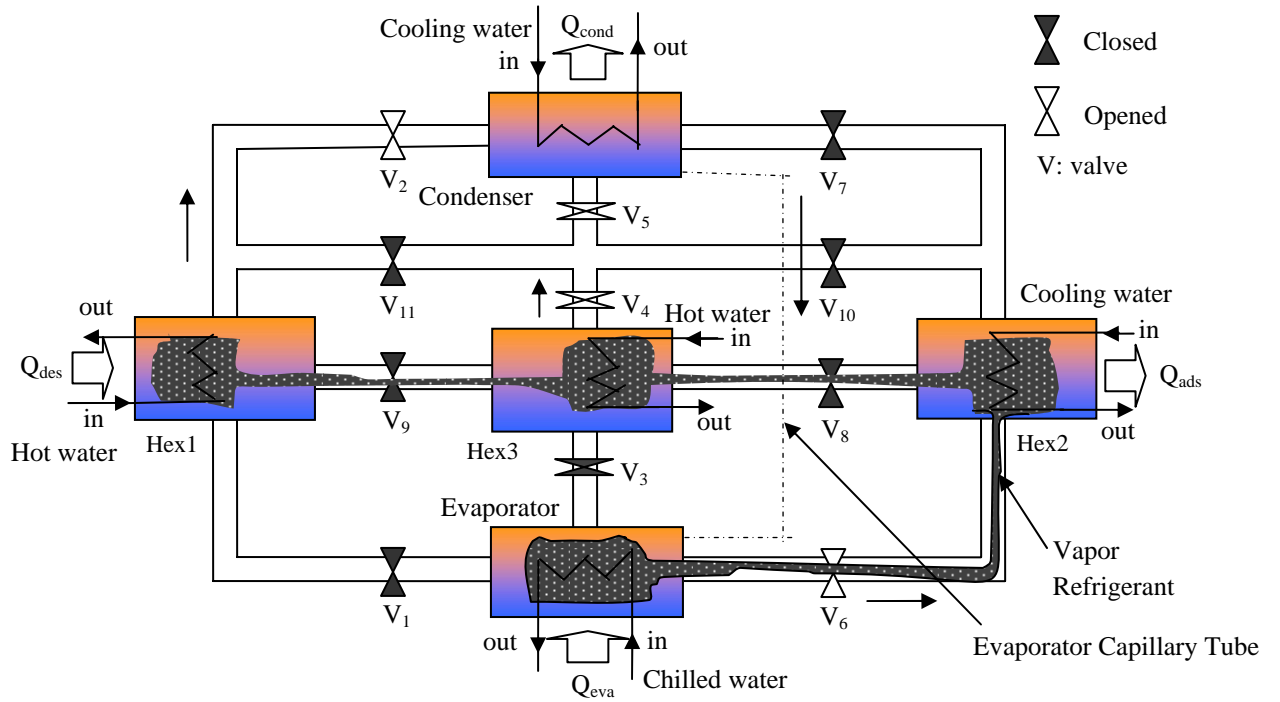


Fig2.1: Schematic of three bed chiller with mass recovery (Mode-K)

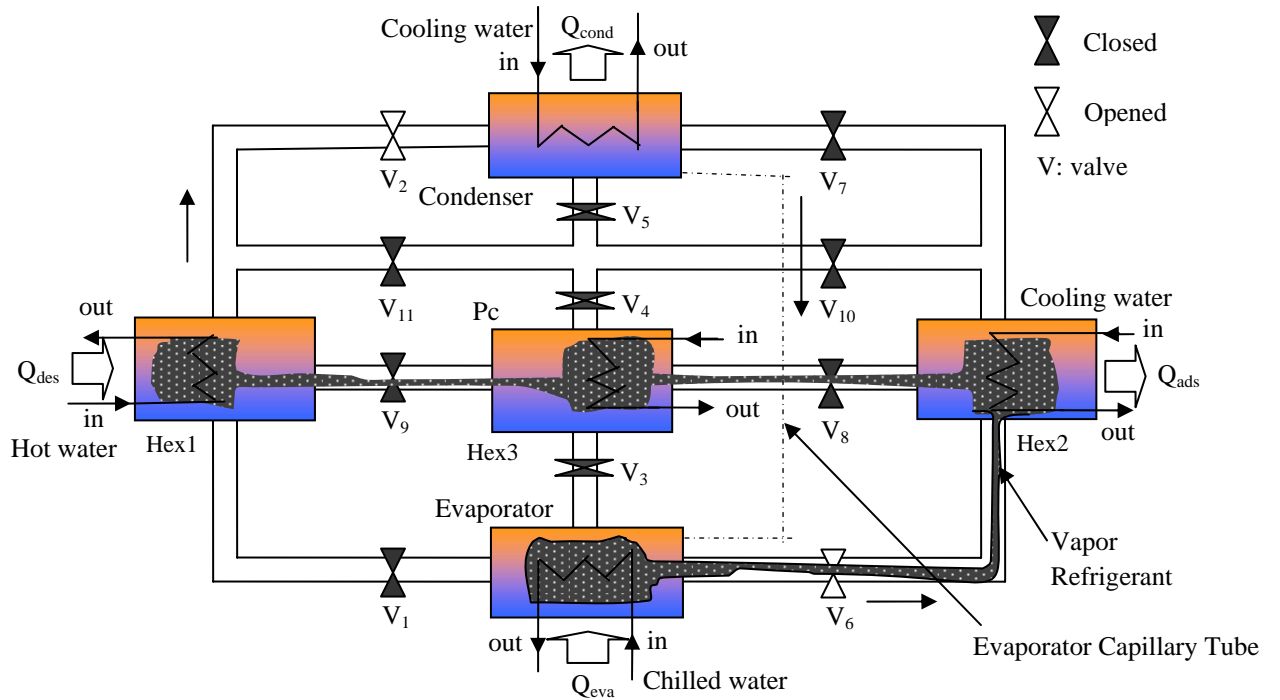


Fig2.1: Schematic of three bed chiller with mass recovery (Mode-L)

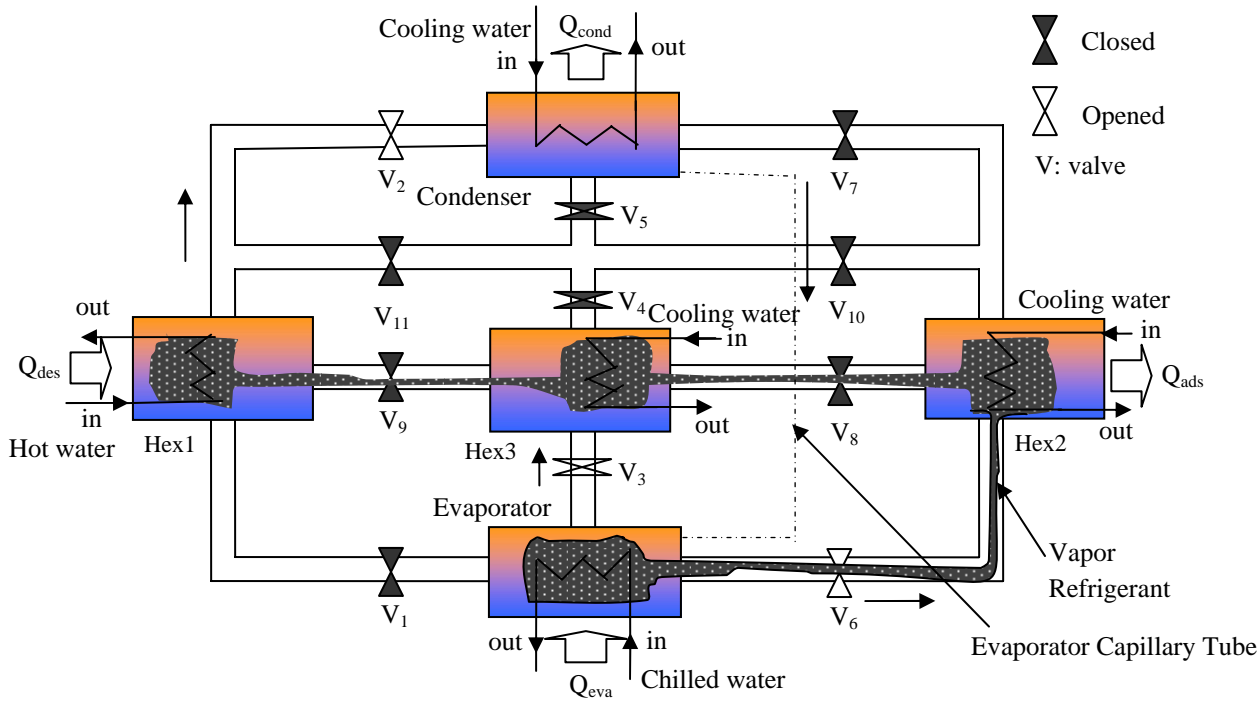


Fig2.1: Schematic of three bed chiller with mass recovery (Mode-M)

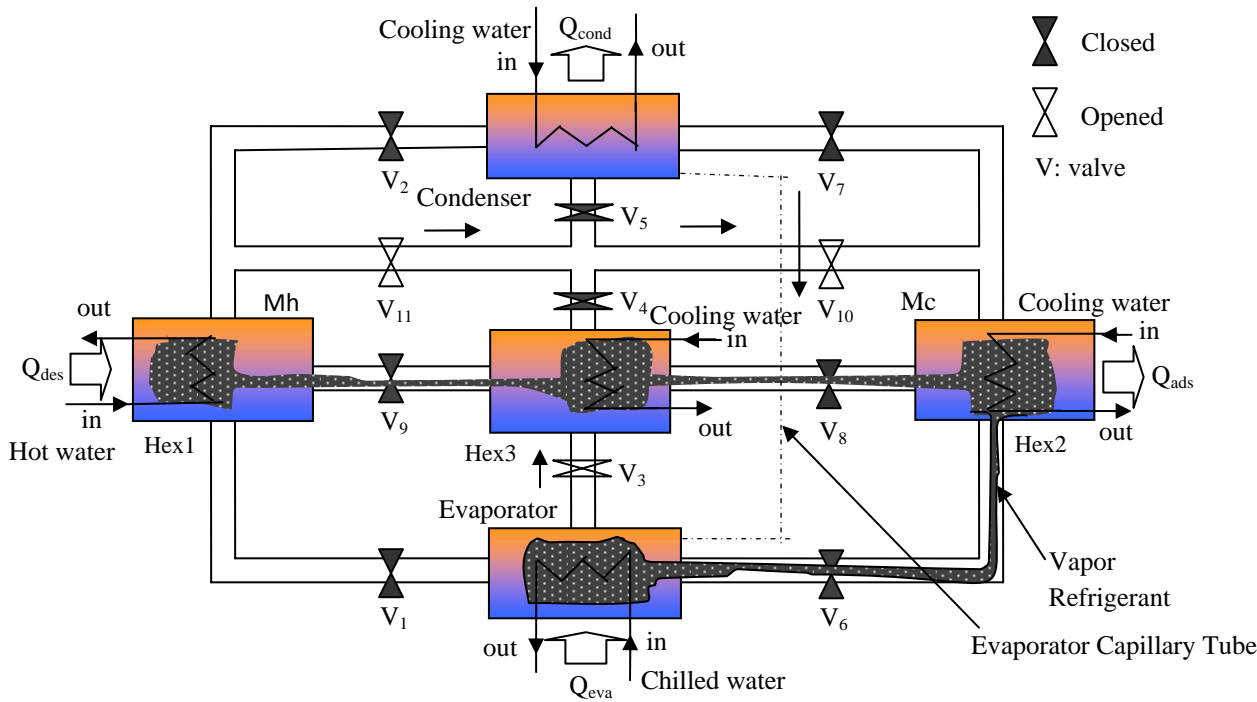


Fig2.1: Schematic of three bed chiller with mass recovery (Mode-N)

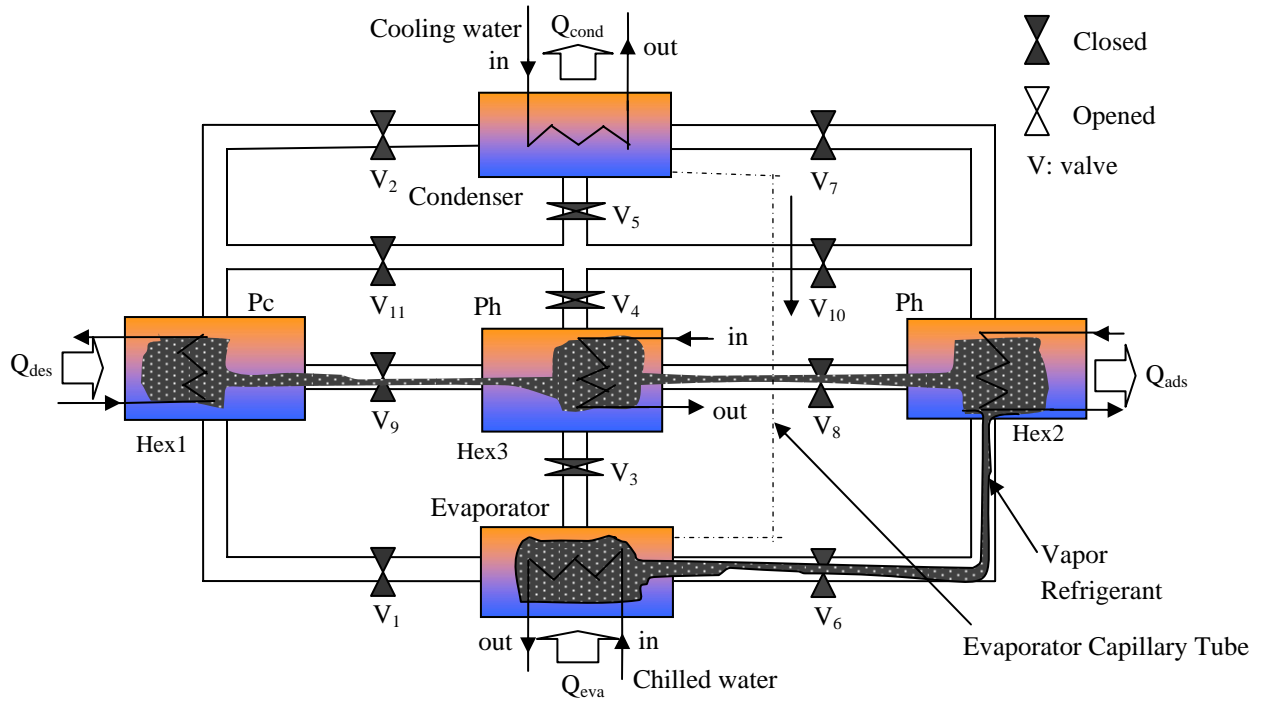


Fig2.1: Schematic of three bed chiller with mass recovery (Mode-O)

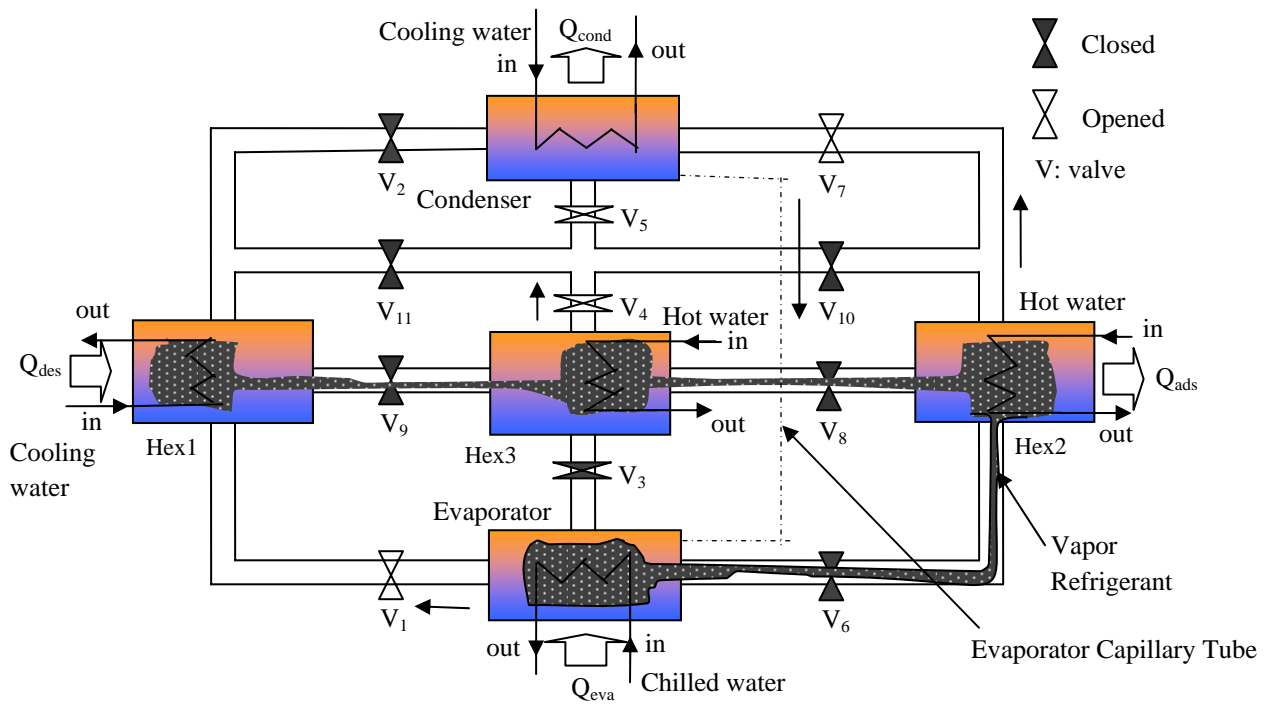


Fig2.1: Schematic of three bed chiller with mass recovery (Mode-P)

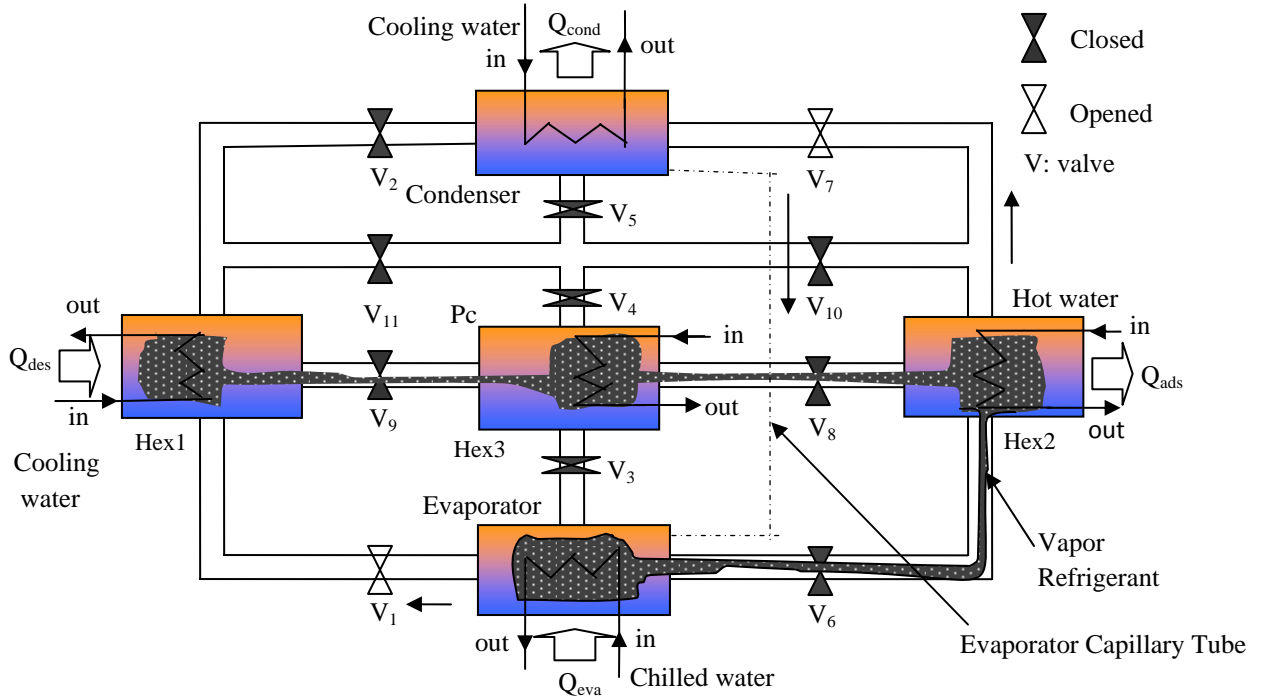


Fig2.1: Schematic of three bed chiller with mass recovery (Mode-Q)

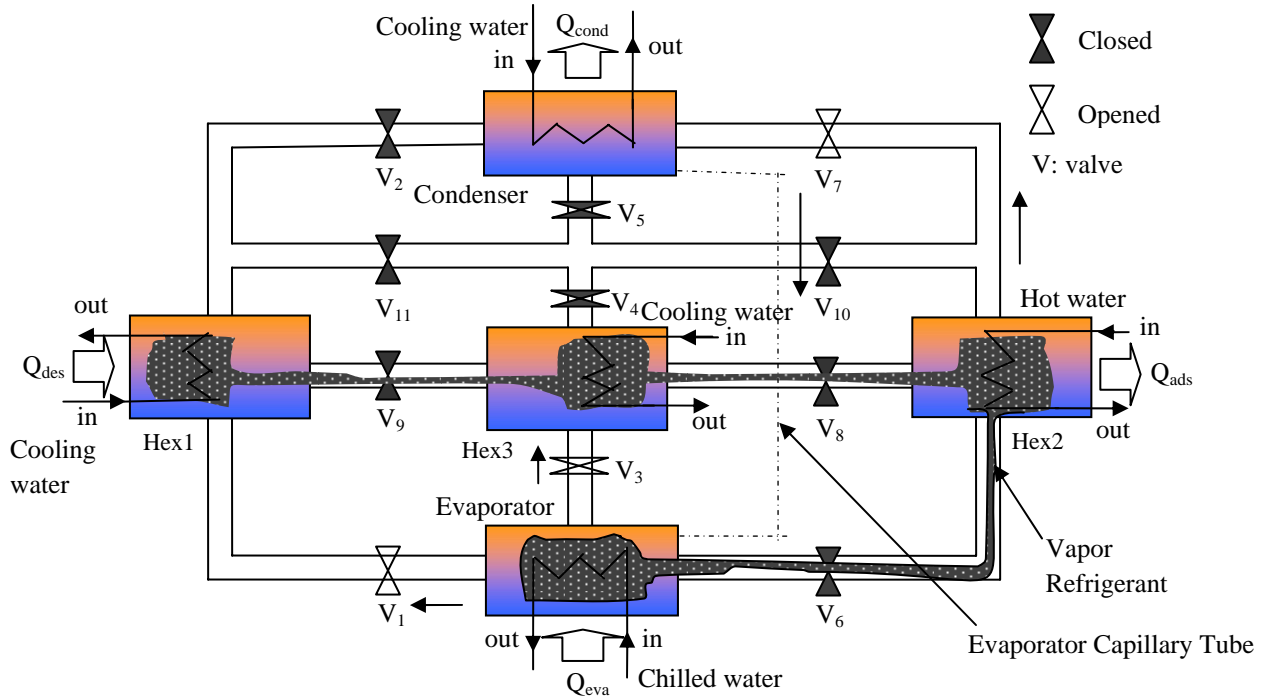


Fig2.1: Schematic of three bed chiller with mass recovery (Mode-R)

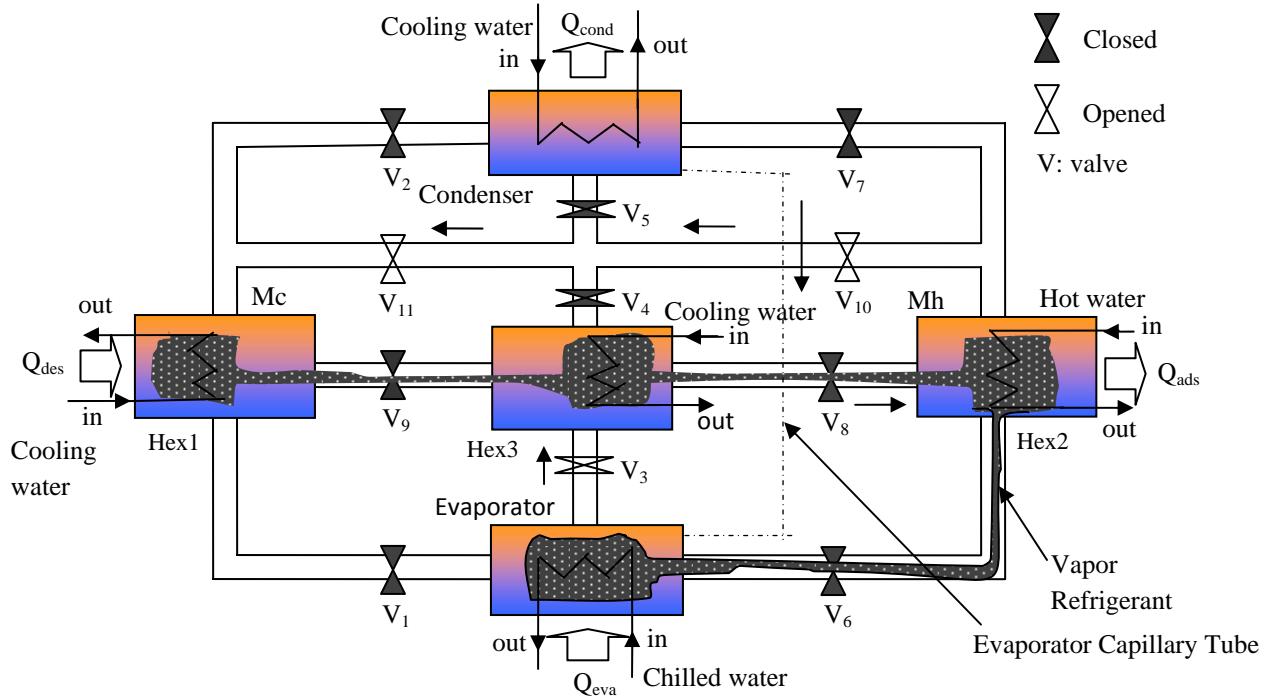


Fig2.1: Schematic of three bed chiller with mass recovery (Mode-S)

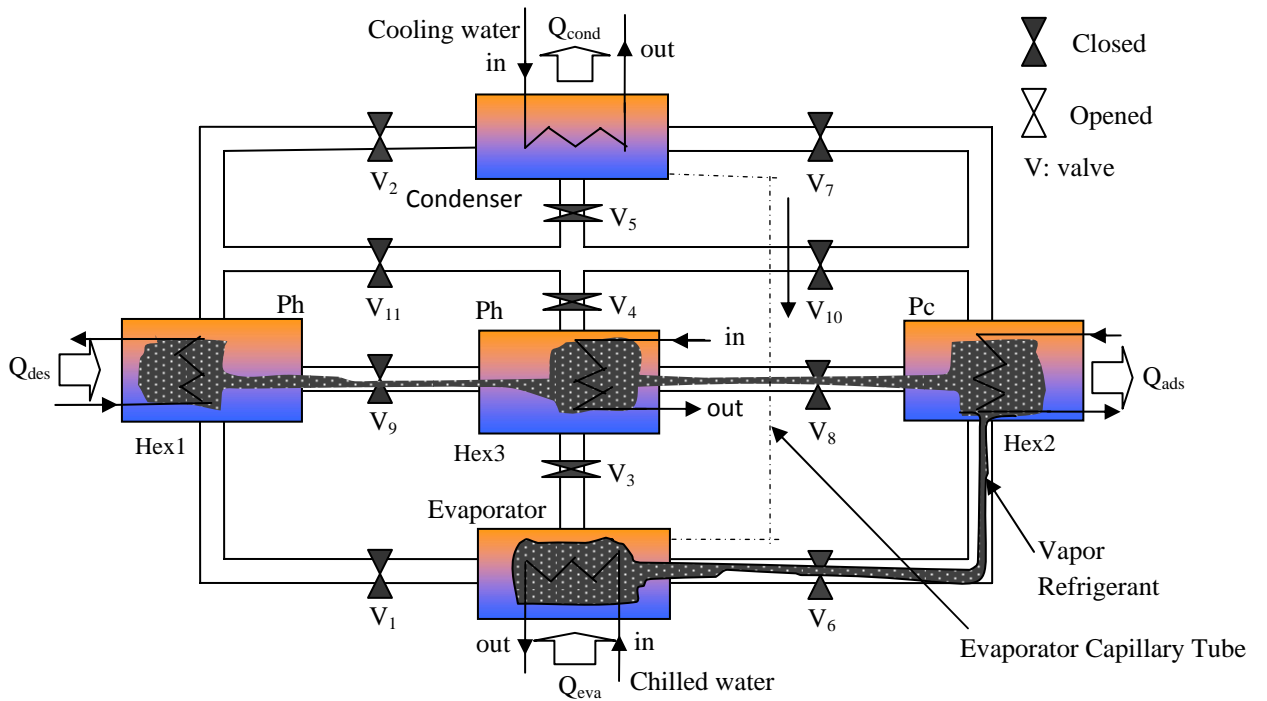


Fig2.1: Schematic of three bed chiller with mass recovery (Mode-T)

In mode A, Hex1 and Hex3 work as desorber. The desorption-condensation process takes place at condenser pressure ( $P_{\text{cond}}$ ). The desorber (Hex1, Hex3) is heated up to temperature ( $T_{\text{des}}$ ) by heat input  $Q_{\text{des}}$ , provided by the driving heat sources. The resulting refrigerant is cooled down by temperature ( $T_{\text{cond}}$ ) in the condenser by the cooling water, which removes condensation heat,  $Q_{\text{cond}}$ . Hex2 works as adsorber in mode A. In the adsorption-evaporation process, refrigerant (water) in evaporator is evaporated at evaporation temperature,  $T_{\text{eva}}$ , and seized heat,  $Q_{\text{eva}}$  from chilled water. The evaporated vapor is adsorbed by adsorbent (silica gel), at which cooling water removes the adsorption heat,  $Q_{\text{ads}}$ .

Mode B is the pre-cooling process for Hex3. In pre-cooling process, Hex3 is isolated from evaporator, condensed or any other beds. Cooling water is supplied to the bed for short time (30s) in this period. Hex1 works as desorber and Hex2 works as adsorber in mode B also.

Mode C is the adsorption process for Hex3, Hex2 and desorption process for Hex1.

In mode D, Hex3 (at the end position of adsorption-evaporation process) and Hex1 (at the end position of desorption-condensation process) are connected with each other continuing cooling water and hot water, respectively that can be classified as two-bed mass recovery process. This time Hex3 is isolated from evaporated and Hex1 is isolated from condensed. Here mass recovery occurs only bed to bed. In this mode Hex2 works as adsorber. When the concentration levels of both beds Hex1 and Hex3 reach in nearly equilibrium levels, then warm up process will start, called mode E (pre-heating or pre-cooling).

In mode E, Hex2 and Hex3 are heated up by hot water, and Hex1 is cooled down by cooling water. When the pressure of Hex2 and Hex3 are nearly equal to the pressure of condenser then Hex2 and Hex3 are connected to condenser. When the pressure of Hex1 is nearly equal to the pressure of evaporator then Hex1 is connected to evaporator.

In mode F, Hex2 and Hex3 work as desorber and Hex1 works as adsorber.

Mode G is the pre-cooling process for Hex3. In this mode, Hex2 works as desorber and Hex1 works as adsorber.

Mode H is the adsorption-evaporation process for Hex1 and Hex3. Hex2 works as desorber in this mode.

In mode I, Hex3 (at the end position of adsorption-evaporation process) and Hex2 (at the end position of desorption-condensation process) are connected with each other continuing cooling water and hot water, respectively that can be classified as two-bed mass recovery process. When the concentration levels of both beds Hex3 and Hex2 reach in nearly equilibrium levels, then warm up process will start, called mode J (pre-heating or pre-cooling). Hex1 works as adsorber in this mode.

Mode J is the pre-heating/pre-cooling process for all bed. In this period, Hex1 and Hex3 are heated up by hot water; Hex2 is cooled down by cooling water.

Modes K, L and M are same as modes A, B and C respectively. In mode K, L and M Hex1 and Hex3 work as desorber and Hex2 works as adsorber.

The mode N is same as mode D. In these modes, Hex2 (at the end position of adsorption-evaporation process) and Hex1 (at the end position of desorption-condensation process) are connected with each other continuing cooling water and hot water respectively. In this mode Hex3 works as adsorber. When the concentration levels of both beds Hex1 and Hex2 reach in nearly equilibrium levels, then warm up process will start, called mode O (pre-heating or pre-cooling). The mode O is same as mode E.

Modes P, Q and R are same as modes F, G and H respectively. In mode P, Q and R, Hex2 and Hex3 work as desorber and Hex1 works as adsorber.

The mode S is same as mode I. In mode S, Hex1 (at the end position of adsorption-evaporation process) and Hex2 (at the end position of desorption-condensation process) are connected with each other continuing cooling water and hot water, respectively that can be classified as two-bed mass recovery process. When the concentration levels of both beds Hex1 and Hex2 reach in nearly equilibrium levels, then warm up process will start, called mode T (pre-heating or pre-cooling). Hex3 works as adsorber in this mode.

Mode T is the pre-heating/pre-cooling process for all bed. In this period, Hex1 and Hex3 are heated up by hot water; Hex2 is cooled down by cooling water. Mode T is the last process for all beds, after this mode, all beds will return to its initial position (Mode A). That's why to complete one cycle, it needs 20 modes.

## 2.3 Mathematical Formulation

### 2.3.1 Energy balance for the adsorber/desorber

Adsorption and desorption heat balances are described by identical equations, where heat transfer fluid (water) temperature term  $T_{in}$  and  $T_{out}$  denotes cooling water upon adsorption and hot water upon desorption.  $T_{hex}$  denotes reactor bed temperature. The adsorbent bed temperature, pressure and concentration are assumed to be uniform throughout the adsorbent bed. The heat transfer and energy balance equations for the adsorbent bed can be described as follows

$$T_{w, out} = T_{hex} + (T_{w, in} - T_{hex}) \exp\left(-\frac{U_{hex} A_{hex}}{\dot{m}_w C_{pw}}\right) \quad (2.1)$$

$$\begin{aligned} \frac{d}{dt} \{ (W_s (C_{ps} + C_{pw} q) + W_{khex} C_{pcu} + W_{fhex} C_{pAl}) T_{hex} \} = W_s Q_{st} \frac{dq}{dt} \\ - \delta W_s C_{pw} \{ \gamma (T_{hex} - T_{eva}) + (1 - \gamma) (T_{hex} - T_{wv}) \} \frac{dq}{dt} + \dot{m}_w C_{pw} (T_{w, in} - T_{w, out}) \end{aligned} \quad (2.2)$$

where,  $\delta$  is either 0 or 1 depending whether the adsorbent bed is working as desorber or adsorber and  $\gamma$  is either 1 or 0 depending on whether the bed is connected with evaporator or another bed.

Equation (2.1) expresses the importance of heat transfer parameters, namely heat transfer area  $A_{hex}$  and heat transfer coefficient  $U_{hex}$ . The left hand side of the adsorber/desorber energy balance equation (2.2) provides the amount of sensible heat required to cool or heat the silica-gel(s), the water (w) contents in bed as well as metallic (hex) parts of the heat exchanger during adsorption or desorption. This term accounts for the input/output of sensible heat required by the batched-cycle operation. The first term on the right hand



side of equation (2.2) represents the release of adsorption heat or the input of desorption heat, while the second and third terms represent for the sensible heat of the adsorbed vapor. The last term on the right hand side of equation (2.2) indicates the total amount of heat released to the cooling water upon adsorption or provided by the hot water for desorption. Equation (2.2) does not account for external heat losses to the environment as all the beds are well insulated.

### 2.3.2 Energy balance for the evaporator

In the present analysis, it is assumed that the tube bank surface is able to hold a certain maximum amount of condensate and the condensate would flow into the evaporator easily. The heat transfer and energy balance equations for evaporator can be expressed as

$$T_{chill, out} = T_{eva} + (T_{chill, in} - T_{eva}) \exp\left(-\frac{U_{eva} A_{eva}}{\dot{m}_{chill} C_{p, chill}}\right) \quad (2.3)$$

$$\begin{aligned} \frac{d}{dt} \{(W_{eva, w} C_{pw} + W_{eva} C_{p, eva}) T_{eva}\} = & -L W_s \frac{dq_{ads}}{dt} - W_s C_{pw} (T_{cond} - T_{eva}) \frac{dq_{des}}{dt} \\ & + \dot{m}_{chill} C_{p, chill} (T_{chill, in} - T_{chill, out}) \end{aligned} \quad (2.4)$$

where the suffixes chill and eva indicate chilled water and evaporator respectively. The left hand side of equation (2.4) represents the sensible heat required by the liquid refrigerant (w) and the metal of heat exchanger tubes in the evaporator. On the right hand side, the first term gives the latent heat of evaporation (L) for the amount of refrigerant adsorbed ( $dq_{ads}/dt$ ), the second term shows the sensible heat required to cool down the incoming condensate from the condensation temperature  $T_{cond}$  to vaporization temperature  $T_{eva}$ , and the last term represents the total amount of heat given away by the chilled water.

### 2.3.3 Energy balance for the condenser

The heat transfer and energy balance equations for condenser can be expressed as

$$T_{cond, out} = T_{cond} + (T_{cw, in} - T_{cond}) \exp\left(-\frac{U_{cond} A_{cond}}{\dot{m}_{cw} C_{pw}}\right) \quad (2.5)$$

$$\begin{aligned} \frac{d}{dt} \left\{ (W_{cw, w} C_{pw} + W_{cond, hex} C_{p, cond}) T_{cond} \right\} = & -L W_s \frac{dq_{des}}{dt} - W_s C_{p, w} (T_{des} - T_{cond}) \frac{dq_{des}}{dt} \\ & + \dot{m}_{cw} C_{pw} (T_{cw, in} - T_{cw, out}) \end{aligned} \quad (2.6)$$

where the subscripts *cw* and *cond* indicate cooling water and condenser, respectively. The left hand side of equation (2.6) represents the sensible heat required by the metallic parts of heat exchanger tubes due to the temperature variations in the condenser. On the right hand side, the first term gives the latent heat of vaporization (*L*) for the amount of refrigerant desorbed ( $dq_{des}/dt$ ), the second term shows the amount of sensible heat requirement to cool down the incoming vapor from the desorber at temperature  $T_{des}$  to condenser at temperature  $T_{conds}$  and the last term represents the total amount of heat released to the cooling water.

### 2.3.4 Mass balance

Mass and heat balances are based on the assumption that both the temperature and the amount of refrigerant adsorbed are uniform in the adsorbent beds. Since the temperature in an adsorption cycle are unsteady state, the energy balance equations (2.2, 2.4, 2.6) must account for sensible heat input and/ or output during cycle period. The mass balance for the refrigerant can be expressed by neglecting the gas phase as

$$\frac{dW_{eva, w}}{dt} = -W_s \left( \frac{dq_{des- cond}}{dt} + \frac{dq_{eva- ads}}{dt} \right) \quad (2.7)$$

where, subscripts *des-cond* and *eva-ads* stand for the vapor flow from desorber to condenser and evaporator to adsorber, respectively.

### 2.3.5 Absorption rate

The absorption rate is expressed as

$$\frac{dq}{dt} = k_s a_p \times (q^* - q) \quad (2.8)$$

where, the overall mass transfer coefficient for absorption is given by

$$k_s a_p = (15D_s)/(R_p)^2 \quad (2.9)$$

The absorption rate is considered to be controlled by surface diffusion inside a gel particle and surface diffusivity is expressed by Sakoda and Suzuki [35] as a function of temperature by

$$D_s = D_{so} \times \exp[-(E_a)/(RT)] \quad (2.10)$$

and  $q^*$  is the amount absorbed in equilibrium with pressure  $P_s(T_w)$  and is derived from the manufacturer property data by the following equation

$$q^* = \frac{0.8 \times [P_s(T_w)/P_s(T_s)]}{1 + 0.5 \times [P_s(T_w)/P_s(T_s)]} , \quad (2.11)$$

where  $P_s(T_w)$  and  $P_s(T_s)$  are the saturation vapor pressure at temperature  $T_w$  (water vapor) and  $T_s$  (silica gel), respectively. The saturation vapor pressure and temperature are correlated by Antoine's equation, which can be written as

$$P_s = 133.32 \times \exp\left(18.3 - \frac{3820}{T - 46.1}\right) \quad (2.12)$$

### 2.3.6 Measurement of the system performance

The performance of a three-bed adsorption chiller with mass recovery is mainly characterized by cooling capacity (CC), coefficient of performance (COP), waste heat recovery efficiency ( $\eta$ ) and can be measured by the following equations

$$\text{Cooling Capacity (CC)} = \frac{\dot{m}_{chill} C_w \int_0^{t_{cycle}} (T_{chill,in} - T_{chill,out}) dt}{t_{cycle}},$$

$$\text{Coefficient of performance (COP)} = \frac{\dot{m}_{chill} C_w \int_0^{t_{cycle}} (T_{chill,in} - T_{chill,out}) dt}{\dot{m}_{hot} C_w \int_0^{t_{cycle}} (T_{hot,in} - T_{hot,out}) dt},$$

$$\text{and the waste heat recovery efficiency } (\eta) = \frac{\dot{m}_{chill} C_w \int_0^{t_{cycle}} (T_{chill,in} - T_{chill,out}) dt}{\dot{m}_w C_w \int_0^{t_{cycle}} (T_{hot,in} - T_{cool,in}) dt}$$

The base line parameter values (Khan et al. [3]) and standard operating conditions adapted in simulation are presented in Table 2.2 and Table 2.3, respectively.

Table 2.2 Baseline parameters

Values Adopted in Simulation		
Symbol	Value	Unit
$A_{hex}$	1.45	$m^2$
$A_{eva}$	0.665	$m^2$
$A_{con}$	0.998	$m^2$
$C_{ps}$	924	J/kg.K
$C_{pw}$	4.18E+3	J/kg.K
$C_{p,chill}$	4.20E+3	J/kg.K
$D_{so}$	2.54E-4	$m^2/s$
$E_a$	2.33E+3	J/kg
$L$	2.50E+6	J/kg
$Q_{st}$	2.80E+6	J/kg
$R$	4.62E+2	J/kg.K

$R_p$	0.35E-3	m
$U_{ads}$	1380	$W/m^2 \cdot K$
$U_{des}$	1540	$W/m^2 \cdot K$
$U_{eva}$	3550	$W/m^2 \cdot K$
$U_{cond}$	4070	$W/m^2 \cdot K$
$W_s$	14	kg
$W_{cw}$	5	kg
$C_{p,cu}$	386	J/kg.K
$C_{p,Al}$	905	J/kg.K
$W_{khex}$	12.67	kg
$W_{fhex}$	5.33	kg
$W_{eva,w}$	25	kg

Table 2.3 Standard operating condition

	Temperature [°C]	Flow rate (kg/s)
Hot water	50 ~ 65	0.4
Cooling water	30	0.74[=0.4(ads)+0.34(cond)]
Chilled water	14	0.11
Cycle Time	2400s=(1100 ads/ des+40 mr+30ph+30pc) s×2	

Ads/des = adsorption/desorption, mr = mass recovery, ph/pc = pre-heat/pre-cool

## 2.4. Solution procedure (Finite difference technique)

In the present analysis, a cycle simulation computer program is developed to predict the performance of the three-bed chiller with mass recovery. The systems of differential equations (2.1) – (2.12) are solved by finite difference approximation with a time step 1

sec. The results taken in the study are from the cyclic steady state conditions. A real chiller starts its operation with unbalanced conditions, however, after a few cycles (typically 2-3 cycles) it reaches its cyclical steady state condition. Therefore, an iteration processes has been employed in solution procedure to fix all the initial values for the cyclic steady state conditions. In the beginning of the solution process, the initial values are assumed and finally those are adjusted for the cyclic steady conditions by the iteration process. When two beds are connected with evaporator or condenser, the vapor pressure is unknown that are calculated through the Antonie's equation as the vapor temperature is calculated from the energy balance equation of evaporator or condenser.

It is however, difficult to calculate the saturated vapor pressure when two-beds are connected with each other, which are essential for the calculation of adsorption/desorption rate inside the adsorbent beds. In this state, vapor pressure is assumed initially and the amounts of vapor adsorbed/desorbed by the beds are calculated.

Conceptually, the desorbed vapor from one reactor bed (Hex1) should be equal to the amount of adsorbed vapor by the other reactor bed (Hex3). If these amounts are not equal then vapor pressure are adjusted for next iteration. Once the satisfactory convergence criterion is achieved, then process goes for the next time step. The convergence factor for all parameters of the present study will be taken as  $10^{-3}$ .

The calculations are shown here for desorber given in equations (2.1) and (2.2).

For heat transfer equation

We know that the heat equation for water as

$$Q_{water} = \dot{m} c_p (T_{wi} - T_{wo})$$

Again, we know from thermodynamics, Logarithms Mean Temperature difference

$$LMTD = \frac{(T_{wo} - T_{ad}) - (T_{wi} - T_{ad})}{\ln\left(\frac{T_{wo} - T_{ad}}{T_{wi} - T_{ad}}\right)}$$

Thus heat equation for water becomes

$$Q_{water} = LMTD * UA$$

$$or, \frac{(T_{wo} - T_{ad}) - (T_{wi} - T_{ad})}{\ln\left(\frac{T_{wo} - T_{ad}}{T_{wi} - T_{ad}}\right)} * UA = \dot{m} c_p (T_{wi} - T_{wo})$$

$$or, \frac{UA}{\ln\left(\frac{T_{wo} - T_{ad}}{T_{wi} - T_{ad}}\right)} = -\dot{m} c_p$$

$$or, \frac{1}{\ln\left(\frac{T_{wo} - T_{ad}}{T_{wi} - T_{ad}}\right)} = -\frac{\dot{m} c_p}{UA}$$

$$or, \ln\left(\frac{T_{wo} - T_{ad}}{T_{wi} - T_{ad}}\right) = -\frac{UA}{\dot{m} c_p}$$

$$or, \left(\frac{T_{wo} - T_{ad}}{T_{wi} - T_{ad}}\right) = \exp\left(-\frac{UA}{\dot{m} c_p}\right)$$

$$or, T_{wo} - T_{ad} = (T_{wi} - T_{ad}) \exp\left(-\frac{UA}{\dot{m} c_p}\right)$$

$$or, T_{wo} = T_{ad} + (T_{wi} - T_{ad}) \exp\left(-\frac{UA}{\dot{m} c_p}\right)$$

For energy balance equation

$$\frac{d}{dt} \{(w_s c_s + w_s c_s q_{des} + w_{des} c_{des}) T_{des}\} = w_s Q_{st} \frac{dq}{dt} + \dot{m} c_w (T_{in} - T_{out})$$

$$(w_s c_s + w_s c_w q + w_{des} c_{des}) \frac{dT_{des}}{dt} + w_s c_w \frac{dq_{des}}{dt} T_{des} = w_s Q_{st} \frac{dq_{des}}{dt} + \dot{m}_w c_w \left\{ T_{in} - T_{des} - (T_{in} - T_{des}) \exp \left( - \frac{UA}{\dot{m}_w c_w} \right) \right\}$$

Let,  $w_s c_s + w_s c_w q + w_{des} c_{des} = \gamma$

$$\text{or, } \gamma \frac{T_i - T_{i-1}}{\Delta t} + w_s c_s T_i \frac{q_i - q_{i-1}}{\Delta t} = w_s Q_{st} \frac{q_i - q_{i-1}}{\Delta t} + \dot{m}_w c_w \left\{ T_{in} - T_{des} - T_{in} \exp \left( - \frac{UA}{\dot{m}_w c_w} \right) + T_{des} \exp \left( - \frac{UA}{\dot{m}_w c_w} \right) \right\}$$

Let,  $NTU = \frac{UA}{\dot{m}_w c_w}$

$$\text{or, } \gamma \frac{T_i - T_{i-1}}{\Delta t} + w_s c_s T_i \frac{q_i - q_{i-1}}{\Delta t} = w_s Q_{st} \frac{q_i - q_{i-1}}{\Delta t} + \dot{m}_w c_w \{ T_{in} (1 - \exp(-NTU)) - T_{des} (1 - \exp(-NTU)) \}$$

$$\text{or, } \gamma \frac{T_i - T_{i-1}}{\Delta t} + w_s c_s T_i \frac{q_i - q_{i-1}}{\Delta t} = w_s Q_{st} \frac{q_i - q_{i-1}}{\Delta t} + \dot{m}_w c_w (1 - \exp(-NTU)) (T_{in} - T_{des})$$

$$\text{or, } \gamma (T_i - T_{i-1}) + w_s c_s T_i (q_i - q_{i-1}) = w_s Q_{st} (q_i - q_{i-1}) + \Delta t \dot{m}_w c_w (T_{in} - T_{des}) (1 - \exp(-NTU))$$

Let,  $EXPN = 1 - \exp(-NTU)$

$$\text{or, } T_i \left\{ \gamma + w_s c_w (q_i - q_{i-1}) + \Delta t \cdot \dot{m}_w c_w EXPN \right\} = \gamma T_{i-1} + w_s Q_{st} (q_i - q_{i-1}) + \Delta t \cdot \dot{m}_w c_w \cdot EXPN T_{in}$$

Let,  $EXPND = \dot{m}_w c_w EXPN$

$$\text{or, } T_i \{ \gamma + w_s c_w (q_i - q_{i-1}) + \Delta t \cdot EXPND \} = \gamma T_{i-1} + w_s Q_{st} (q_i - q_{i-1}) + \Delta t \cdot T_{in} \cdot EXPND$$

$$\text{or, } T_i = \frac{\gamma T_{i-1} + w_s Q_{st} (q_i - q_{i-1}) + \Delta t \cdot T_{in} \cdot EXPND}{\gamma + w_s c_w (q_i - q_{i-1}) + \Delta t \cdot EXPND}$$



$$\text{or, } T_i = \frac{\gamma T_{i-1} + w_s Q_{st} \Delta q + \Delta t \cdot T_{in} \cdot EXPND}{(w_s c_s + w_s c_w q_i + w_{des} c_{des}) + w_s c_w (q_i - q_{i-1}) + \Delta t \cdot EXPND} \quad [q_i - q_{i-1} = \Delta q]$$

$$\text{or, } T_i = \frac{\gamma T_{i-1} + w_s Q_{st} \Delta q + \Delta t \cdot T_{in} \cdot EXPND}{w_s c_s + w_s c_w (2q_i - q_{i-1}) + w_{des} c_{des} + \Delta t \cdot EXPND}$$

Similarly, we can discretize the energy balance equations for the evaporator and condenser.

## 2.5. Results and discussion

In order to clarify the performance of mass recovery cycle, cycle simulation runs are performed. Since our main interest is to utilize the low grade waste heat as the driving source, the investigation was conducted for hot water between 50<sup>0</sup>C and 65<sup>0</sup>C.

### 2.5.1 Effect of driving heat source temperature on CC and COP

Figures 2.2(a) and 2.2(b) show heat source temperature variation on CC and COP, respectively. It is seen that CC for three-bed mass recovery chiller increases with the increase of heat source temperature from 50<sup>0</sup>C to 65<sup>0</sup>C with a cooling water inlet temperature of 30<sup>0</sup>C. This is because the amount of refrigerant circulated increases, due to increased refrigerant desorption with higher driving source temperature. Another reason is that, in the proposed cycle, Hex1 and Hex2 connect with Hex3 one by one during mass recovery, which accelerates cooling effect. The CC is improved due to the mass recovery process. The mass recovery process generates more desorption heat and that is transferred from the desorber through desorbed vapor. So, in the low heat source temperature (50<sup>0</sup>C-65<sup>0</sup>C), proposed chiller gives better performance. The optimum COP value is 0.6214 for hot water inlet temperature at 65<sup>0</sup>C along with the coolant and chilled water inlet temperature are at 30<sup>0</sup>C and 14<sup>0</sup>C, respectively. The delivered chilled water temperature is 6<sup>0</sup>C for this operation condition.

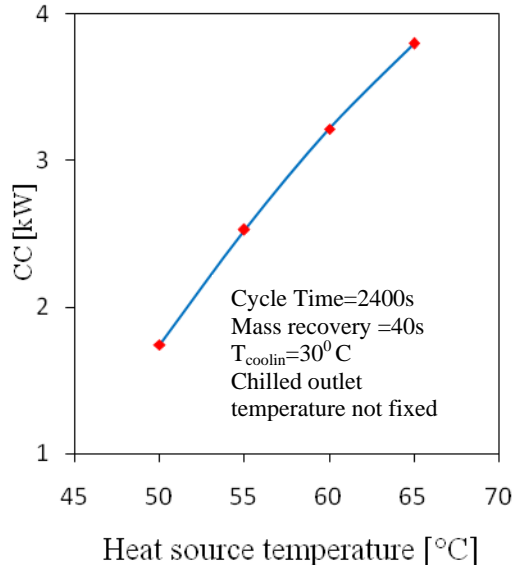


Fig 2.2(a): The effect of heat source temperature on CC

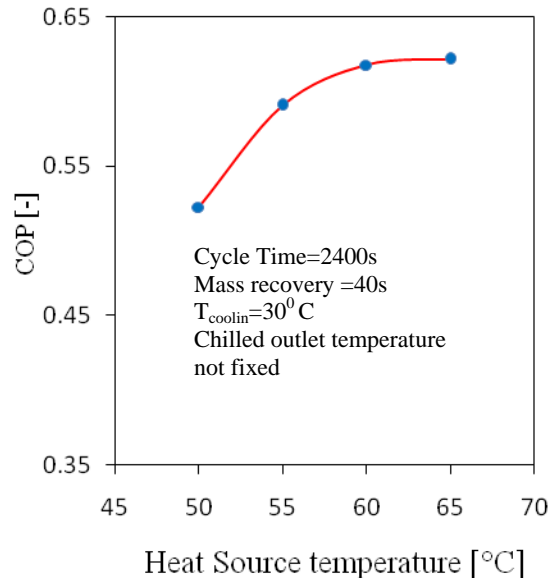


Fig 2.2(b): The effect of heat source temperature on COP

## 2.5.2 Effect of cooling source temperature on CC and COP

Figure 2.3(a) and 2.3(b) show the effect of cooling water inlet temperatures on CC and COP, respectively. In the present simulation, cooling water mass flow rate into adsorber is taken as 0.4kg/s, while for the condenser the coolant mass flow rate is taken as 0.34 kg/s. The CC increases steadily as the cooling water inlet temperature is lowered from 40°C to 20°C. This is due to the fact that lower adsorption temperatures result in larger amounts of refrigerant being adsorbed and desorbed during each cycle. The simulated COP values also increases with lower cooling water inlet temperature. For the three bed chiller the COP value reaches 0.6975 with 65°C driving source temperature in combination with a coolant inlet temperature of 20°C.

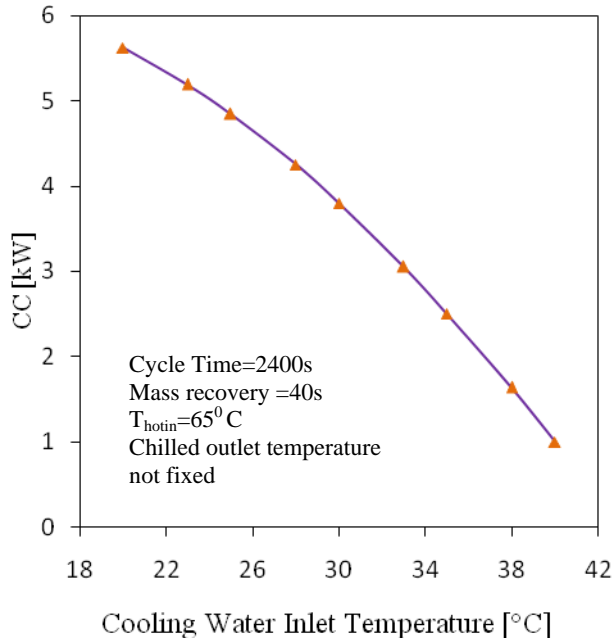


Fig 2.3(a): The effect of cooling water inlet temperature on CC

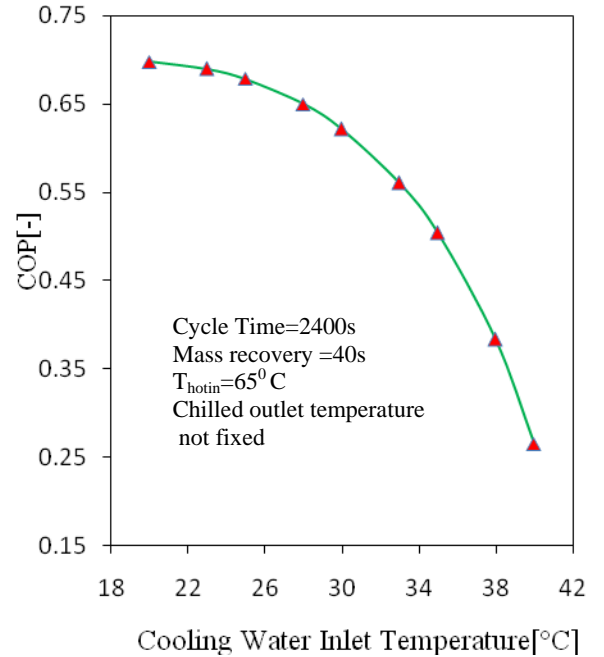


Fig 2.3(b): The effect of cooling water inlet temperature on COP

### 2.5.3 Effect of driving heat source temperature on chiller efficiency, $\eta$

Figure 2.4(a) presents the waste heat recovery efficiency,  $\eta$ , as a function of heat source temperature. For three-bed proposed cycle employing mass recovery scheme with heating/cooling,  $\eta$  rises from 0.0522 to 0.0649 as the hot water inlet temperature is increased from 50°C to 65°C with a cooling source 30°C. This is because improvement of cooling capacity of the proposed chiller in this range.

### 2.5.4 Effect of driving heat source temperature on chilled water outlet temperature

The effect of heat source temperature on average chilled water outlet temperature is depicted in Fig. 2.4(b). The chilled water temperature level needs to be considered according to demand side requirement. Mass flow rate of chilled water can control the outlet temperature of chilled water. From Fig. 2.4(b), it is seen that the cyclic average chilled water outlet temperature of the proposed cycle decreases with the increase of the driving heat source temperature. Low chilled water outlet temperature is expected from real machine.

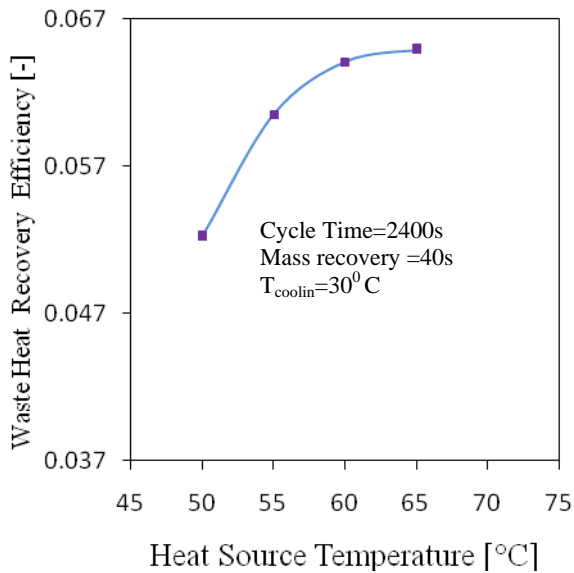


Fig 2.4(a): The effect of heat source temperature on waste heat recovery efficiency [-]

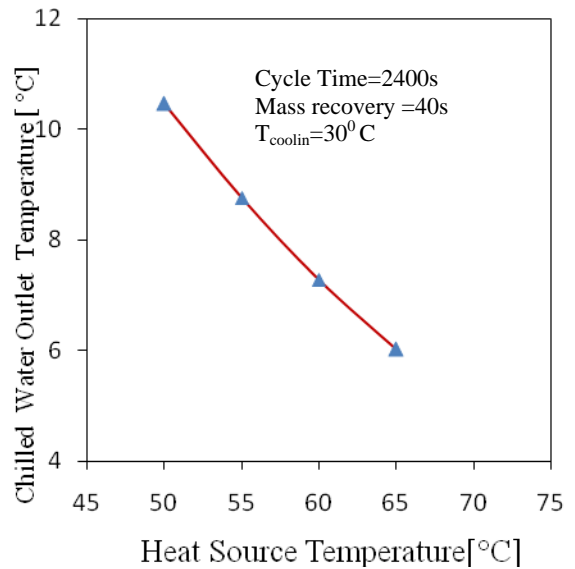


Fig 2.4(b): The effect of heat source temperature on chilled water outlet temperature

### 2.5.5 Effect of cycle time on CC and COP

CC and COP variations with adsorption/desorption cycle time are depicted in Fig.2.5(a). The sensible heating/cooling time is kept constant 30s. The highest CC values are obtained for cycle time between 2100s and 2700s. When cycle times are shorter than 900s, there is not enough time for adsorption or desorption, so CC decreases abruptly. On the other hand, when cycle times are greater than 2700s, CC decreases gradually as the adsorbent approaches to its equilibrium condition. From the same Figure, it can also be observed that COP increases uniformly with longer cycle time. This is because of the lower consumption of driving heat with longer adsorption/desorption cycles.

### 2.5.6 Effect of mass recovery time on CC and COP

Mass recovery cycle is very simple but effective to operate. For operating conditions such as high-condensing temperatures, low-evaporation temperatures, or low-generation temperatures, mass recovery operation is strongly recommended by Wang [15].

Figure 2.5(b) shows the effect of mass recovery process time on CC and COP. It is shown that both CC and COP values are decreased with the increase of mass recovery time. Both CC and COP values are maximized when mass recovery time is 40s with 65<sup>0</sup>C driving source temperature.

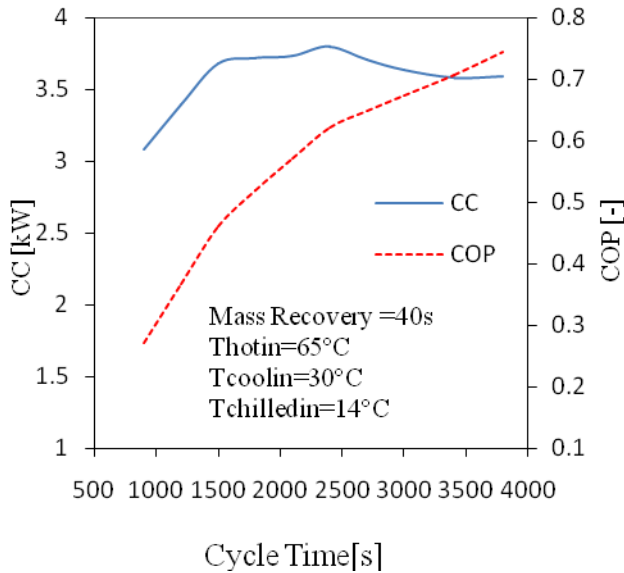


Fig 2.5(a): Cycle time effect on CC and COP

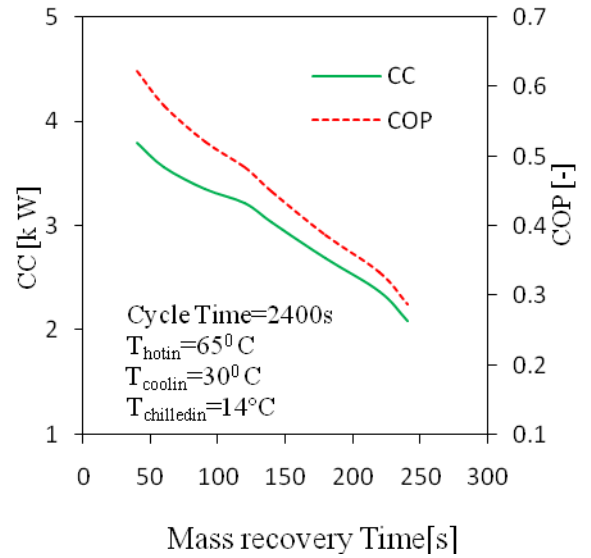


Fig 2.5(b): Effect of mass recovery time on CC and COP

## 2.6 Comparison of the results

In comparison to the three-bed chiller with mass recovery cycle, the chiller performance of the proposed cycle is higher compared to the conventional cycle in terms of the CC and COP values, especially for heat source temperatures 65<sup>0</sup>C. Both of the cycles were tested at different conditions are presented in Table 2.4 and Table 2.5 respectively.

Table 2.4: Cycle time = 2400s, Mass recovery = 40s (Proposed Cycle)

Heat Source Temperature[°C]	CC[kW]	COP[-]	T <sub>chillout</sub> [°C]
50	1.7463	0.5226	10.4585
55	2.5285	0.5906	8.7646
60	3.2153	0.6178	7.2771
65	3.7981	0.6214	6.0148

Table 2.5: Cycle time = 1800s, Mass recovery = 140s (Khan et al. [2])

Heat Source Temperature[°C]	CC[kW]	COP[-]	T <sub>chillout</sub> [°C]
50	0.4197	0.1791	13.4095
55	1.1796	0.3713	11.7633
60	1.8779	0.4786	10.2505
65	2.5168	0.5480	8.8664
70	3.0703	0.5921	7.6674
75	3.5490	0.6227	6.6304
80	3.9472	0.6425	5.7679
85	4.2679	0.6541	5.0732
90	4.5110	0.6574	4.5468

From Table 2.4, it is clearly found that the coefficient of performances (COP) of the proposed cycle is higher than that of the conventional mass recovery cycle if heat source temperature is 65<sup>0</sup>C. It is also seen that the coefficient of performances (COP) can be improved up to 13% than that of the conventional cycle if heat source temperature is considered to be 65<sup>0</sup>C. A novel adsorption chiller, namely, “Three-bed adsorption chiller” is also investigated by Saha et al. [5] and shown that the COP value of the three-bed chiller is 0.38 with driving source temperature at 80<sup>0</sup>C. In this circumstance, two adsorber beds will be connected with the evaporator and will enhance evaporation. Most of the research in this field focuses on developing advanced cycles in order to improve chiller performance to be competitive with other systems. So in the low heat source temperature, the proposed cycle gives better COP value than Saha et al. [5]. It should be noted that the cooling capacity (CC) of the proposed cycle is much better than that of the conventional mass recovery cycle (see Table 2.4) in the range of heat source temperature from 50<sup>0</sup>C to 65<sup>0</sup>C. However, the proposed cycle produces a high cooling capacity. The cooling capacity can be improved more than 50% using the proposed cycle from that of conventional cycle.

The ability to produce a low chilled water outlet is one of the indicators to test the performance of the new cycle. The performance of the proposed cycle is much better than that of the conventional cycle because the chilled water outlet temperature of the conventional cycle is higher than that of the proposed cycle as shown in Table 2.4. According to Table 2.4, the proposed cycle is able to produce chilled water at lower temperature than that of the conventional cycle.

## 2.7 Conclusion

A three-bed mass recovery chiller (equal bed) with silica gel as adsorbent and water as adsorbate is proposed and the performances are evaluated by numerical technique. There is an increasing need for energy efficiency and requirement for the system driven with low temperature heat source. For the utilization of the demand, multi-bed mass recovery cycle is presented and the effects of operating conditions are investigated. The following concluding remarks can be drawn from the present analysis:

- (i) The main feature of the proposed chiller is the ability to be driven by relatively low temperature heat source. The chiller can utilize the fluctuated heat source temperature between  $50^{\circ}\text{C}$  to  $65^{\circ}\text{C}$  to produce effective cooling along with a coolant inlet at  $30^{\circ}\text{C}$ .
- (ii) In the cycle simulation study, hot and cooling water temperatures are the most influential parameters. CC increases with the increase of hot water temperature and opposite tendency for cooling water temperature. Highest COP value (0.6214) is obtained for hot water inlet temperature at  $65^{\circ}\text{C}$ .
- (iii) In the low heat source temperature, COP improves significantly.
- (iv) Waste heat recovery efficiency,  $\eta$  rises from 0.0522 to 0.0649 as the hot water inlet temperature is increased from  $50^{\circ}\text{C}$  to  $65^{\circ}\text{C}$  with cooling source at  $30^{\circ}\text{C}$ .
- (v) Delivered outlet chilled water temperature of the proposed cycle decreases with the increase of driving heat source temperature.
- (vi) The mass recovery process has greater influence on the performance with a lower heat source temperature, such as  $65^{\circ}\text{C}$ , which may help to obtain a COP increase of more than 13%.

---

### Performance Evaluation on Mass Recovery Three-Bed Adsorption Chiller (Unequal Bed)

#### 3.1 Introduction

The thermodynamic framework of a three-bed adsorption chiller (unequal bed) employing mass recovery scheme, which is driven by low temperature heat source is portrayed in this chapter and the performance of the proposed chiller is evaluated numerically. The innovative chiller is powered by waste heat or renewable energy sources of temperature between 50<sup>0</sup>C and 90<sup>0</sup>C along with a coolant of inlet temperature at 30<sup>0</sup>C for air-conditioning purpose. The three-bed adsorption chiller comprises with three adsorber/desorber heat exchanger, one evaporator and one condenser. In the present strategy, mass recovery process occurs in all bed where the configuration of Hex1 and Hex2 are identical, but the configuration of Hex3 is taken as half of Hex1 or Hex2. The cycle simulation calculation indicates that the COP value of the three-bed adsorption chiller with mass recovery is 0.6003 with a driven heat source temperature at 65<sup>0</sup>C in combination with coolant inlet and chilled water inlet temperatures at 30<sup>0</sup>C and 14<sup>0</sup>C, respectively.

#### 3.2 Working Principle of the Mass Recovery Chiller

The schematic diagram and time allocation of the proposed three-bed mass recovery chiller are shown in Fig.3.1 and Table 3.1, respectively. The three-bed mass recovery chiller comprises with three sorption elements (adsorber / desorber heat exchangers), a condenser, an evaporator, and metallic tubes for hot, cooling and chilled water flows as shown in Fig. 3.1. The design criteria of the three-bed mass recovery chiller are almost similar to that of the three-bed chiller without mass recovery which is proposed and developed by Saha et al. [2003] and [2006].

Operational strategy 2 of the proposed chiller is shown in Table 3.1. In proposed design, mass recovery process occurs in all bed. To complete a full cycle for the proposed

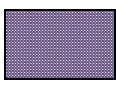



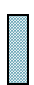



system, the chiller needs 20 modes, namely A, B, C, D, E, F, G, H, I, J, K, L, M, N, O, P, Q, R, S and T as can be seen from Table 3.1.

Table 3.1: Operational strategy 2 of three bed chiller with mass recovery

Mode	A	C	D	F	G	H	I	J	K	L	M	N	O	P	Q	R	S	
Hex1	Desorption		Mass recovery with heating	Adsorption			Mass recovery with heating	Desorption		Mass recovery with cooling	Adsorption		Mass recovery with heating	Desorption		Mass recovery with cooling	Pre-cooling	
Hex2	Adsorption			Mass recovery with cooling	Desorption		Mass recovery with heating	Adsorption			Mass recovery with cooling	Desorption		Mass recovery with heating	Adsorption		Mass recovery with cooling	Pre-heating
Hex3	Desorption	Adsorption	Mass recovery with cooling	Desorption	Adsorption	Desorption	Adsorption	Desorption	Adsorption	Desorption	Adsorption	Desorption	Adsorption	Desorption	Adsorption	Desorption	Adsorption	

	Desorption		Mass recovery with heating		Pre-heating
	Adsorption		Mass recovery with cooling		Pre-cooling

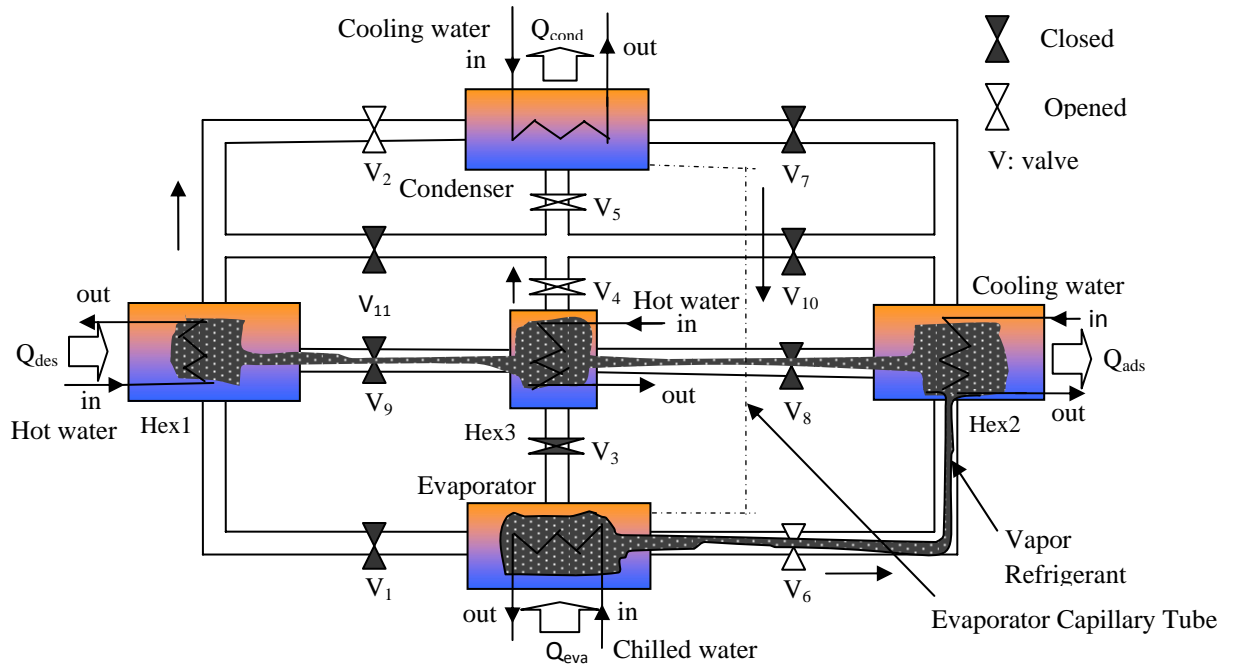


Fig3.1: Schematic of three bed chiller with mass recovery

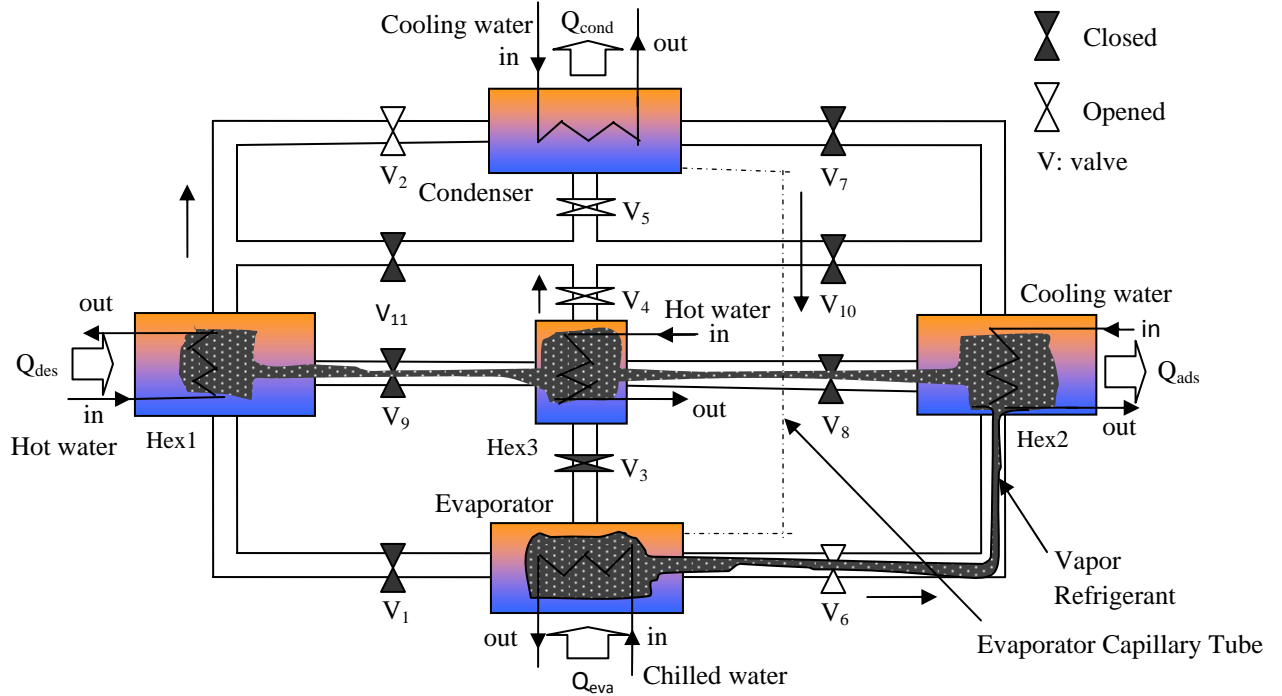


Fig3.1: Schematic of three bed chiller with mass recovery (Mode-A)

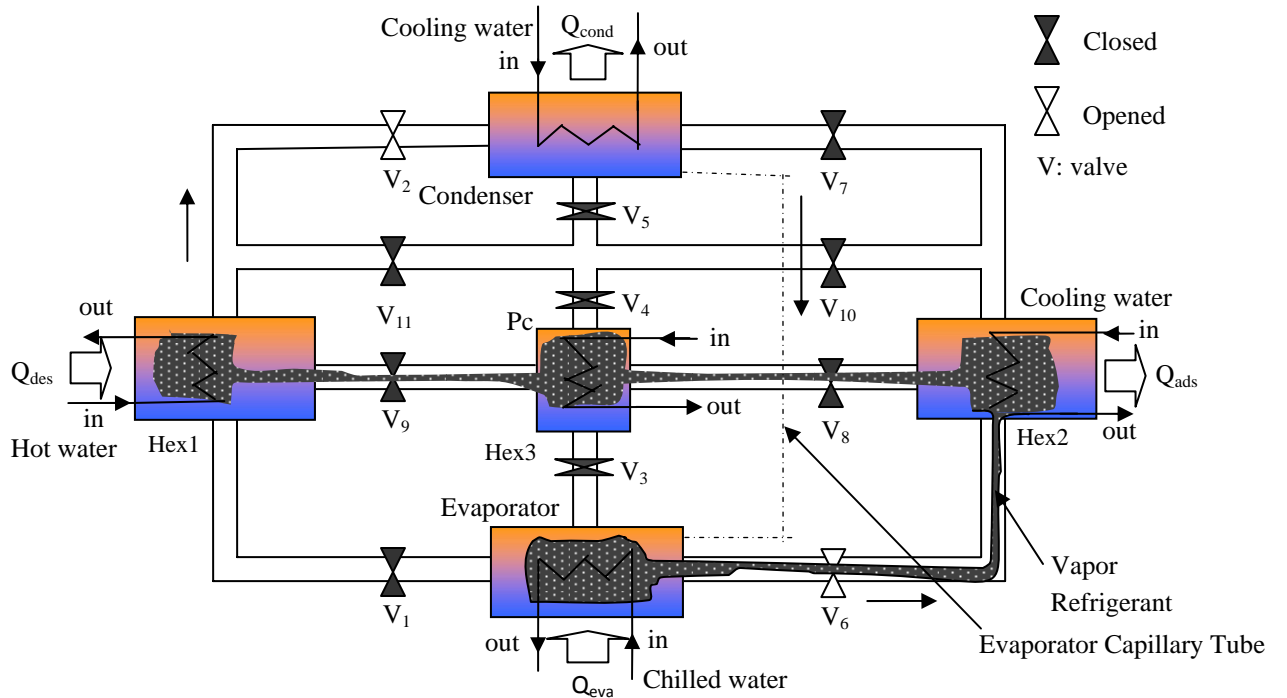


Fig3.1: Schematic of three bed chiller with mass recovery (Mode-B)

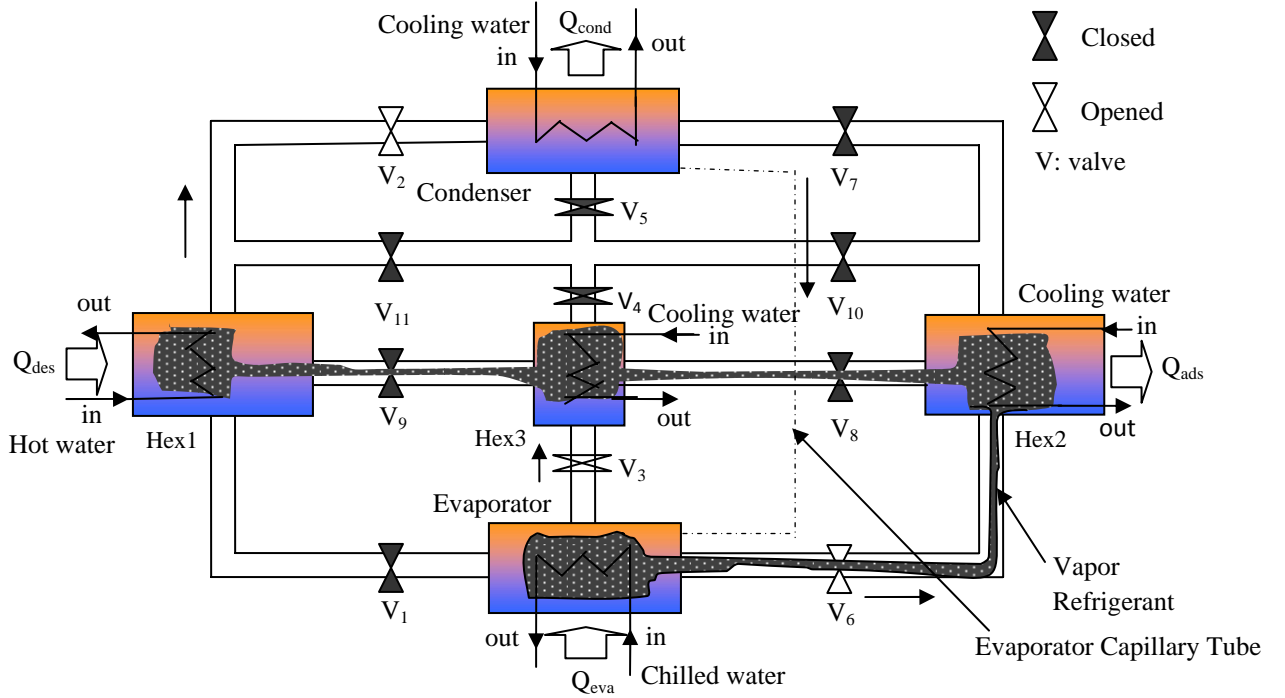


Fig3.1: Schematic of three bed chiller with mass recovery (Mode-C)

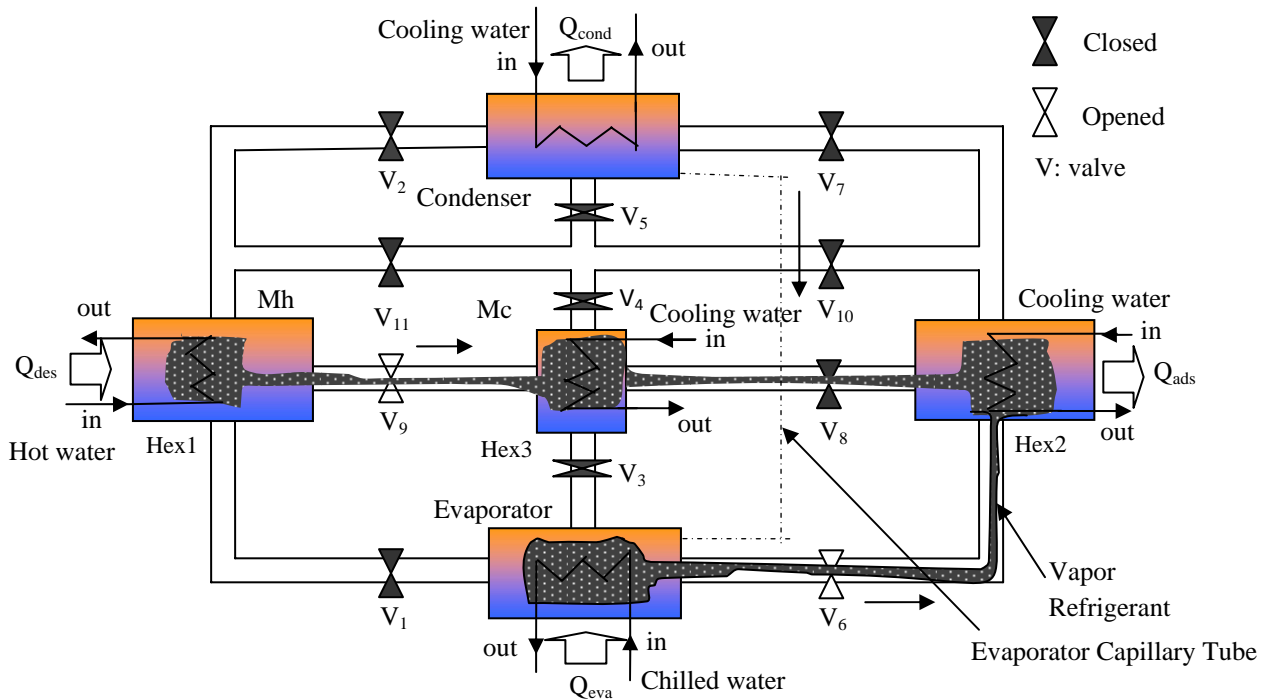


Fig3.1: Schematic of three bed chiller with mass recovery (Mode-D)

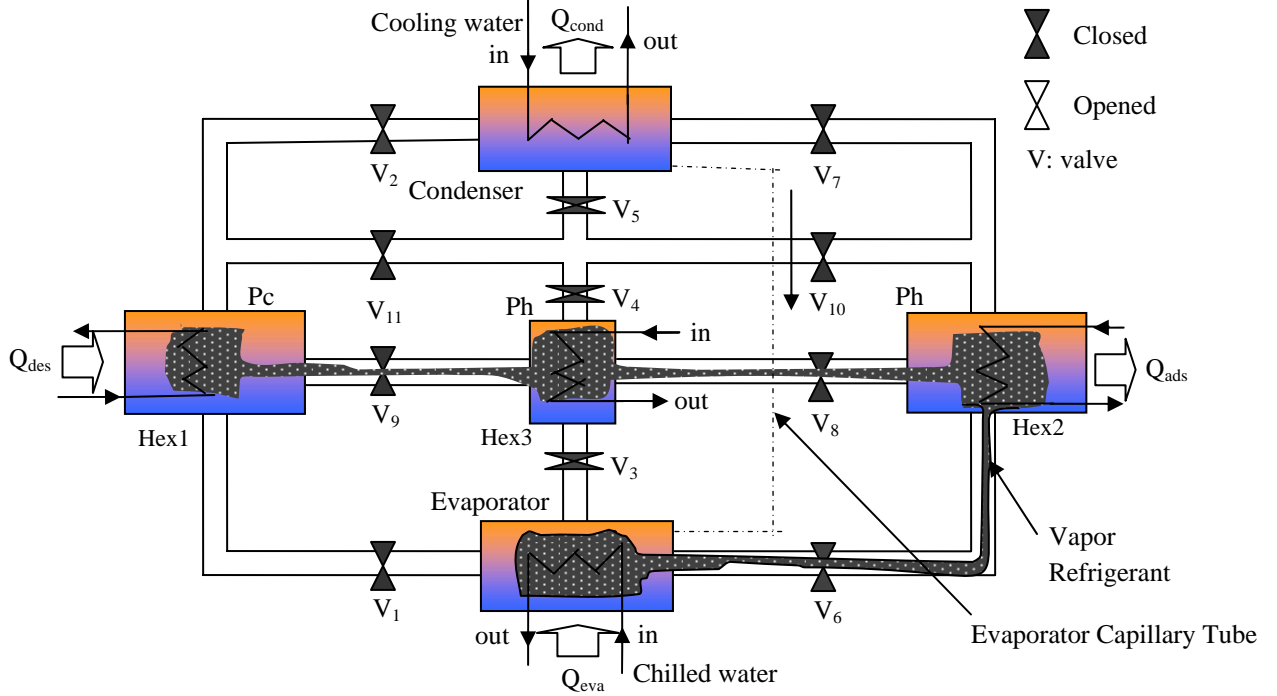


Fig3.1: Schematic of three bed chiller with mass recovery (Mode-E)

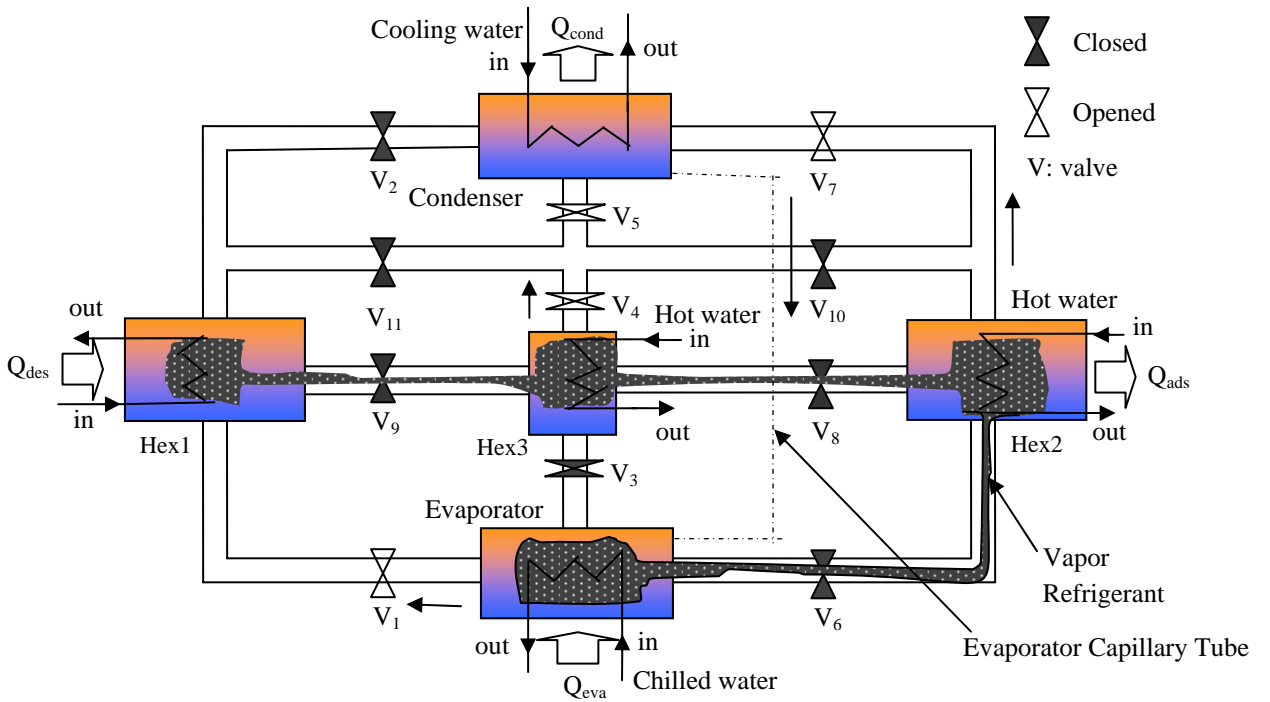


Fig3.1: Schematic of three bed chiller with mass recovery (Mode-F)

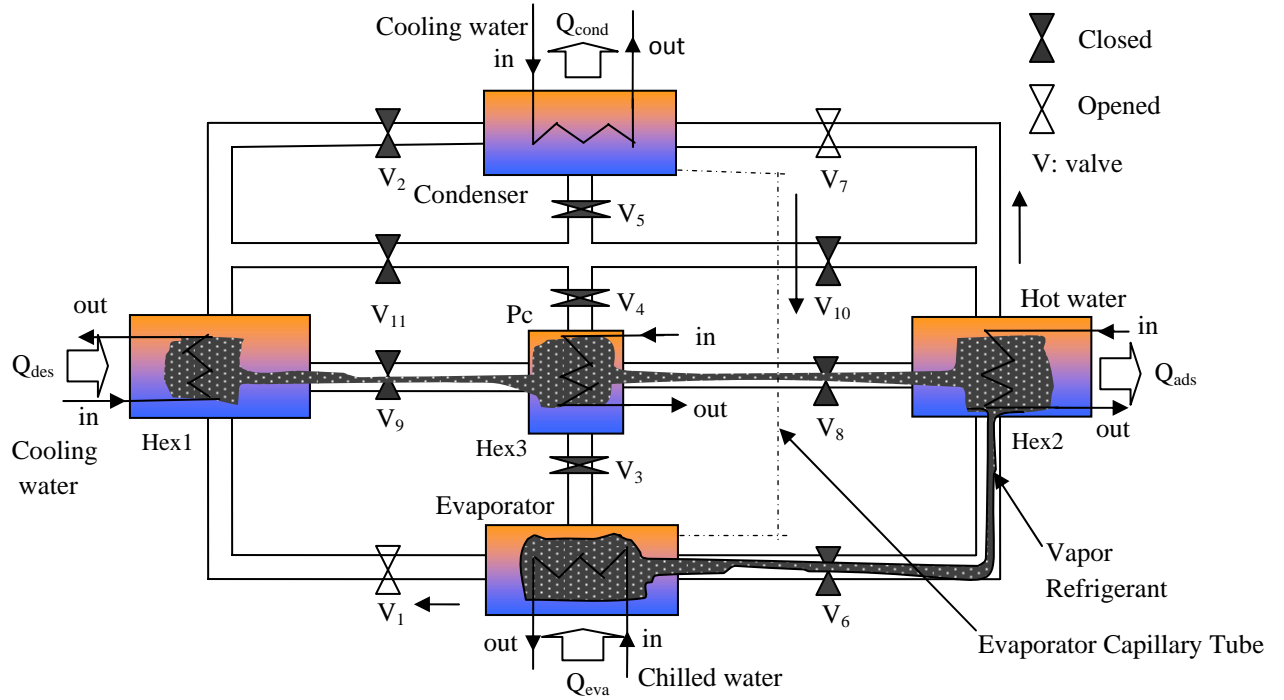


Fig3.1: Schematic of three bed chiller with mass recovery (Mode-G)

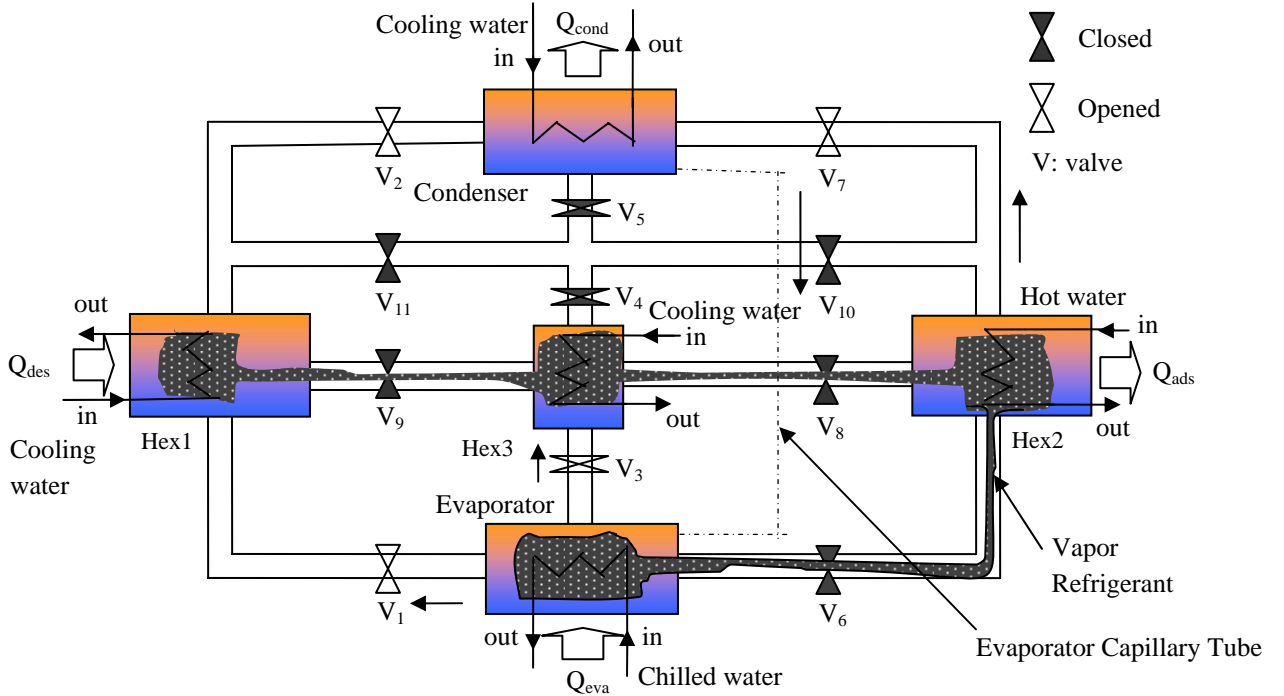


Fig3.1: Schematic of three bed chiller with mass recovery (Mode-H)

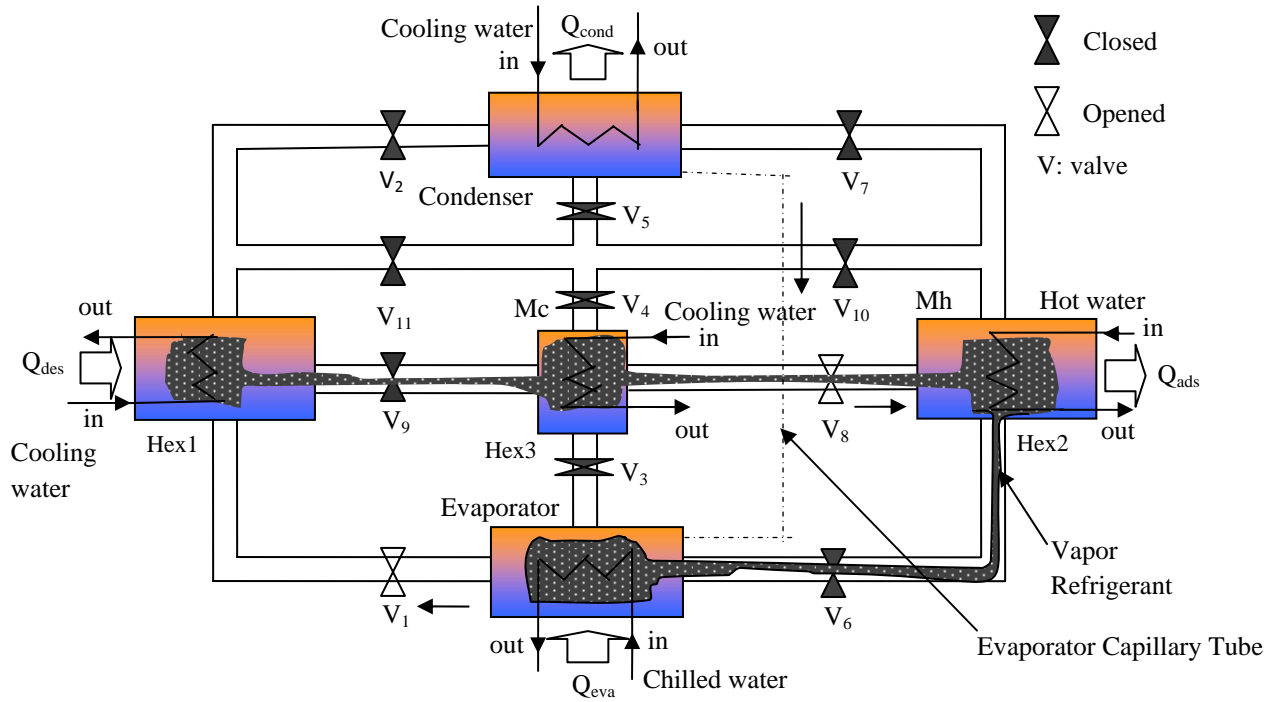


Fig3.1: Schematic of three bed chiller with mass recovery (Mode-I)

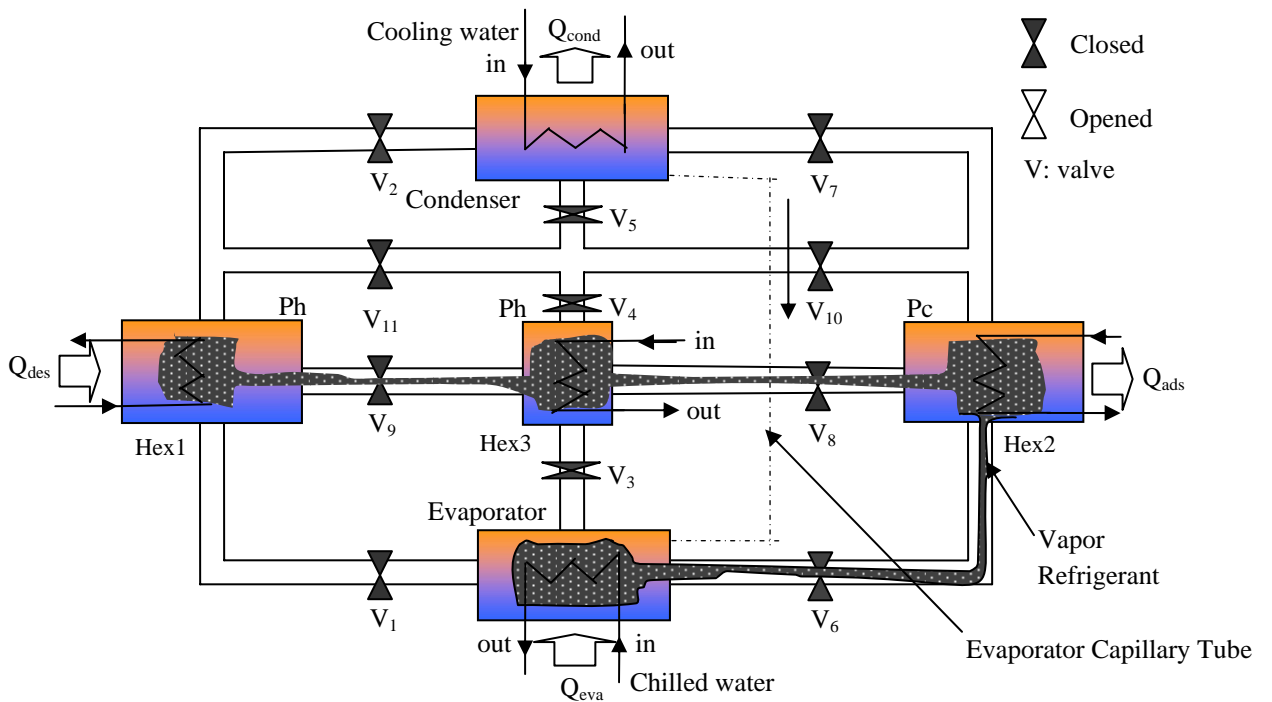


Fig3.1: Schematic of three bed chiller with mass recovery (Mode-J)

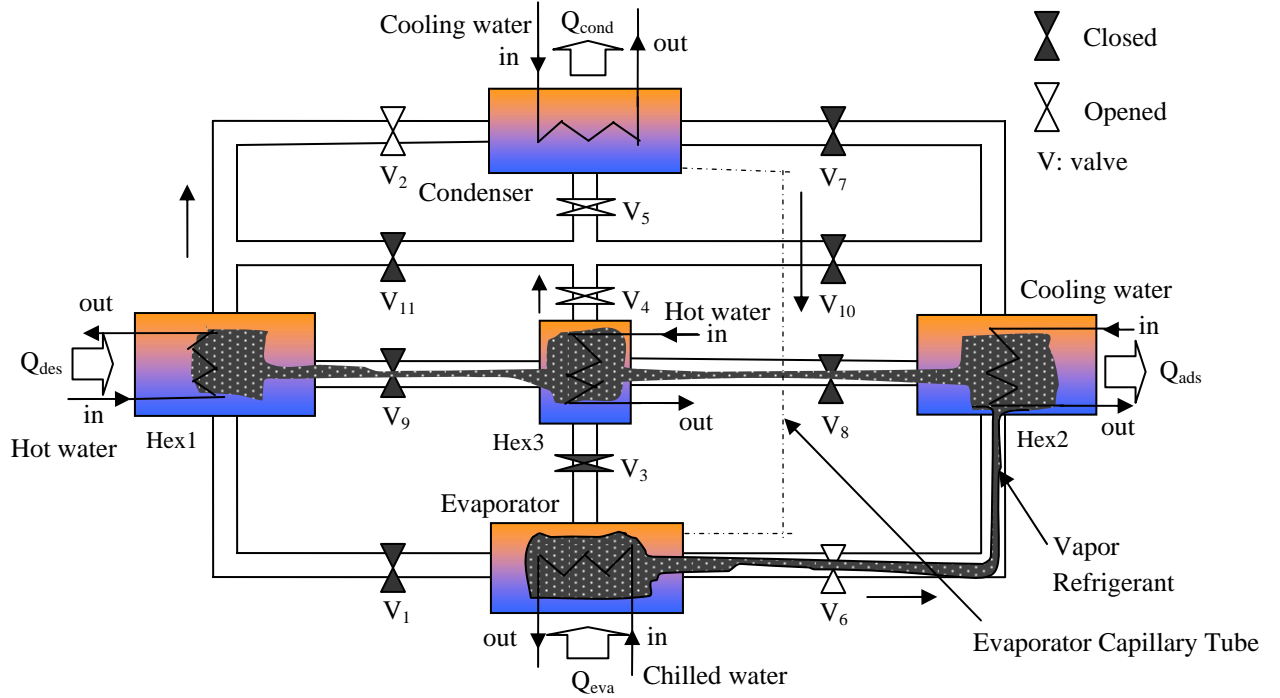


Fig3.1: Schematic of three bed chiller with mass recovery (Mode-K)

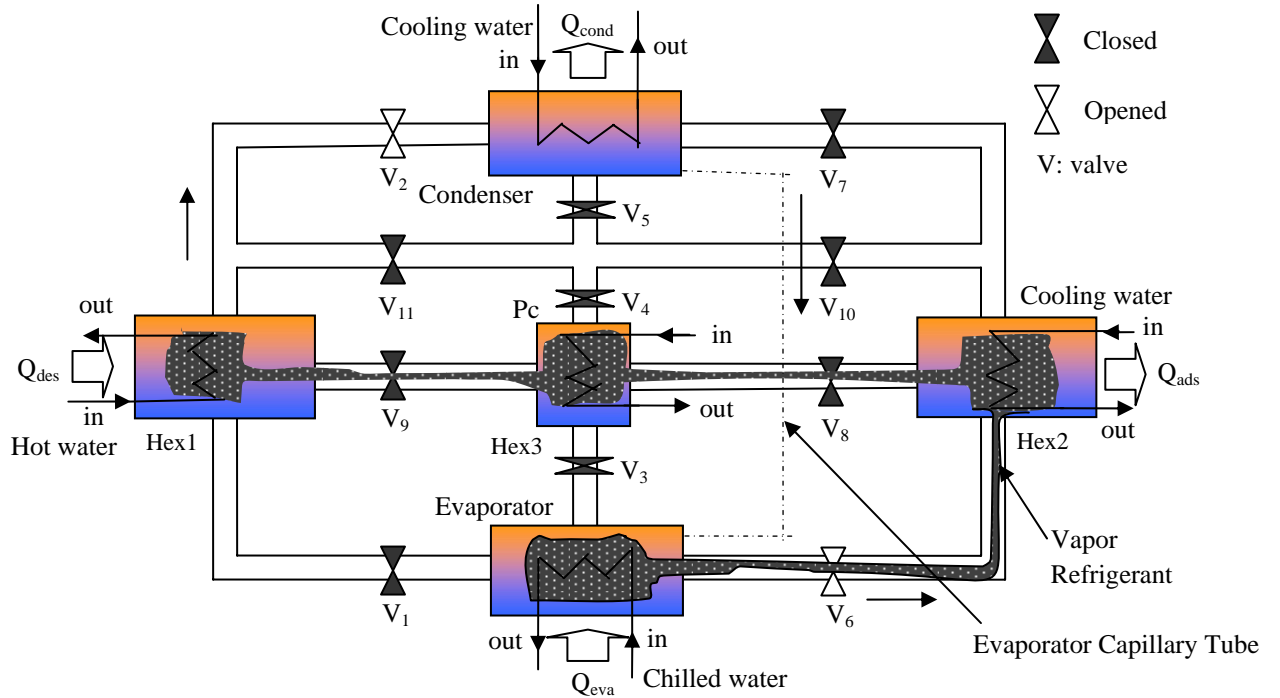


Fig3.1: Schematic of three bed chiller with mass recovery (Mode-L)

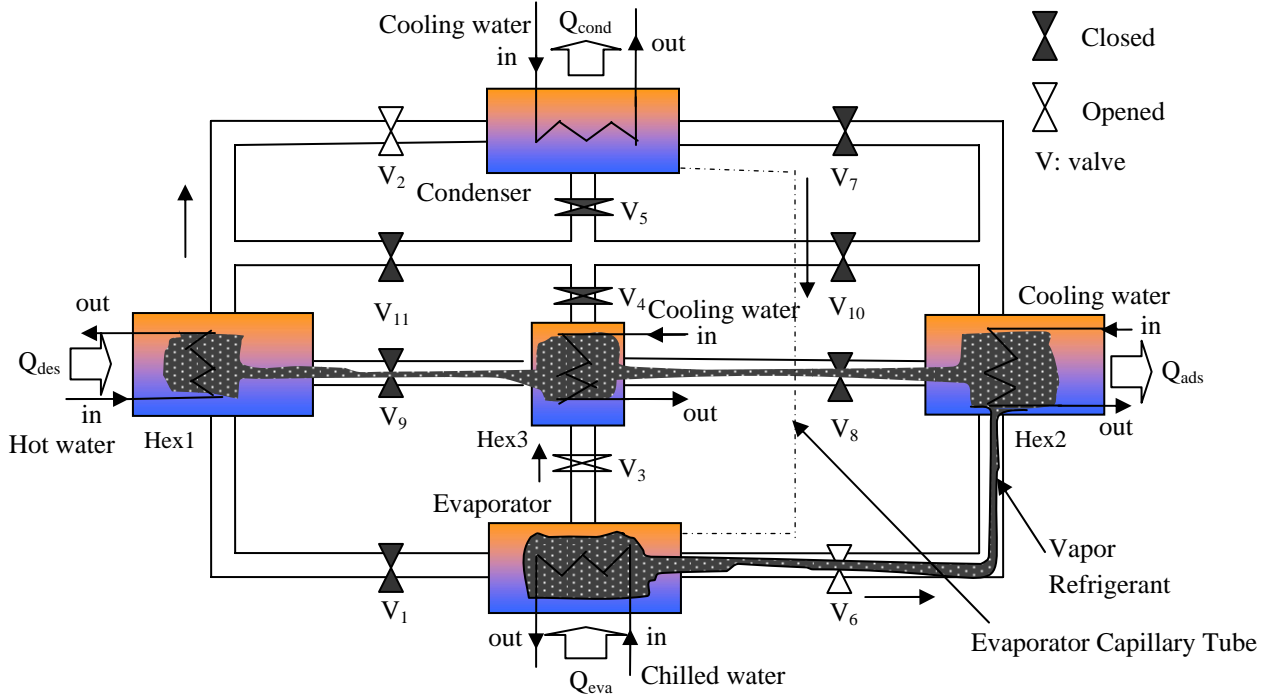


Fig3.1: Schematic of three bed chiller with mass recovery (Mode-M)

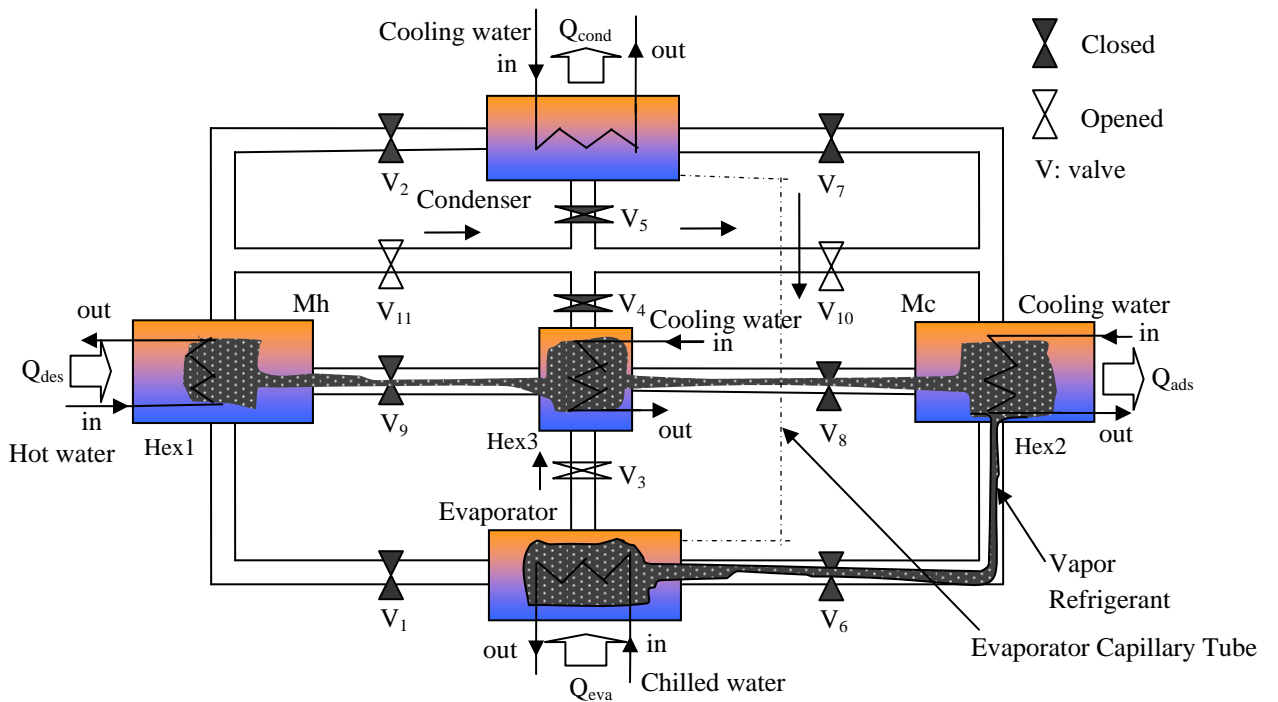


Fig3.1: Schematic of three bed chiller with mass recovery (Mode-N)



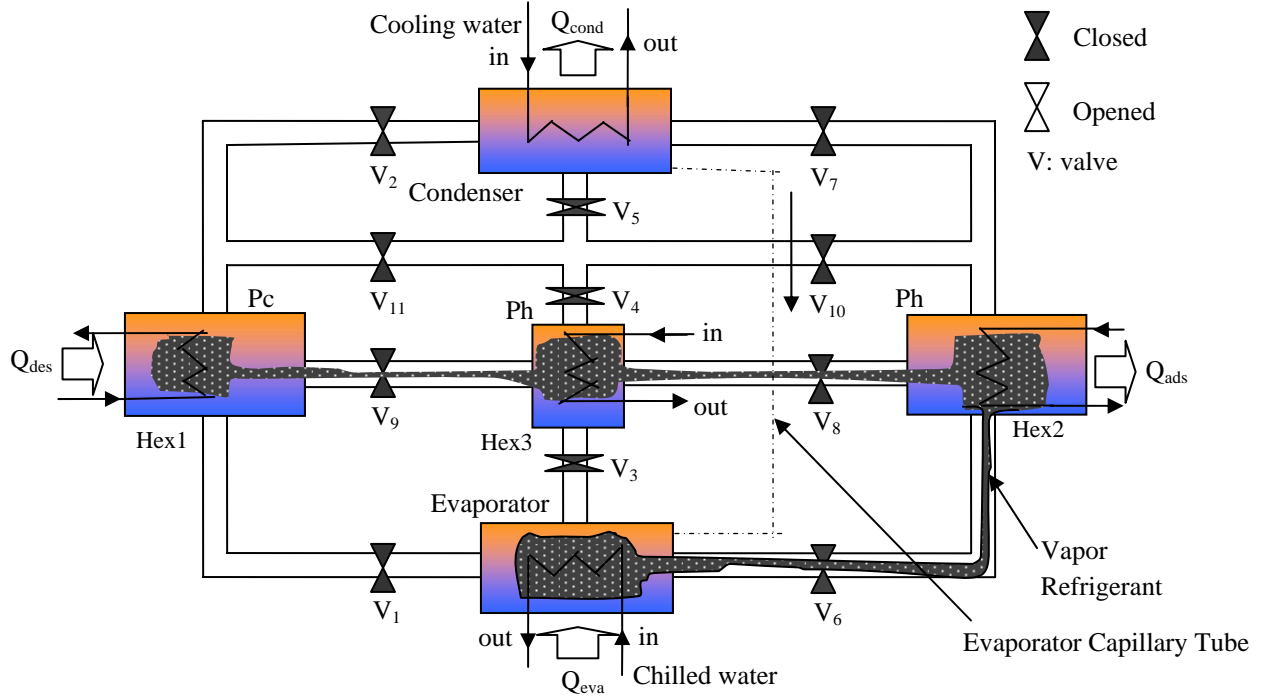


Fig3.1: Schematic of three bed chiller with mass recovery (Mode-O)

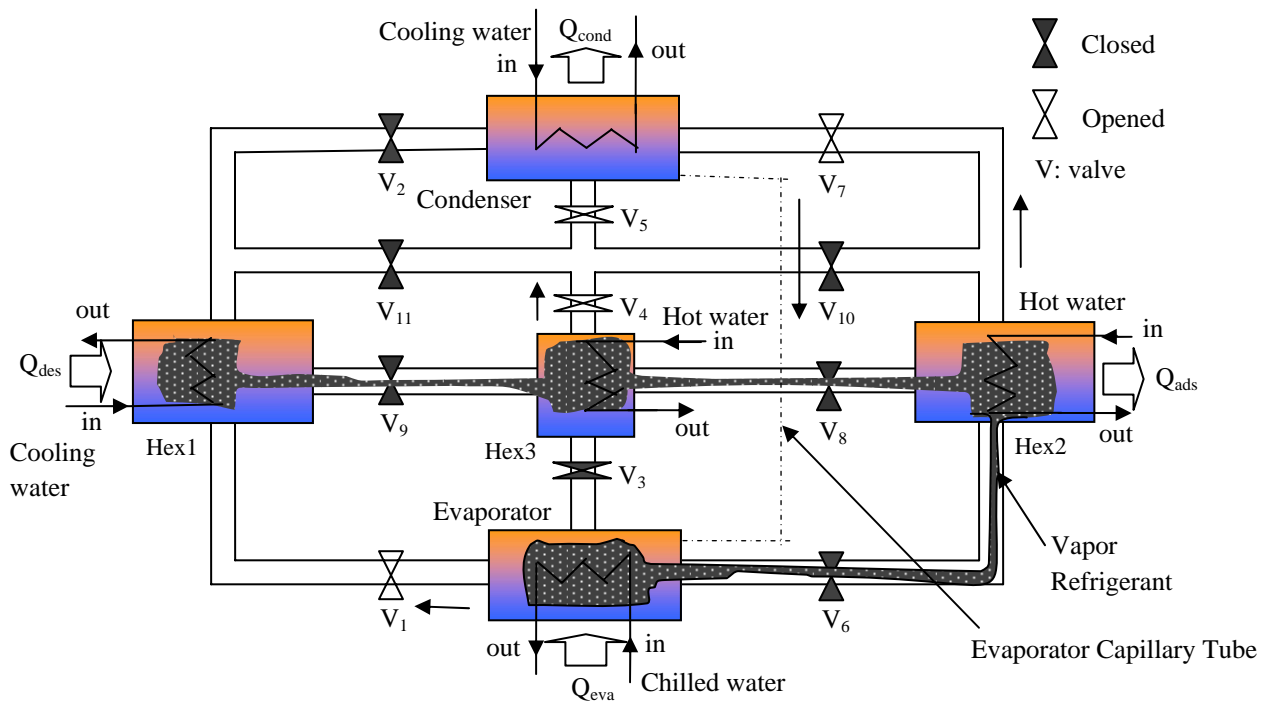


Fig3.1: Schematic of three bed chiller with mass recovery (Mode-P)

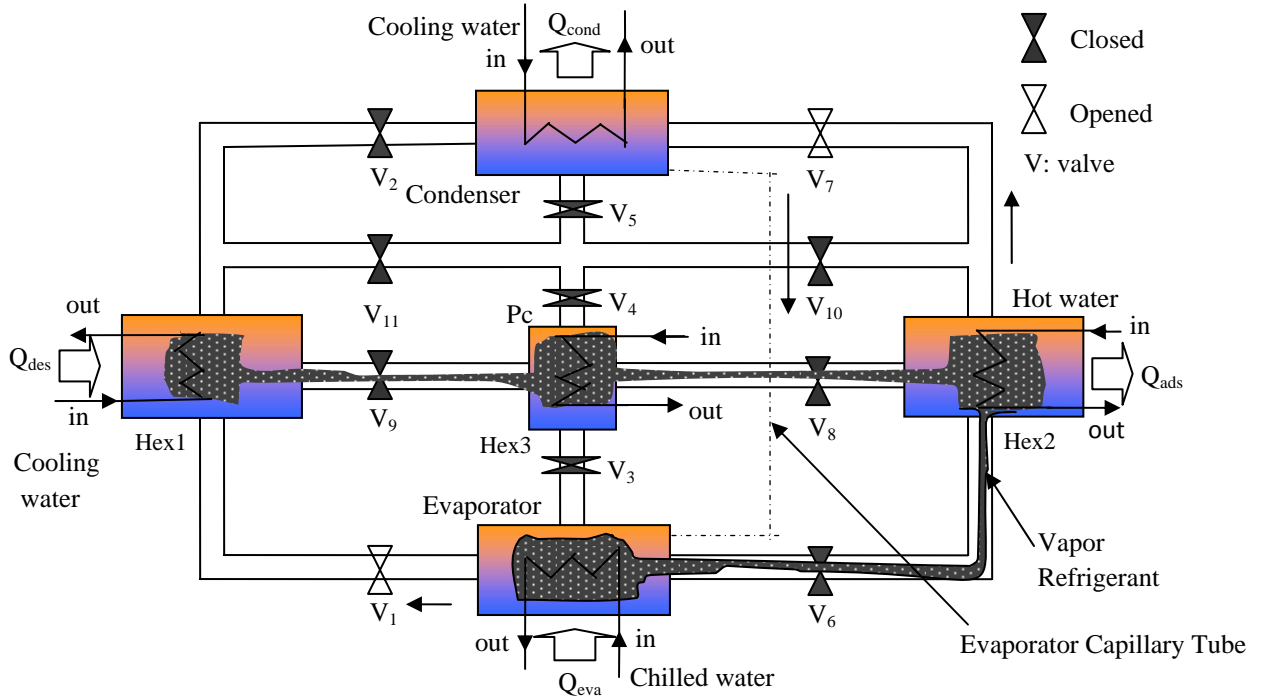


Fig3.1: Schematic of three bed chiller with mass recovery (Mode-Q)

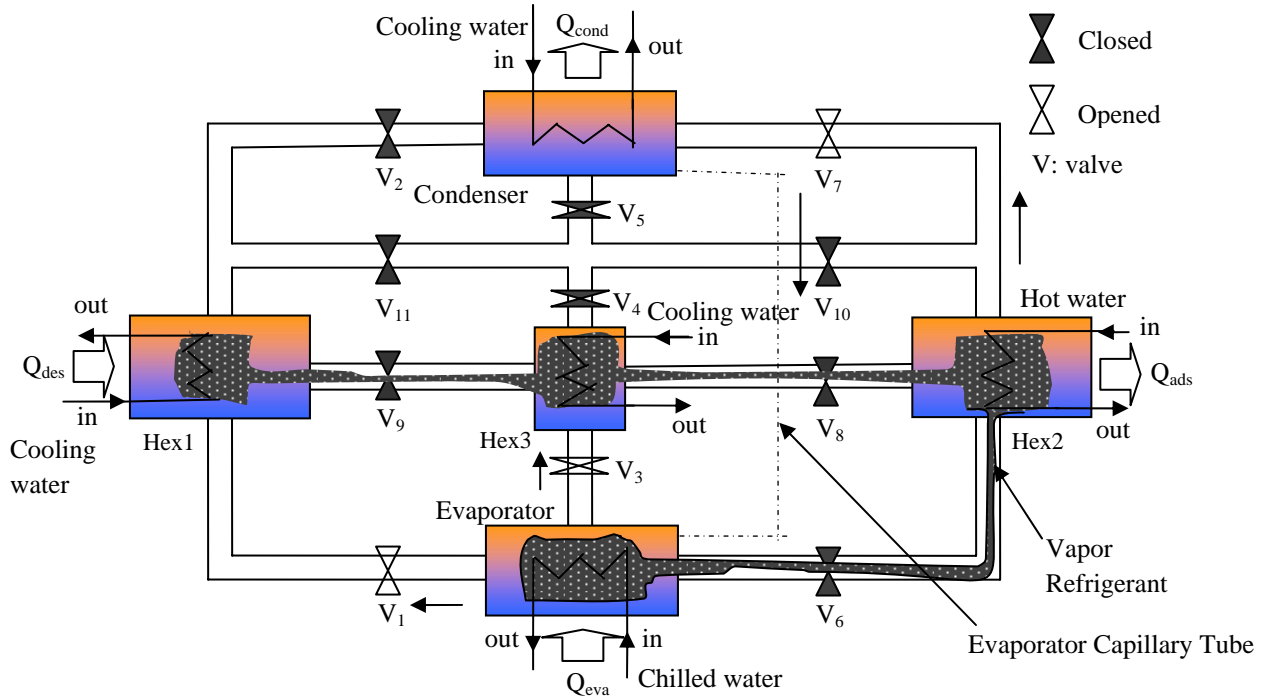


Fig3.1: Schematic of three bed chiller with mass recovery (Mode-R)

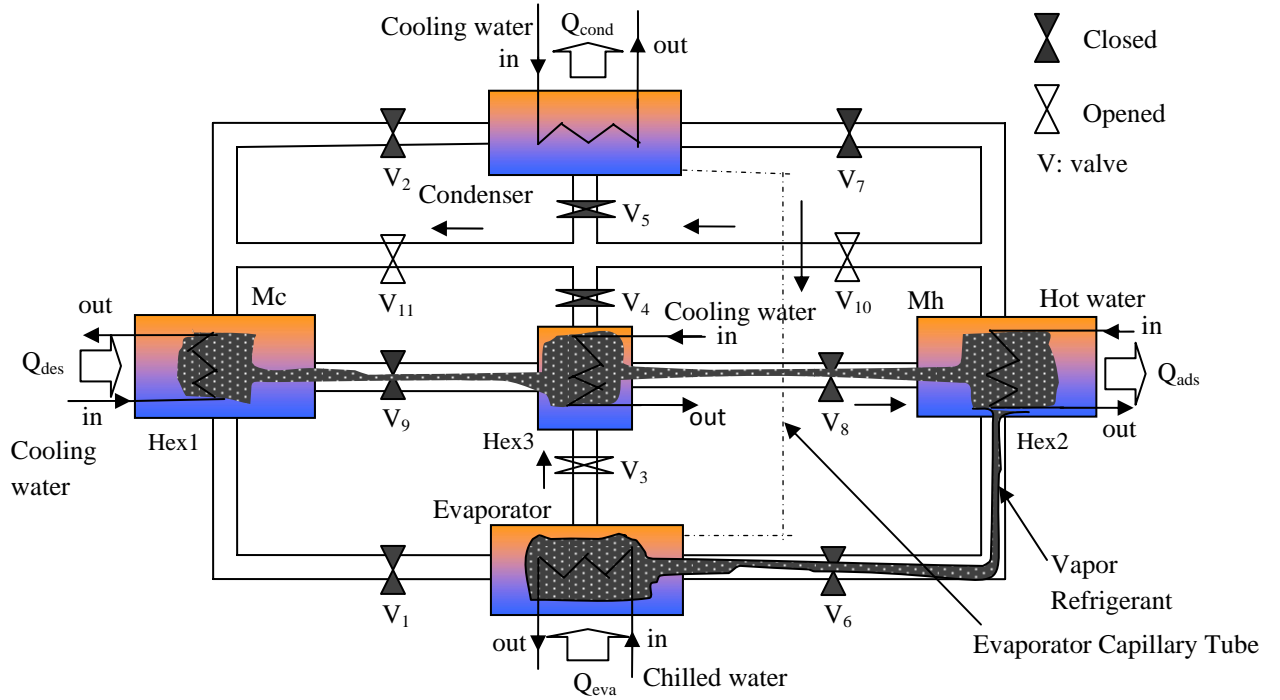


Fig3.1: Schematic of three bed chiller with mass recovery (Mode-S)

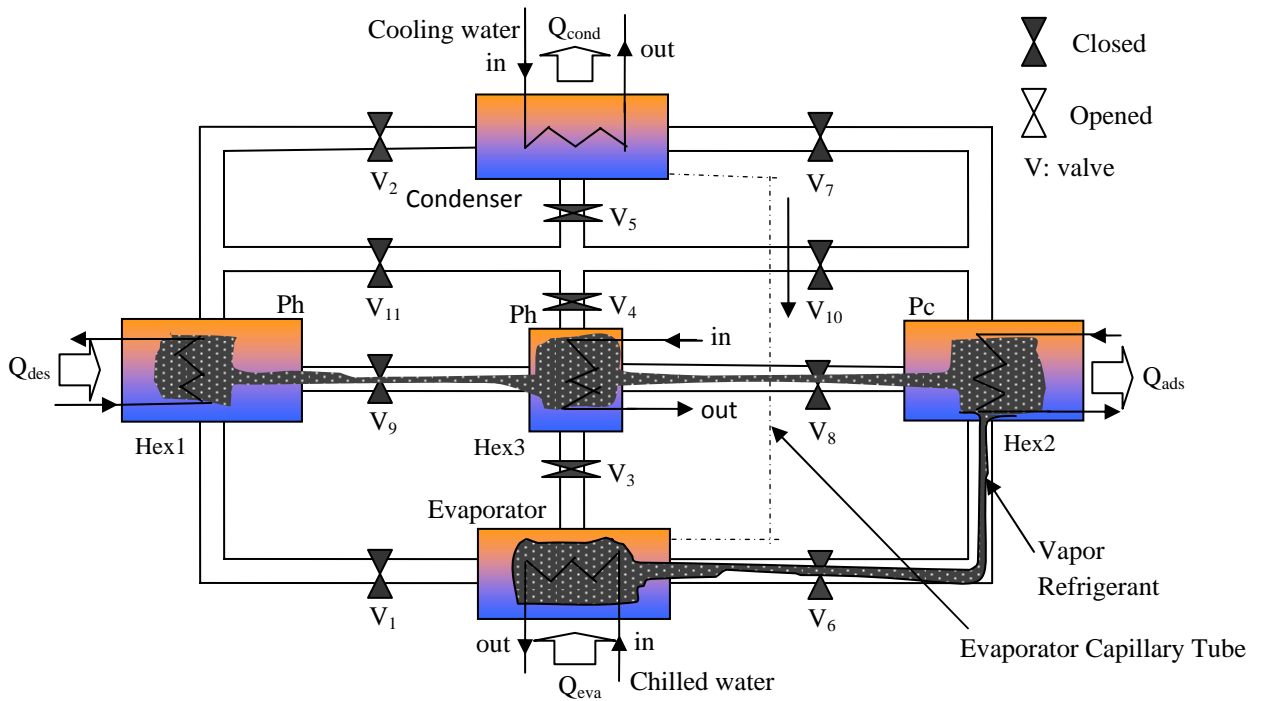


Fig3.1: Schematic of three bed chiller with mass recovery (Mode-T)

In mode A, Hex1 and Hex3 work as desorber. The desorption-condensation process takes place at condenser pressure ( $P_{\text{cond}}$ ). The desorber (Hex1, Hex3) is heated up to temperature ( $T_{\text{des}}$ ) by heat input  $Q_{\text{des}}$ , provided by the driving heat sources. The resulting refrigerant is cooled down by temperature ( $T_{\text{cond}}$ ) in the condenser by the cooling water, which removes condensation heat,  $Q_{\text{cond}}$ . Hex2 works as adsorber in mode A. In the adsorption-evaporation process, refrigerant (water) in evaporator is evaporated at evaporation temperature,  $T_{\text{eva}}$ , and seized heat,  $Q_{\text{eva}}$  from chilled water. The evaporated vapor is adsorbed by adsorbent (silica gel), at which cooling water removes the adsorption heat,  $Q_{\text{ads}}$ .

Mode B is the pre-cooling process for Hex3. In pre-cooling process, Hex3 is isolated from evaporator, condensed or any other beds. Cooling water is supplied to the bed for short time (30s) in this period. Hex1 works as desorber and Hex2 works as adsorber in mode B also.

Mode C is the adsorption process for Hex3, Hex2 and desorption process for Hex1.

In mode D, Hex3 (at the end position of adsorption-evaporation process) and Hex1 (at the end position of desorption-condensation process) are connected with each other continuing cooling water and hot water, respectively that can be classified as two-bed mass recovery process. This time Hex3 is isolated from evaporated and Hex1 is isolated from condensed. Here mass recovery occurs only bed to bed. In this mode Hex2 works as adsorber. When the concentration levels of both beds Hex1 and Hex3 reach in nearly equilibrium levels, then warm up process will start, called mode E (pre-heating or pre-cooling).

In mode E, Hex2 and Hex3 are heated up by hot water, and Hex1 is cooled down by cooling water. When the pressure of Hex2 and Hex3 are nearly equal to the pressure of condenser then Hex2 and Hex3 are connected to condenser. When the pressure of Hex1 is nearly equal to the pressure of evaporator then Hex1 is connected to evaporator.

In mode F, Hex2 and Hex3 work as desorber and Hex1 works as adsorber.

Mode G is the pre-cooling process for Hex3. In this mode, Hex2 works as desorber and Hex1 works as adsorber.

Mode H is the adsorption-evaporation process for Hex1 and Hex3. Hex2 works as desorber in this mode.

In mode I, Hex3 (at the end position of adsorption-evaporation process) and Hex2 (at the end position of desorption-condensation process) are connected with each other continuing cooling water and hot water, respectively that can be classified as two-bed mass recovery process. When the concentration levels of both beds Hex3 and Hex2 reach in nearly equilibrium levels, then warm up process will start, called mode J (pre-heating or pre-cooling). Hex1 works as adsorber in this mode.

Mode J is the pre-heating/pre-cooling process for all bed. In this period, Hex1 and Hex3 are heated up by hot water; Hex2 is cooled down by cooling water.

Modes K, L and M are same as modes A, B and C respectively. In mode K, L and M Hex1 and Hex3 work as desorber and Hex2 works as adsorber.

The mode N is same as mode D. In these modes, Hex2 (at the end position of adsorption-evaporation process) and Hex1 (at the end position of desorption-condensation process) are connected with each other continuing cooling water and hot water respectively. In this mode Hex3 works as adsorber. When the concentration levels of both beds Hex1 and Hex2 reach in nearly equilibrium levels, then warm up process will start, called mode O (pre-heating or pre-cooling). The mode O is same as mode E.

Modes P, Q and R are same as modes F, G and H respectively. In mode P, Q and R, Hex2 and Hex3 work as desorber and Hex1 works as adsorber.

The mode S is same as mode I. In mode S, Hex1 (at the end position of adsorption-evaporation process) and Hex2 (at the end position of desorption-condensation process) are connected with each other continuing cooling water and hot water, respectively that can be classified as two-bed mass recovery process. When the concentration levels of both beds Hex1 and Hex2 reach in nearly equilibrium levels, then warm up process will start, called mode T (pre-heating or pre-cooling). Hex3 works as adsorber in this mode.

Mode T is the pre-heating/pre-cooling process for all bed. In this period, Hex1 and Hex3 are heated up by hot water; Hex2 is cooled down by cooling water. Mode T is the last process for all beds, after this mode, all beds will return to its initial position (Mode A). That's why to complete one cycle, it needs 20 modes.

The standard operating condition for the chiller operation is presented in Table 3.2

Table 3.2 Standard operating condition

	Temperature [ <sup>0</sup> C]	Flow rate (kg/s)
Hot water	50 ~ 90	0.2
Cooling water	30	0.54[=0.2(ads)+0.34(cond)]
Chilled water	14	0.11
Cycle Time	2100s=(950 ads/ des+40 mr+30ph+30pc) s×2	

### 3.3. Results and discussion

Since our main interest is to utilize the low grade waste heat as the driving source, the investigation was conducted for hot water between 50<sup>0</sup>C and 90<sup>0</sup>C. The effect of operating temperature (hot and cooling water) is calculated by the simulation runs.

#### 3.3.1 Effect of driving heat source temperature on CC and COP

Figures 3.2(a) and 3.2(b) show heat source temperature variation on CC and COP, respectively. It is seen that CC for three-bed mass recovery chiller increases with the increase of heat source temperature from 50<sup>0</sup>C to 90<sup>0</sup>C with a cooling water inlet temperature of 30<sup>0</sup>C. This is because the amount of refrigerant circulated increases, due to increased refrigerant desorption with higher driving source temperature. Another reason is that, in the proposed cycle, Hex1 and Hex2 connect with Hex3 one by one during mass recovery, which accelerates cooling effect. The CC is improved due to the mass recovery process. The mass recovery process generates more desorption heat and that is transferred from the desorber through desorbed vapor. So, in the low heat source

temperature (55<sup>0</sup>C -65<sup>0</sup>C), proposed chiller gives better performance. The optimum COP value is 0.6003 for hot water inlet temperature at 65<sup>0</sup>C along with the coolant and chilled water inlet temperature are at 30<sup>0</sup>C and 14<sup>0</sup>C, respectively. The delivered chilled water temperature is 8<sup>0</sup>C for this operation condition.

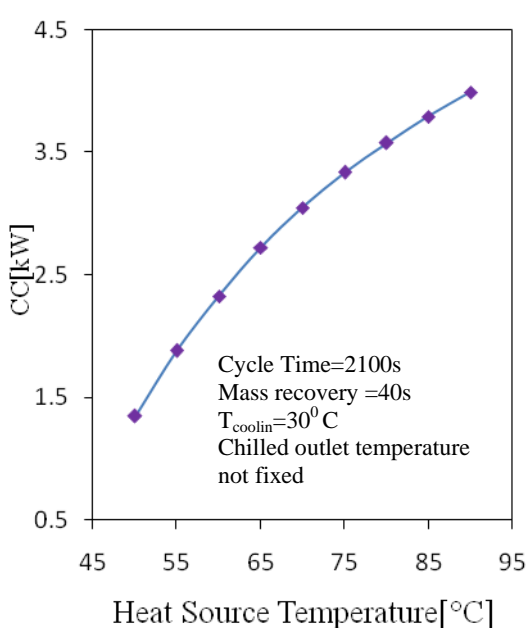


Fig 3.2(a): The effect of heat source temperature on CC

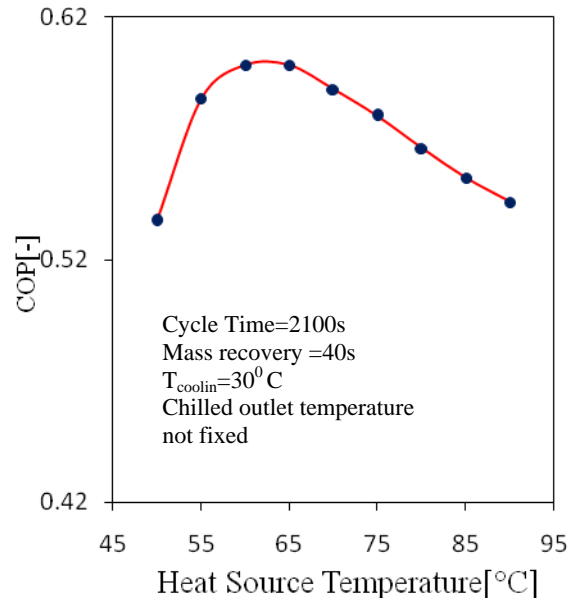


Fig 3.2(b): The effect of heat source temperature on COP

### 3.3.2 Effect of cooling source temperature on CC and COP

Figure 3.3(a) and 3.3(b) show the effect of cooling water inlet temperatures on CC and COP, respectively. In the present simulation, cooling water mass flow rate into adsorber is taken as 0.2 kg/s, while for the condenser the coolant mass flow rate is taken as 0.34 kg/s. The CC increases steadily as the cooling water inlet temperature is lowered from 40 to 20<sup>0</sup>C. This is due to the fact that lower adsorption temperatures result in larger amounts of refrigerant being adsorbed and desorbed during each cycle. The simulated COP values also increases with lower cooling water inlet temperature. For the three bed chiller the COP value reaches 0.6519 with 65<sup>0</sup>C driving source temperature in combination with a coolant inlet temperature of 20<sup>0</sup>C.

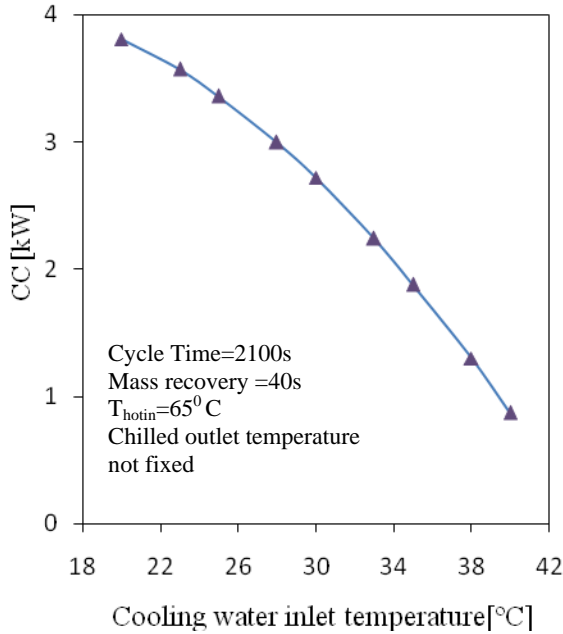


Fig 3.3(a): The effect of cooling water inlet temperature on CC

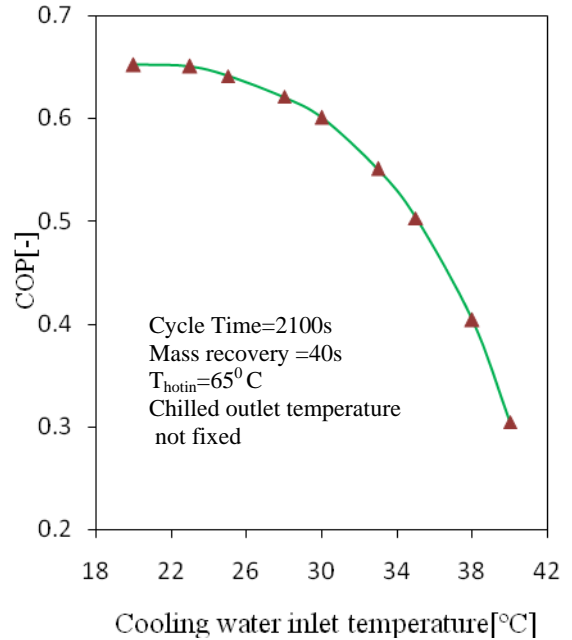


Fig 3.3(b): The effect of cooling water inlet temperature on COP

### 3.3.3 Effect of driving heat source temperature on chiller efficiency, $\eta$

Figure 3.4(a) presents the waste heat recovery efficiency,  $\eta$ , as a function of heat source temperature. For three-bed proposed cycle employing mass recovery scheme with heating/cooling,  $\eta$  rises from 0.0805 to 0.0931 as the hot water inlet temperature is increased from 50°C to 65°C with a cooling source 30°C. This is because improvement of cooling capacity of the proposed chiller in this range. It is also observed that  $\eta$  is boosted by about 25% than that of conventional cycle demonstrated by Khan et al.(2005).

### 3.3.4 Effect of driving heat source temperature on chilled water outlet temperature

The effect of heat source temperature on average chilled water outlet temperature is depicted in Fig.3.4 (b). The chilled water temperature level needs to be considered according to demand side requirement. Mass flow rate of chilled water can control the outlet temperature of chilled water. From Fig.3.4 (b), it is seen that the cyclic average chilled water outlet temperature of the proposed cycle decreases with the increase of the driving heat source temperature. Low chilled water outlet temperature is expected from real machine.



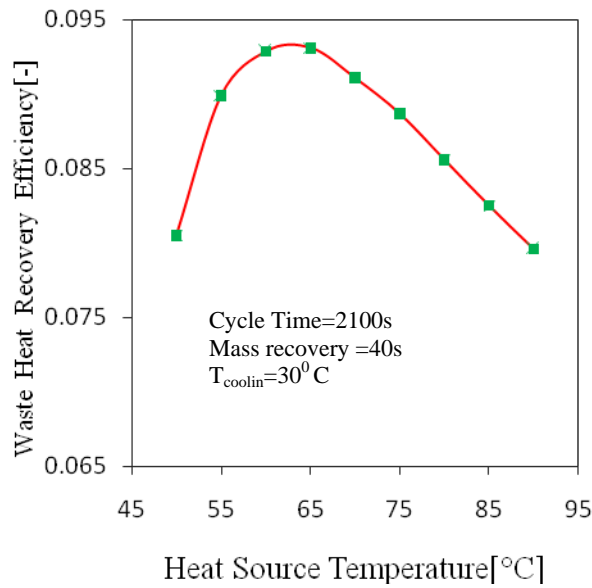


Fig 3.4(a): The effect of heat source temperature on waste heat recovery efficiency [-]

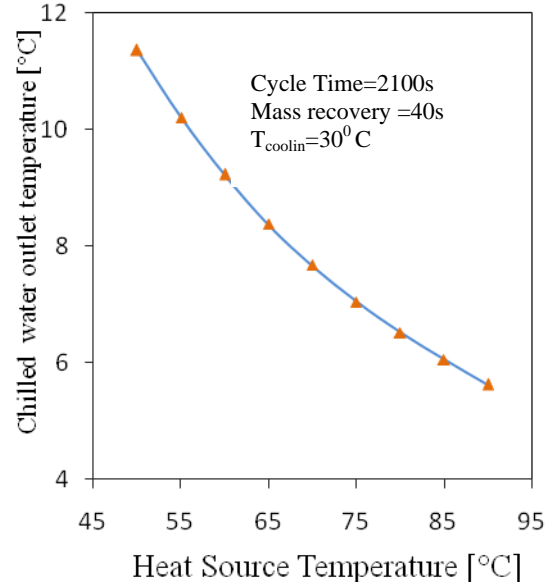


Fig 3.4(b): The effect of heat source temperature on chilled water outlet temperature

### 3.3.5 Effect of cycle time on CC and COP

CC and COP variations with adsorption/desorption cycle time are depicted in Fig.3.5 (a). The sensible heating/cooling time is kept constant 30s. The highest CC values are obtained for cycle time between 1800 and 2400 s. When cycle times are shorter than 900s, there is not enough time for adsorption or desorption, so CC decreases abruptly. On the other hand, when cycle times are greater than 2400s, CC decreases gradually as the adsorbent approaches to its equilibrium condition. From the same Figure, it can also be observed that COP increases uniformly with longer cycle time. This is because of the lower consumption of driving heat with longer adsorption/desorption cycles.

### 3.3.6 Effect of mass recovery time on CC and COP

Mass recovery cycle is very simple but effective to operate. For operating conditions such as high-condensing temperatures, low-evaporation temperatures, or low-generation temperatures, mass recovery operation is strongly recommended by Wang [15].

Figure 3.5 (b) shows the effect of mass recovery process time on CC and COP. It is shown that both CC and COP values are decreased with the increase of mass recovery time. Both CC and COP values are maximized when mass recovery time is 40s with 65<sup>0</sup>C driving source temperature.

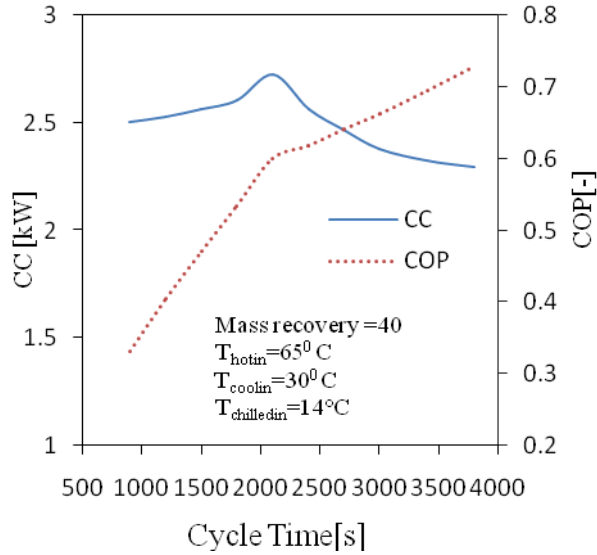


Fig 3.5(a): Cycle time effect on CC and COP

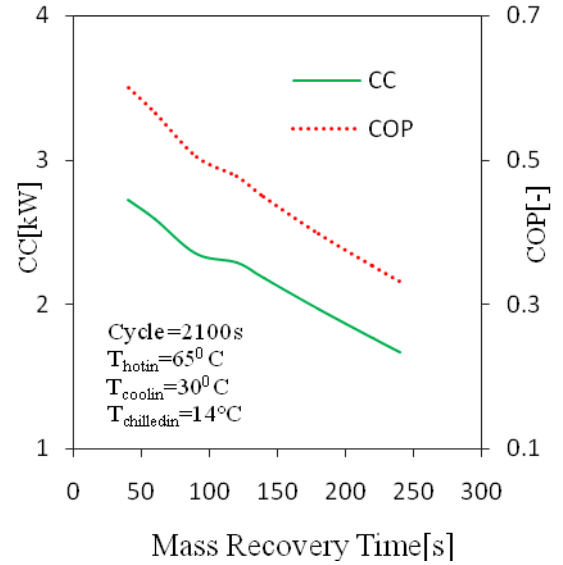


Fig 3.5(b): Effect of mass recovery time on CC and COP

### 3.4 Comparison of the results

In comparison to the three-bed chiller with mass recovery cycle, the chiller performance of the proposed cycle is higher compared to the conventional cycle in terms of the CC and COP values, especially for heat source temperatures 65<sup>0</sup>C. Both of the cycles were tested at different conditions are presented in Table 3.4 and Table 3.5 respectively.

Table 3.3: Cycle time = 2100s, Mass recovery = 40s (Proposed Cycle)

Heat Source Temperature[°C]	CC[kW]	COP[-]	T <sub>chillout</sub> [°C]
50	1.3453	0.5359	11.3605
55	1.8792	0.5866	10.2041
60	2.3289	0.6003	9.2299

65	2.7227	0.6003	8.3769
70	3.0467	0.5901	7.6751
75	3.3364	0.5793	7.0477
80	3.5788	0.5658	6.5225
85	3.7942	0.5537	6.0560
90	3.9930	0.5437	5.6254

Table 3.4: Cycle time = 1800s, Mass recovery = 140s (Khan et al.[2])

Heat Source Temperature[°C]	CC[kW]	COP[-]	T <sub>chillout</sub> [°C]
50	0.4197	0.1791	13.4095
55	1.1796	0.3713	11.7633
60	1.8779	0.4786	10.2505
65	2.5168	0.5480	8.8664
70	3.0703	0.5921	7.6674
75	3.5490	0.6227	6.6304
80	3.9472	0.6425	5.7679
85	4.2679	0.6541	5.0732
90	4.5110	0.6574	4.5468

From Table 3.3, it is clearly found that the coefficient of performances (COP) of the proposed cycle is higher than that of the conventional mass recovery cycle if heat source temperature is 65<sup>0</sup>C. It is also seen that the coefficient of performances (COP) can be improved up to 9.5% than that of the conventional cycle if heat source temperature is considered to be 65<sup>0</sup>C. It should be noted that the cooling capacity (CC) of the proposed cycle is much better than that of the conventional mass recovery cycle (see Table 3.3) in the range of heat source temperature from 50<sup>0</sup>C to 65<sup>0</sup>C. The cooling capacity can be improved more than 8% using the proposed cycle from that of conventional cycle.

The ability to produce a low chilled water outlet is one of the indicators to test the performance of the new cycle. The performance of the proposed cycle is much better than that of the conventional cycle because the chilled water outlet temperature of the conventional cycle is higher than that of the proposed cycle as shown in Table 3.3. According to Table 3.3, the proposed cycle is able to produce chilled water at lower temperature than that of the conventional cycle.

### **3.5 Conclusion**

A novel three-bed chiller (unequal bed) with mass recovery scheme is proposed and the performances are evaluated by numerical technique. There is an increasing need for energy efficiency and requirement for the system driven with low temperature heat source. The following concluding remarks can be drawn from the present analysis:

- (i) The main feature of the proposed chiller is the ability to be driven by relatively low temperature heat source. The chiller can utilize the fluctuated heat source temperature between  $50^{\circ}\text{C}$  to  $90^{\circ}\text{C}$  to produce effective cooling along with a coolant inlet at  $30^{\circ}\text{C}$ .
- (ii) Cooling capacity of the proposed chiller is increased as heat source temperature is increased from  $50^{\circ}\text{C}$  to  $90^{\circ}\text{C}$  and cooling water inlet temperature is decreased from  $40^{\circ}\text{C}$  to  $20^{\circ}\text{C}$ .
- (iii) The optimum COP value (0.6003) is obtained for hot water inlet temperature at  $65^{\circ}\text{C}$  in combination with the coolant and chilled water inlet temperatures are  $30^{\circ}\text{C}$  and  $14^{\circ}\text{C}$ , respectively. The delivered chilled water temperature is obtained at  $8^{\circ}\text{C}$ .
- (iv) Adsorption/desorption cycle time is very sensitive to the heat source temperature. The highest CC values are obtained for cycle time between 1800s and 2400 s in the present study.

### Comparison of the Result between Two Cycles

#### 4.1 Introduction

The comparison of the numerical results between the proposed cycle1 and the proposed cycle 2 are discussed in this chapter. In cycle1, the configuration of beds in the three bed chiller with mass recovery were taken as uniform in size but in cycle 2 the configuration of Hex3 is taken as half of Hex1 or Hex2 (where Hex1 and Hex2 are identical). Results show that the cooling capacity (CC) and coefficient of performance (COP) of the proposed cycle1 is much better than that of the proposed cycle 2 in the range of heat source temperature from 50<sup>0</sup>C to 70<sup>0</sup>C.

Table 4.1: Cycle time = 2100s, Mass recovery = 40s

Heat Source Temperature [°C]	Proposed Cycle1			Proposed Cycle2		
	CC[kW]	COP[-]	T <sub>chillout</sub> [°C]	CC[kW]	COP[-]	T <sub>chillout</sub> [°C]
50	1.6332	0.4524	10.7371	1.0652	0.4128	11.9672
55	2.4351	0.5289	9.0003	1.6190	0.4853	10.7674
60	3.1288	0.5615	7.4978	2.0845	0.5130	9.7593
65	3.7298	0.5703	6.1962	2.4967	0.5248	8.8662
70	4.2444	0.5674	5.0816	2.8432	0.5247	8.1156

#### 4.2 Comparison of the result between two cycles

Figures 4.1(a)-4.1(c) show the comparison of the numerical results between the proposed cycle1 and the proposed cycle 2. Both of the cycles were tested at the same conditions based on the input parameters presented in Table 4.1. From the figure 4.1(b), it is clearly found that COP of the proposed cycle1 is higher than that of the proposed cycle 2 if heat source temperature is 65<sup>0</sup>C. It should be noted that the cooling capacity (CC) of the

proposed cycle1 is much better than that of the proposed cycle 2 (see Fig.4.1(a)) in the range of heat source temperature from 50°C to 70°C.

The ability to produce a low chilled water outlet is one of the indicators to test the performance of the new cycle. The performance of the proposed cycle1 is much better than that of the proposed cycle 2 because the chilled water outlet temperature of the proposed cycle 2 is higher than that of the proposed cycle1 as shown in Figure 4.1(c). According to Figure 4.1(c), the proposed cycle1 is able to produce chilled water at lower temperature than that of the proposed cycle 2.

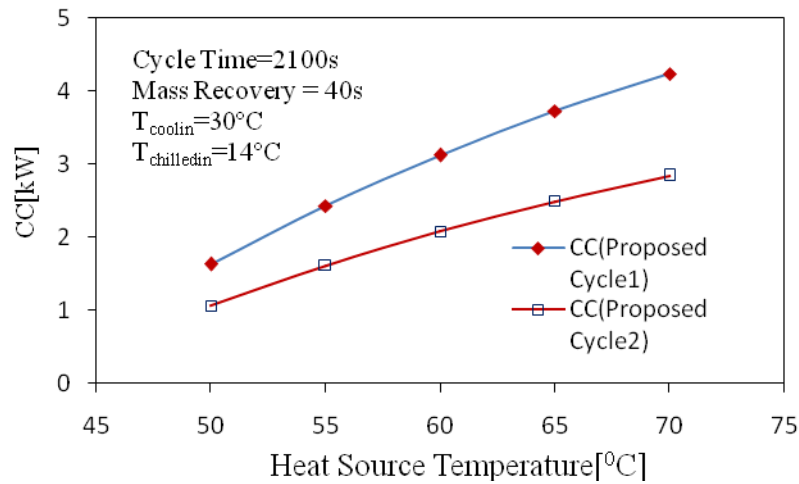


Fig 4.1(a): Performance comparison of CC between the proposed cycle1 and cycle2

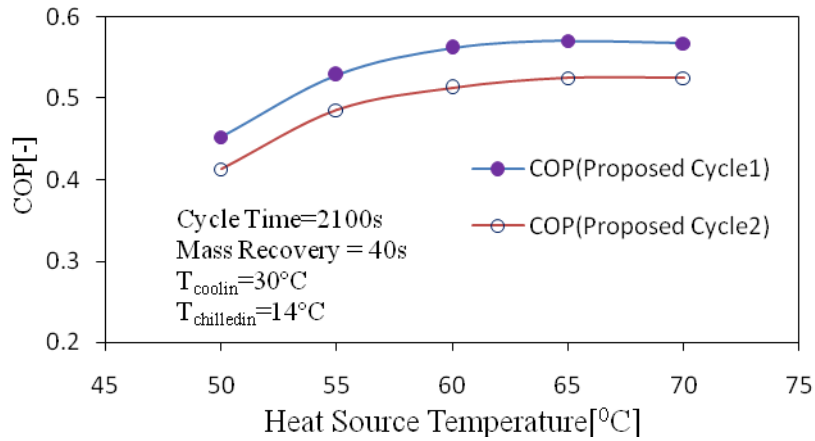


Fig 4.1(b): Performance comparison of COP between the proposed cycle1 and cycle2

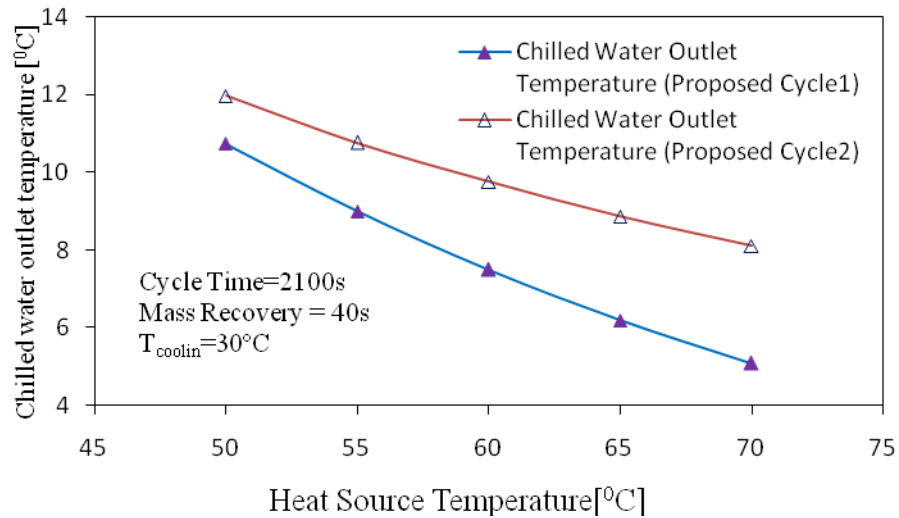


Fig 4.1(c): Performance comparison of outlet chilled water between the proposed cycle1 and cycle2

### 4.3 Conclusion

The comparison of the numerical results between the proposed cycle1 and the proposed cycle 2 are discussed in this chapter. Both of the cycles were tested at the same conditions based on the input parameters. The following possible outcomes can be drawn from the present analysis:

- (i) The main feature of the proposed chiller is the ability to be driven by relatively low temperature heat source. The chiller can utilize the fluctuated heat source temperature between 50<sup>0</sup>C to 70<sup>0</sup>C to produce effective cooling along with a coolant inlet at 30<sup>0</sup>C.
- (ii) The cooling capacity (CC) and coefficient of performance (COP) of the proposed cycle1 is much better than that of the proposed cycle2 in the range of heat source temperature from 50<sup>0</sup>C to 70<sup>0</sup>C. The optimum COP value is obtained for hot water inlet temperature at 65<sup>0</sup>C.
- (iii) The performance of the proposed cycle1 is much better than that of the proposed cycle2 because the proposed cycle1 is able to produce chilled water at lower temperature than that of the proposed cycle 2.

## Overall Conclusion

A three-bed adsorption chiller with different cycle has been numerically studied to improve the cooling effect (using mass recovery scheme). The main feature of the proposed chiller is the ability to be driven by relatively low temperature heat source below 100<sup>0</sup>C. The chiller can utilize the fluctuated heat source temperature between 50<sup>0</sup>C to 65<sup>0</sup>C (for cycle1) and 50<sup>0</sup>C to 90<sup>0</sup>C (for cycle 2) respectively to produce effective cooling along with a coolant inlet at 30<sup>0</sup>C. It is found that the cooling capacity (CC) increases with the increase of hot water temperature and reverse tendency for cooling water temperature. In the low heat source temperature, COP improves significantly. It is also seen that the cooling capacity (CC) and coefficient of performances (COP) can be improved up to 50%, 13% (for cycle1) and 8%, 9.5% (for cycle 2) respectively than that of the conventional mass recovery cycle for fixed heat source temperature 65<sup>0</sup>C. It should be noted that the proposed cycle is able to produce low outlet chilled water than that of the conventional cycle. The highest CC values are obtained for cycle time between 2100 s and 2700s (for cycle 1) and 1800s and 2400s (for cycle 2) respectively in the present study. Finally, it may be concluded that the mass recovery process has greater influence on the performance with a lower heat source temperature, such as 65<sup>0</sup>C, which may help to improve COP more than 13% (for cycle1) and 9.5% (for cycle2) respectively.



## **Extension of this work**

- ❖ This thesis deals with the numerical study of a three-bed adsorption chiller with different cycles, where connection of the bed with the evaporator is excluded during pre-heating or pre-cooling time. If we connect any one of the bed with the evaporator may give better performance to the existing system, which may pave the way for the provision of future works related to this system.

## References

---

- [1] Saha, B.B., Akisawa, A. and Kashiwagi, T., Solar/waste heat driven two-stage adsorption chiller: The Prototype, *Renewable Energy*, Vol-23(4), pp 93-101, 2001.
- [2] Khan, M.Z.I., Saha, B.B., Alam, K.C.A., Akisawa, A., Kashiwagi, T., Performance investigation on mass recovery three-bed adsorption cycle, *International Conference on Mechanical Engineering*, pp 28-30, 2005.
- [3] Khan, M.Z.I., Sultana, S., Akisawa, A., Kashiwagi, T., Numerical simulation of advanced adsorption refrigeration chiller with mass recovery, *Journal of Naval Architecture and Marine Engineering*, Vol-3(2), pp 59-67, 2006.
- [4] Saha, B.B., Koyama, S., Kashiwagi, T., Akisawa, A., Ng, K.C., Chua, H.T., Waste heat driven dual-mode, multi-stage, multi-bed regenerative adsorption system, *International Journal of Refrigeration*, Vol-26, pp 749-757, 2003.
- [5] Saha, B.B., Koyama, S., Lee, J. B., Kuwahara, K., Alam, K. C. A., Hamamoto, Y., Akisawa, A. and Kashiwagi, T., Performance evaluation of a low-temperature waste heat driven multi-bed adsorption chiller, *International Journal of Multiphase Flow*, Vol-29, pp 1249-1263, 2003.
- [6] Kashiwagi, T., Akisawa, A., Yoshida, S., Alam, K.C.A., Hamamoto, Y., Heat driven sorption refrigerating and air conditioning cycle in Japan, *International Proceeding of the International Sorption Heat Pump Conference*, pp 50-62, 2002.
- [7] Douss, N., and Meunier, F., Experimental study of cascading adsorption cycles, *Chemical Engineering Science*, Vol-44, pp 225-235, 1989.
- [8] Stitou, D., Spinner, B., Satzger, P., and Ziegler, F., Development and comparison of advanced cascading cycles coupling a solid/gas thermochemical process and a liquid/gas absorption process, *Applied Thermal Engineering*, Vol-20, pp 1237-1269, 2000.

- [9] Wang, W., Qu, T.F., and Wang, R.Z., Influence of degree of mass recovery and heat regeneration on adsorption refrigeration cycles, *Energy Convers Manage*, Vol-43, pp 733-741, 2002.
- [10] Leong, K.C., and Liu, Y., Numerical study of a combined heat and mass recovery adsorption cooling cycle, *International Journal of Heat Mass Transfer*, Vol-47(22) pp 4761-4770, 2004.
- [11] Shelton, S.V., Wepfer, J.W. and Miles, D.J., Ramp wave analysis of the solid/vapor heat pump, *ASME Journal Energy Resources technology*, Vol-112, pp 69-78, 1990.
- [12] Critoph, R.E., Forced convection adsorption cycles, *Applied Thermal Engineering*, Vol-18, pp 799-807, 1998.
- [13] Meunier, F, Theoretical performances of solid adsorbent cascading cycles using the zeolite-water and active carbon-methanol pairs: four case studies, *Heat recovery & CHP systems*, Vol-6(6), pp 491-498, 1986.
- [14] Pons, M. and Poyelle, F., Adsorptive machines with advantaged cycles for heat pumping or cooling applications, *International Journal of Refrigeration*, Vol-22(1), pp 27-37, 1999.
- [15] Wang, R. Z., Performance improvement of adsorption cooling by heat and mass recovery operation, *International Journal of Refrigeration*, Vol-24, pp 602-611, 2001.
- [16] Akahira, A., Alam, K.C.A., Hamamoto, Y., Akisawa, A., Kashiwagi, T., Mass recovery adsorption refrigeration cycle-improving cooling capacity, *International Journal of Refrigeration*, Vol-27, pp225-234, 2004.
- [17] Alam, K.C.A., Akahira, A., Hamamoto, Y., Akisawa, A. and Kashiwagi, T., A four-bed mass recovery adsorption refrigeration cycle driven by low temperature waste/renewable heat source, *Renewable Energy*, Vol-29, pp 1461-1475, 2004.
- [18] Saha, B.B., Koyama, S., Ng, K.C., Hamamoto, Y., Akisawa, A. and Kashiwagi, T., Study on a dual-mode, multi-stage, multi-bed regenerative adsorption chiller, *Renewable*

- Energy, Vol-31(13), pp 2076-2090, 2006.
- [19] Khan, M.Z.I., Alam, K.C.A., Saha, B.B., Hamamoto, Y., Akisawa, A. and Kashiwagi, T., Parametric study of a two-stage adsorption chiller using re-heat-the effect of overall thermal conductance and adsorbent mass on system performance, International Journal of Thermal Sciences, Vol-45, pp511-519, 2006.
- [20] Saha, B.B., Akisawa, A., Kashiwagi, T., Silica gel/water advanced adsorption refrigeration cycle, Energy , Vol-22(4), pp 437-447, 1997.
- [21] Chua, H.T., Ng, K.C., Malek, A., Kashiwagi, T., Akisawa, A., Saha, B.B., Multi-bed regenerative adsorption chiller-improving the utilization of waste heat and reducing the chilled water outlet temperature fluctuation, International Journal of Refrigeration, Vol-24, pp124-136, 2001.
- [22] Alam, K.C.A., Hamamoto, Y., Akisawa, A. and Kashiwagi, T., Advanced adsorption chiller driven by low temperature heat source, International Proceedings of 21<sup>st</sup> International Congress of Refrigeration, Washington, DC, USA Paper No136, 2003.
- [23] Ng, K.C., Wang, X., Lim, Y.S., Saha, B.B., Chakarborty, A., Koyama, S., Akisawa, A., Kashiwagi, T., Experimental study on performance improvement of a four-bed adsorption chiller by using heat and mass recovery, International Journal of Heat Mass Transfer, Vol-49, pp 3343-3348, 2006.
- [24] Qu, T.F., Wang, R.Z., Wang, W., Study on heat and mass recovery in adsorption refrigeration cycles, Applied Thermal Engineering, Vol-21, pp 439-452, 2001.
- [25] Chu, H.T., Ng, K.C., Wang, W., Yap, C., Wang, X.L., Transient modeling of a two-bed silica gel-water adsorption chiller, International Journal of Heat Mass Transfer, Vol-47, pp 659-669, 2004.
- [26] Ng, K.C., Chua, H.T., Chung, C.Y., Loke, C.Y., Kashiwagi, T., Akisawa, A., Saha, B.B., Experimental investigation of the silica gel-water adsorption isotherm characteristics, Applied Thermal Engineering, Vol-21, pp 1631-1642, 2001.

- [27] Saha, B.B., Boelman, E.C., Kashiwagi, T., Computational analysis of an advanced adsorption-refrigeration cycle, *Energy*, Vol-20, pp 983-994, 1995.
- [28] Akahira, A., Alam, K.C.A., Hamamoto, Y., Akisawa, A., Kashiwagi, T., Experimental investigation of mass recovery adsorption refrigeration cycle, *International Journal of Refrigeration*, Vol-28, pp 749-572, 2005.
- [29] Akahira, A., Alam, K.C.A., Hamamoto, Y., Akisawa, A., Kashiwagi, T., Mass recovery four-bed adsorption refrigeration cycle with energy cascading, *Applied Thermal Engineering*, Vol-25, pp 1764-1778, 2005.
- [30] Alam, K., Khan M., Uyun, A.S., Hamamoto, Y., Akisawa, A., Kashiwagi, T., Experimental study of a low temperature heat driven re-heat two-stage adsorption chiller, *Applied Thermal Engineering*, Vol-27, pp 1686-1692, 2007.
- [31] Khan, M.Z.I., Alam, K.C.A., Saha, B., Akisawa, A., Kashiwagi, T., Performance evaluation of multi-stage, multi-bed adsorption chiller employing re-heat scheme, *Renewable Energy*, Vol-33, pp 88-98, 2008.
- [32] Khan, M.Z.I., Saha, B.B., Alam, K.C.A., Akisawa, A., Kashiwagi, T., Study on solar/waste heat driven multi-bed adsorption chiller with mass recovery, *Renewable Energy*, Vol-32, pp 365-381, 2007.
- [33] Uyun, A.S., Akisawa A., Miyazaki, T., Ueda, Y., Kashiwagi, T., Numerical analysis of an advanced three-bed mass recovery adsorption refrigeration cycle, *Applied Thermal Engineering*, July17, 2009.
- [34] Khan, M.Z.I., Saha, B.B. and Akisawa, A., Experimental study on a three-bed adsorption chiller, *International Journal of Air-Conditioning and Refrigeration*, Vol-19(4), pp 285-290, 2011.